UNIVERSITY OF EDUCATION, WINNEBA

COLLEGE OF TECHNOLOGY EDUCATION – KUMASI

DEPARTMENT OF MECHANICALAND AUTOMOTIVE TECHNOLOGY EDUCATION

NUMERICAL ANALYSIS OF CRANKSHAFT USED ON TVS DELUXE AUTO-RICKSHAW(PRAGYA)

SAMUEL PASSIM ASSAM

2021

UNIVERSITY OF EDUCATION, WINNEBA

COLLEGE OF TECHNOLOGY EDUCATION – KUMASI

DEPARTMENT OF MECHANICAL AND AUTOMOTIVE TECHNOLOGY EDUCATION

NUMERICAL ANALYSIS OF CRANKSHAFT USED ON TVS DELUXE AUTO-RICKSHAW(PRAGYA)

SAMUEL PASSIM ASSAM

(200029498)

A Thesis in the Department of Mechanical and Automotive Technology Education, Faculty of Technology Education, Submitted to the School of Graduate Studies,University of Education, Winneba in partial fulfilment of the requirements for the award of Master of Philosophy (Automotive Engineering Technology) degree

.

SEPTEMBER, 2021

DECLARATION

STUDIES' DECLARATION

I, Samuel Passim Assam declare that this thesis, with the exception of quotations and references contained in published works which have all been identified and duly acknowledged, is entirely my own original work, and it has not been submitted, either in part or whole, for another degree elsewhere.

NAME: SAMUEL PASSIM ASSAM

SIGNATURE: ……

DATE: ……

SUPERVISOR'S DECLARATION

I hereby declare that the preparation and presentation of this work was supervised in accordance with the guidelines for supervision of thesis as laid down by the University of Education, Winneba

NAME: ING. ENOCKA. DUODU (PhD)

SIGNATURE: ……...

DATE: ……

DEDICATION

To God the Father, God the Son and God the Holy Ghost be praise, Glory and Honourforever and ever. May the purpose of God for my life be accomplished and made manifest. I wish to dedicate this work to my father, Mr. Akparibilla Assam and my mother Mrs. AssamAwieya all of blessed memory. Also, I wish to dedicate this material to my lovely wife Mrs. Assam Salomey and my children Joycelyn Teiwin Assam, Gabriella Win-Pang Assam, Godwin Win-Nongeti Assam and Joshua Win-Yangya Assam for your spiritual and moral support during this period of my studies, most especially when you needed me by your side.

ACKNOWLEDGEMENT

I am most grateful to the Almighty God for the grace given me to go through this programme successfully. To him alone be praise and glory.

Great deals of appreciation go to my able supervisor Ing. Enock A.Duodu (PhD) for his attention and support towards the success of this whole project.

I also wish to express my profound gratitude to all the academic staff of Department of Mechanical and Automotive Technology Education of the University of Education, Winneba- Kumasi Campus teaching for their cooperation during the period of this programme.

I am most grateful to the entire management of Tamale Technical University for the opportunity to pursue this programme. I am also very thankful to Mr. Jonathan Afrifa and Mr. Jacob K. Nkrumah for their support in making this work a success.

My gargantuan appreciation is directed to my better half MrsSalomey Assam, my colleague Priest Rev. Fr. John A. Atua, all my course mates and my family members for their prayers and support.

Finally, my thanks go to all senior and junior members of the Automobile Engineering Department of Tamale Technical University for their wonderful cooperation.

ABSTRACT

This study was motivated by the need for numerical analysis of crankshaft used on TVS Deluxe Auto-Rickshaw (Pragya)to determine the structural deformation it goes through under load. A crankshaft can be called the heart of every internal combustion engine because of the vital role it places in an engine. The main function of the crankshaft is to convert the reciprocating motion of the connecting rod into rotary motion of the flywheel. The primary objective of this study was to ascertain the possibility of using structural steel to model a TVSDeluxe Auto-Rickshaw(Pragya) crankshaft for weight optimisation whiles maintaining strength of the crankshaft. The crankshaft was modelled using Autodesk inventor 2017 software based on computed dimensions. The modelled crankshaft was imported onto the ANSYS Workbench observing boundary conditions. Static structural and modal analysis was performed on the crankshaft using both the control and implementing materialsto ascertain the suitability or otherwise of the implementing material. The result showed that, the weights of crankshafts made of the controlled materials (mild steel and forged steel) were the same, while the weight of the implementing material (structural steel) was 82.6g less than that of the controlled materials. Structural steel can be considered as one of the materials for TVS king tricycle (Pragya) crankshaft. Numerical results showed that structural steel can withstand the induced stresses and was also lighter in weight as compared to the controlled materials. Therefore, it is recommended that structural steel must be used as one of the materials for TVS king tricycle (Pragya) crankshaft. Simulated results showed that it can withstand the induced stresses, and also lighter in weight as compared to the control materials.

TABLE OF CONTENTS

LIST OF TABLES

LIST OF FIGURES

NOMENCLATURES

FEM	Finite element method
3D	Three dimensions
PRO/E	Pro Engineer
CrMov13	Chromium Molybdenum vanadium
FEA	Finite element analysis
SAE	Society of Automotive Engineers
AISI	American Iron and Steel Institute
ASTM	American Society for Testing and Materials
cc	Capacity
T_1	Belt tension in the tight side
T_2	Belt tension in the slack side
W	Weight of flywheel acting downward
F_P	Gas load on piston
H_1 &H_2	Horizontal reactions at bearings 1 and 2
D	Piston diameter or Bore diameter
P	Maximum intensity of pressure on the piston
P_b	Permissible bearing pressure
t	Thickness of crank web
d_c	Diameter of crankpin
l_c	Length of crankpin
M_c	Bending moment at the centre of the crankpin
d_s	Shaft diameter
w	Width of crank web
M	Maximum bending moment on the crank web
Z	Section modulus
M_w	Bending moment due to weight of flywheel
M_T	Bending moment due to belt tension

M_s	Bending moment at the shaft
F_Q	Thrust on the connecting rod
F_T	Tangential force
F_R	Radial force
T_c	Twisting moment of the crankpin
T_e	Equivalent twisting moment at the crankpin
T_s	Twisting moment at the shaft
Ø	Angle of inclination of the connecting rod with the line of stroke
θ	Angle of twist
τ	Allowable shear stress in the crankpin
M_R	Bending moment due to the radial component of F_Q
b	Distance between bearing 1 & 2
H_{T1}	Tangential reaction at bearing 1
H_{T1}	Tangential reaction at bearing 2
T	Twisting moment on arm
σ_{max}	Total or maximum stress
σ_b	Allowable bending stress for the crankpin
σ_c	Direct compressive stress on the crank web
σ_{bR}	Bending stress in the radial direction
σ_{bT}	Bending stress in the tangential direction
σ_d	Directional compressive stress
$(\sigma_c)_{max}$	Maximum or combined stress

CHAPTER ONE

INTRODUCTION

1.1 Background to the Study

The crankshaft is a component of a reciprocating engine that converts the power created from the power strokes of the pistons in the engine cylinders (linear power delivery) into rotational movement and passes this power onto the transmission system, drive train and road wheels (Hillier 2004). It's the largest single component of an internal combustion engine. Other applications of a crankshaft range from small one-cylinder lawnmower engines to very large multi cylinder marine engine crankshafts. In Ghana today, tricycles have become the commonest means of transport in rural, urban, peri-urban and cities. TVSDeluxe Auto-Rickshawis one of the leading brands of tricycle in Ghana, hence the need to conduct a study on its crankshaft.

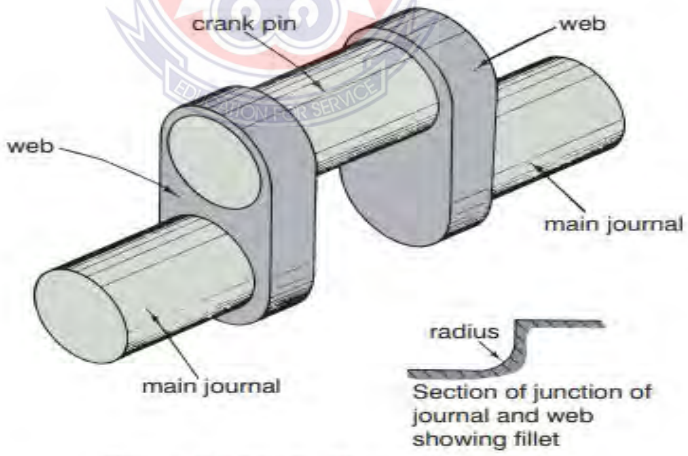

Figure 1.1 Single-Throw Crankshaft

As shown in Figure 1.1, the crankshaft of an internal combustion engine is formed of a number of sections. The main bearings and the crankpin or a crank journal to which the big-end of the connecting rod is fitted, is offset from the main journal by a distance called the crank radius. The webs connect the main journals to the crankpin, and where the journals join the webs a fillet or radius is formed to avoid

sharp corner which would be a source of weakness (Hillier& Coombes, 2004).Therefore, the need for improvement in the design of fillets cannot be overemphasized. A crankshaft may consist of as few as two main journal bearings, even in four-cylinder engines, provided their rating is low. However, in highly rated engines there is usually in addition, one between each pair of crank throws, though some four-cylinder units have only three bearings. In the latter event, the shaft has to be very stiff, otherwise at certain speeds and loads, it would whip heavily, loading the central bearing as it does so, possibly causing it to fail. This tendency can be completely eliminated, or at least reduced, by balance weight on the crank webs at each side of that bearing (Hillier, 2004).

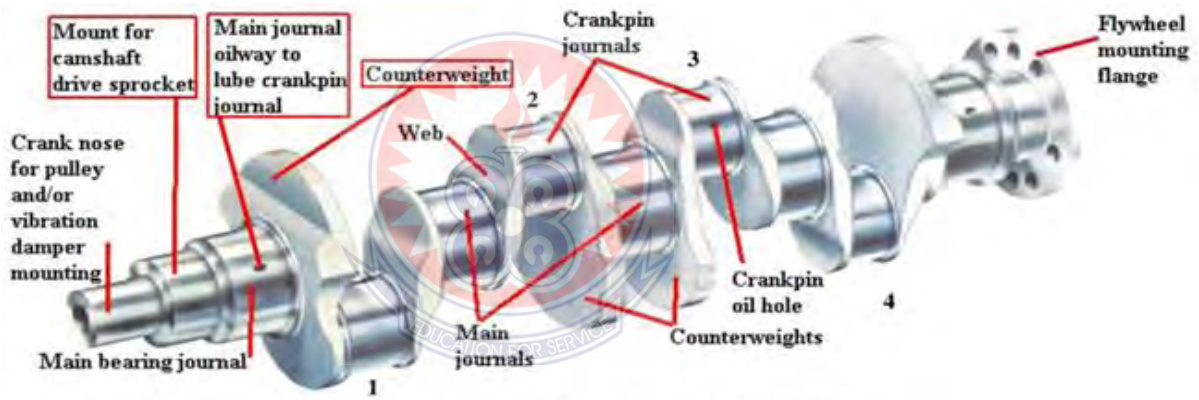

Figure 1.2 COMPONENTS OF CRANKSHAFT

According to Pratiksha (2015), the linear displacement of an engine caused by the combustion chamber is not smooth and therefore leads to sudden shocks. The concept of using crankshaft is to change these sudden displacements to a smooth rotary output, which is the input to devices such as generators, pumps and compressors. It should also be stated that, the use of a flywheel helps in smoothing the shock. Bending stresses and torsional stresses act upon the crankshaft due to various forces caused by the variable gas pressure during working of the engine. Hillier (2004) states that, in some cases the webs are extended to form balance masses, which

are used in certain types of engines to ensure that the rotating parts are balanced as effectively as possible and will cause little or no vibration when the engine is running. The number of crank-pins depends on the type of engine and number of cylinders. A single cylinder engine will have only one crank-pin and two webs. An example of a single cylinder engine is the tricycle engine.

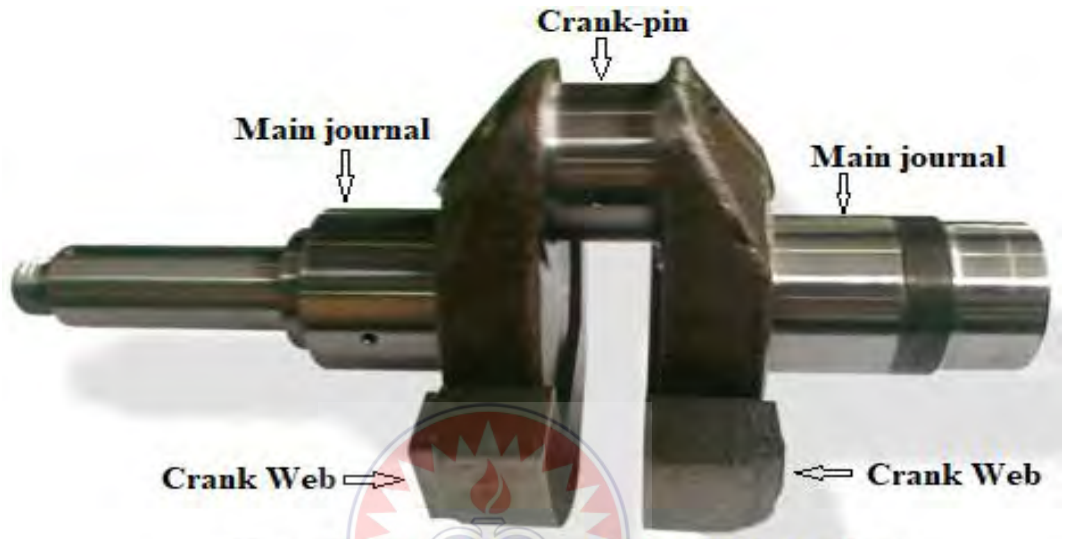

Figure 1.3 Crankshaft of Single-cylinder Engine

Multi-cylinder engines will have one crank-pin per piston if the engine is a straight engine, meaning that all cylinders are in a line.

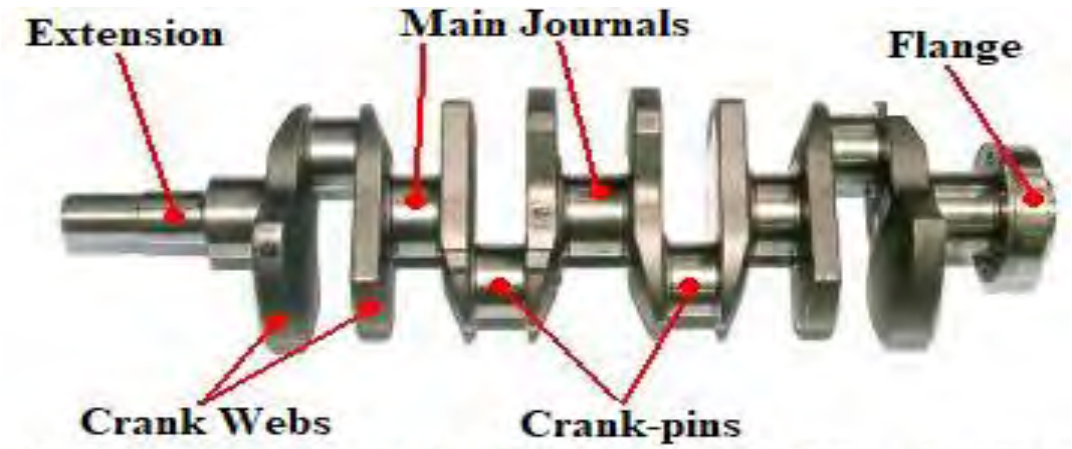

Figure 1.4 Crankshaft of Four-cylinder Inline Engine

If the engine is a V-engine, the cylinders are arranged such that, one bank of cylinders are on each side of the crankshaft, with two pistons attached to the same crank-pin.

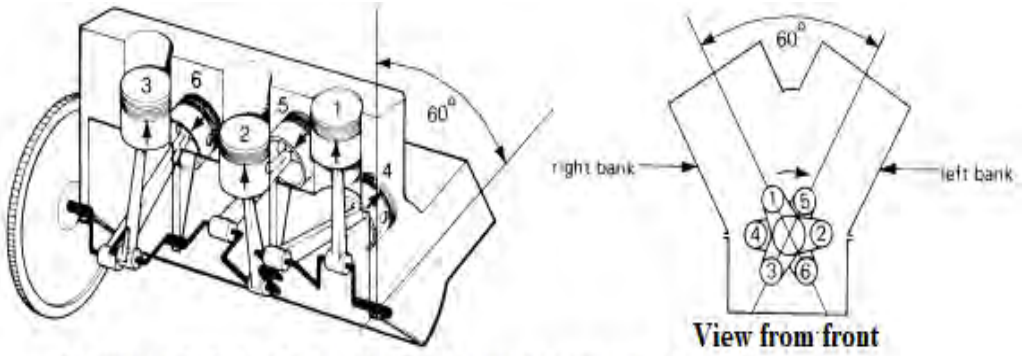

Figure 1.5 Cylinder and Crank arrangement for V6 Engine

Usually, crankshafts are classified by the number of "crank throws" or simply "throws". A crank throw or throw is the combination of the two webs and crank-pin.

1.2 Statement of the Problem

If there is no crankshaft, there is certainly not going to be an internal combustion engine and the associated numerous benefits derived from its operation. Crankshaft is one of the most important rotating parts in internal combustion engine. It is the largest rotating component with a complex geometry in an internal combustion engine which converts the reciprocating motion of the piston into a rotary motion. This study was motivated by the need for numerical analysis of crankshaft used on TVSDeluxe Auto-Rickshaw(Pragya) to determine the structural deformation it goes through under load. Also, to optimiseTVSDeluxe Auto-Rickshawcrankshaft using structural steel which will lead to reduction in weight compared to the traditional mild steel and forged Steel. Furthermore, to perform a modal analysis on crankshaft to give the behaviour of its structure through different mode shapes at different frequencies and help determine resonance frequencies. Crankshaft is one of the most important components of an internal combustion engine. It is the largest and heaviest single component in an engine. It converts reciprocating motion into rotary motion which is transmitted through the transmission system to the final drive to propel the vehicle and tricycles. Most tricycles parked in Tamale is as a result of

crankshaft failure. This paper intends to analyse the structural deformation on the crankshaft under load and optimization of the crankshaft in order to reduce weight while maintaining strength.To achieve this, other materials for the production of crankshafts used on TVSDeluxe Auto-Rickshaw(Pragya) are introduced.

1.3 Purpose of the Study

The main aim of the study is to usenumerical methods to analyse the crankshaft of four-stroke spark ignition engine on TVSDeluxe Auto-Rickshaw(Pragya).

1.4Research Objectives

The following specific research objectives were formulated to guide the study;

- To model a TVS king tricycle engine crankshaft
- To conduct static structural analysis on different materials for TVS crankshaft.
- To perform modal analysis of three crankshafts made of different materials.
- To use structural steel as a material for TVS crankshaft to reduce weight and prolong service life.
- To compare the simulation results with theoretical results to validate the model.

1.5Organisation of the Study

The study comprises of five chapters; Chapter One contains the introduction to the study,which includes background to the study, statement of the problem, purpose of the study and research objectives. Chapter Two discusses relevant and relatedliterature of scholarly works related to the subject area. Chapter Three contains the methods and materials used for the study. Chapter Fourpresents the results and

discussion of the study. Chapter five contains a summary of the main findings, conclusion, and recommendations.

CHAPTER TWO

LITERATURE REVIEW

2.1 Introduction

This chapter reviews the earlier studies conducted on crankshaft in general and single cylinder crankshaft in particular, which motivated the current study. This review covered articles from many journals, thesis and dissertations, and web publications, some of which are not directly related to the single cylinder crankshaft but rather crankshaft in general.

2.2 Load on crankshaft

The crankshaft is subjected to two types of stress, static and dynamic. Combustion pressure, inertial forces of the piston and con-rod, bearing load and drive torque all cause static stress. The vibration causes dynamic stress. If it occurs at the resonating frequency, the deformation will be very high and will instantly rupture the crankshaft. In order to achieve good acceleration, the crankshaft must have high static and high dynamic rigidity as well as low weight (Yamagata, 2005).

According to Basavaraj S. T. et al (2015) using ANSYS for “Static Structural Analysis of 2-Cylinder Crankshaft, it is observed that using ANSYS” the crankshaft has to sustain the load from other parts of the engine such as the connecting rod and piston, in order perform it operation.The study observed that, these loads make the crankshaft liable to structural damages.

The majority of external loads are applied to the crankshaft perpendicular to its rotational centerline, and the reaction forces are thus transmitted through the rod

and main bearings. However, in addition to these loads, the crankshaft is exposed to some thrust loading – loading applied along the axis of crankshaft rotation. Thrust loads occur as the clutch in a manual-transmission application is engaged or disengaged. With an automatic transmission, the load transfer through the torque converter includes a thrust component. If the camshaft is driven with a gear train using helical gears, a further thrust load is transmitted to the crankshaft. Finally, dimensional stack-up between the crankshaft and the connecting rods and cylinder bore centerlines results in a small thrust load. For all of these reasons, the crankshaft must include a thrust bearing surface. This is typically provided in conjunction with one of the main bearings. Because the largest thrust loads are generated at the rear of the crankshaft, the thrust bearing is often placed at or near the rear main bearing; for packaging reasons the second-to-rear main bearing is often used since the rear main bearing must also incorporate the rear oil seal (Springer, 2006).

Raja, I. J. et al (2018) in a study 'Design and Dynamic Analysis of Crankshaft in Light Weight', whose main objective was to analyze the average von-misses stress and principle shear stress over the crankshaft. ANSYS was used to conduct static and dynamic analysis on the crankshaft to find total deformation and frequency of the crankshaft. The studyobserved that while converting the reciprocating motion into rotary motion, the crankshaft is subjected to vertical load and vibrations. The study as well checked the load carrying capacity of the crankshaft when subjected to both vibration and rotation.

Another obvious source of forces applied to a crankshaft is the product of combustion chamber pressure acting on the top of the piston. High-performance, normally-aspirated Spark-ignition (SI) engines can have combustion pressures in the 100-bar neighbourhood (1450 psi), while contemporary high-performance

Compression-Ignition (CI) engines can see combustion pressures in excess of 200 bar (2900 psi). A pressure of 100 bar acting on a 4.00-inch diameter piston will produce a force of 18,221 pounds. A pressure of 200 bar acting on a 4.00-inch diameter piston produces a force of 36,442 pounds. That level of force exerted onto a crankshaft rod journal produces substantial bending and torsional moments and the resulting tensile, compressive and shear stresses. However, there is another major source of forces imposed on a crankshaft, namely 'Piston Acceleration'. The combined weight of the piston, ring package, wristpin, retainers, the connecting rod small end and a small amount of oil are being continuously accelerated from rest to very high velocity and back to rest twice each crankshaft revolution. Since the force it takes to accelerate an object is proportional to the weight of the object times the acceleration (as long as the mass of the object is constant), many of the significant forces exerted on those reciprocating components, as well as on the connecting rod beam and big-end, crankshaft, crankshaft bearings, and engine block are directly related to piston acceleration (Mechanical Engineering, 2014). So due to the number of forces acting on the crankshaft, makes it one of the main force bearing components in an engine, hence, its' production process identified as very important and the need to be precise and accurate.

2.3 Finite Element Modelling

According to Metkar, R. et al (2011), finite element method is the most favorite method to solve stress and fatigue analysis and it is commonly used for analysing engineering problems. The report also deliberated on stress life, strain life and FEM to solve fatigue analysis. A good number of Softwares are accessible for use

in finite element analysis applications. Software such as: Autodesk Inventor, ANSYS, Abaqus, Nastran, and MSC.

In astudy conducted by Rinkle& Sunil (2012), a crankshaft model and crank throw were created by Pro/E Software and then imported onto ANSYS bench. The result shows that when the weight of the crankshaft is reduced, the strength of the crankshaft at the maximum limits of stress, total deformation, and the strain is also reduced. As the weight of the crankshaft is decreased this will decrease the cost of the crankshaft and increase the internal combustion engine performance.

Brahmbhatt et al. (2017) created a 3D model in SOLID WORKS and simulation was done in ANSYS. Dynamic analysis was done to calculate the stress in critical areas. The results showed that the edge of the main journal was the maximum stress region and the center of crankpin shows the maximum deformation area.

Jian et al. (2011) analysed three-dimensional model of 380 diesel engine crankshafts. They used Pro/E and ANSYS as FEA tools. The study checked the crankshaft's static strength and fatigue evaluations, whichthen provided theoretical foundation for the optimisation and improvement of engine design. The maximum deformation occurs in the end of the second cylinder balance weight.

According to Pachpande J. E. et al as cited in Muse D. et al (2017), a study was conducted on 'Optimisation of Crankshaft using FEA, the modal analysis of a 3-cylinder crankshaft of SWARAJ 855 XM tractor.' ANSYS suit was used for static structural analysis. The comparison of analysis results of two different materials will show the effect of stresses on different materials and to evaluate the most suitable material for manufacturing crankshaft which gives good performance and to avoid possible structural damages on the crankshaft surface.

2.4 Fatigue analysis of crankshaft

Raju &Namcharaiah, (2018), in a study 'Design and Fatigue Analysis of Crankshaft', the material composition and the manufacturing processes usually followed for crankshafts and also the possible causes of failure were discussed.Based on the numerical results obtained, it was observed that there has been considerable increase in the Von-mises stress (max.) for Grey Cast Iron as compared to steel.Also, fatigue life will be more for Grey Cast Iron compared to steel since it was derived that, the maximum deformation value is 5.572e-3mm for Grey Cast Iron and 5.821e-3mm for Steel.

Wang, J. H (2011) observed in a study that, fatigue rupture is the major reason of crankshaft parts failure. Traditional fatigue analysis is fairly complicated and causes a great error. The finite element model of S195 engine crankshaft is created under Solid Works environment, whose static analysis and fatigue analysis is carried out by using Simulation module. Also, the vibration character of the crankshaft is calculated through modal analysis. Result shows the fatigue strength of the crankshaft is enough and it will not produce resonance in operation.

Metkar, R.M. et al (2011), review on fatigue life of crankshaft was to investigate the behavior of crankshaft under complex loading conditions. Automobile industries are always interested to develop a new product which will be innovative and fulfill market expectations. Various other factors also play important role in mechanical fatigue failure of crankshaft, such as, misalignment of crankshaft on assembly, improper journal bearing, and vibration due to some problem with main bearing or due to high stress concentration caused by incorrect fillet size, oil leakage, overloading, and high operating oil temperature. The study observed that, heat and

stresses during contact bearing with repetition of heating and cooling would eventually create thermal fatigue cracks which will propagate with time.

Katari, et al. (2011) in a study considered three (3) different crankshafts made up of same material, i.e., forged steel which is used in train. The investigation shows that crankshaft failure is due to fatigue which is supported through examination of mechanical properties of crankshaft material. The study observed that, failure regions shows semi-elliptical fracture, indicating progressive fracture growth. Also, cracks are produced due to combined effect of mechanical and thermal fatigue load. It was confirmed by the study that, heat and stresses during contact bearing with repetition of heating and cooling would eventually create thermal fatigue cracks and it will propagate with time.

2.5 Modal analysis of crankshaft

A study conducted by Sriramireddy, K. et al (2018) observed that, stress and fatigue that the crankshaft can handle decides the satisfactory working period of the crankshaft. Thestudy further reveals that, any defect in the crankshaft deteriorates the performance of the engine. Hence, it is important to analyse the crankshaft and predict its failures before a severe damage occurs. It was further observed that, vibrations give a good amount of information on the characteristics of the vibrating structure and hence vibration analysis can be used to inspect and evaluate the crankshaft. Based on the proceeding information, the study conducted a dynamic analysis of the whole crankshaft.

According to Jagrti&Baarjibbe (2016) in the study “Experimental and Numerical Analysis of Crankshaft used in Hero Honda Splendor Motorcycle”, the ANSYS workbench was used to simulate on the modal and stress analysis of

crankshaft to check the safety. The study results on stress and deformation distributions, and natural frequency of crankshaft were obtained.

Talikoti1, B. et al (2015) in a study observed that, the operation of Crankshaft makes it liable to vibrations due to different types of stresses and loads. Modal analysis when conducted on crankshaft, gives the behavior of its structure through different mode shapes at different frequencies and also helps to determine resonance frequencies. The study further observed that modal analysis is the primary stage of many useful analysis like harmonic analysis and transient dynamic analysis, which give the dynamic behavior of the crankshaft.

2.6 Optimisation for weight reduction of crankshaft

According to Muse, D. et al (2017) in the study'Optimization and Finite Element Analysis of Single Cylinder Engine Crankshaft for improving Fatigue Life', an effort was done to improve fatigue life for single cylinder engine crankshaft with geometric optimisation. After conducting the Finite Element Analysis (FEA), the study discovered that the maximum stress appears at the fillet areas between the crankshaft journal and crank web. The study also observed that, failure in the crankshaft initiated at the fillet region of the journal, and fatigue is the dominant mechanism of failure. The study concluded that, the result of geometric optimisation parameter; like changing crankpin fillet radius and crankpin diameter were changes in model of crankshaft to improve fatigue life of crankshaft.

Shahane&Pawar (2016)using ANSYS for "Optimisation of the Crankshaft using Finite Element Analysis," the study conducted a static structural and dynamic simulation on a single cylinder four stroke diesel engine crankshaft to obtain the variation of stresses at different critical locations of the crankshaft. Optimisation of

the crankshaft was studied in the area of geometry and shape on the existing crankshaft. The optimised crankshaft helps to improve the performance of the engine and causes reduction in weight. This optimisation study of the crankshaft helps to reduce 4.37% of the weight in the original crankshaft.

According to Montazersadgh&Fatemi (2009) in the study which dynamic simulation was conducted on a forged steel crankshaft from a single cylinder four stroke engine,finite element analysis was performed to obtain the variation of the stress magnitude at critical locations. The dynamic analysis resulted in the development of the load spectrum applied to the crankpin bearing. The first step in the optimisation process was weight reduction of the component considering dynamic loading. This required the stress range under dynamic loading not to exceed the magnitude of the stress range in the original crankshaft. The optimisation process resulted in an 18% weight reduction, increased fatigue strength, and a reduced cost of the crankshaft.

According to Rinkle&Sunil (2017), a study was conducted on static analysis of a cast iron crankshaft from a single cylinder four stroke engine. Finite element analysis was performed to obtain the variation of the stress magnitude at critical locations. Results obtained from the analysis were used in optimisation of the cast iron crankshaft. This requires the stress range not to exceed the magnitude of the stress range in the original crankshaft. The optimisation process included geometry changes without changing connecting rod and engine block.

Pandiyan, A. (2018) carried out the study‘Design and Optimisation of Crankshaft for Single Cylinder four– Stroke Spark Ignition Engine Using Coupled Steady-State Thermal Structural Analysis.’ The aim of the study was design and optimisation of crankshaft for a single cylinder four stroke over head valve (OHV)

spark ignition engine. Thestudy used reverse engineering techniques, in order to obtain an existing physical model. The results obtained from simulation and parametric optimisation concluded that, the modified design is safe along the selected materials for AISI 1045 and shows the maximum von-misses stresses 184.21 MPa, factor of safety (n) is 2.4428 and the reduced weight of the crankshaft was 63 grams which is 4.04 % less as compared to existing crankshaft model without compromising the strength to weight ratio.

2.7 Materials of crankshaft

Crankshafts are made of high-quality steel or iron. These materials are processed by either forging or casting. Forging gives greater strength, but stiffness is of more importance than strength alone. Most modern shafts have large journals and relatively short throws that allow the crankpins to overlap the journals when viewed from the end of the shaft. This feature allows the shaft to be cast, which results in a lighter shaft and is cheaper to manufacture because it requires less machining. In addition, modem nodular irons are exceptionally strong and, when ground to a fine finish and then surface-hardened, provide an excellent bearing surface. In this case the term ‘nodular’ applies to the inclusion of minute rounded lumps of graphite, (carbon). These particles are not combined with the base material so their existence in a free state classifies the material as iron and not steel (Hillier, 2004).

Crankshafts are generally steel forgings, though high carbon, high copper, chromium silicon iron has been used and nodular, or spheroidal graphite (SG), cast iron is becoming increasingly popular. Best of the steels for crankshafts, but the costliest, are the nitrogen-hardened types, less costly, though also inferior to a significant degree, are the high carbon or alloy steels, surface hardened by the flame

or induction methods, Last in order of durability come the heat-treated high carbon or alloy steels that have not been surface hardened, for which only the soft white metal bearings are suitable. Factors favouring cast iron crankshafts are the low cost of this material, which also has a high hysteresis for damping out vibrations; shafts can be produced in more complex shapes without need for costly tooling or machining; and the larger sections required for heavily loaded shafts on account of the lower tensile strength of the material would, in any case, tend to be necessary also with steel ones, to obtain adequate stiffness. The significance of being able to produce more complex shapes is that balance weights can be cast integrally, instead of having to be bolted on during the balancing operation and, if hollow journals are called for, to reduce weight, they can be cored in the casting instead of having to be machined subsequently at a high cost. Bosses usually have to be left in the hollow sections, so that oilways from the main to the big end journals can be drilled through them. Spheroidal graphite (SG) irons used for crankshafts have both better tensile strength and fatigue resistance and better bearing qualities than the cast irons containing graphite in flake form. They include the following grades: 600/3, 650/2, 700/2, and 800/2 where the larger figure represents its ultimate tensile strength in N/ mm2 and the smaller one its percentage elongation. The graphite is converted to SG form by the injection of magnesium inoculants during smelting and by controlling the cooling (Garrett, 2001).

Kadir A. (2010) in thestudy “Crack Analysis of a Gasoline Engine Crankshafts” states that; the study was conducted on a crankshaft made of nodular graphite cast iron, it was discovered that cracks propagated axially on surface of the 4th pin journal. Microscopic observation was conducted on the surface of journals. Mechanical and metallurgical properties of the crankshaft including chemical composition, micro-hardness, tensile properties and roughness were studied and

compared with the specified properties of the crankshaft materials. The simulation results observed that,the main reason of failure was thermal fatigue because of contact of journal and bearing surface, a condition which leads to the formation and growth of fatigue cracks.

"Structural Static Analysis of Crankshaft" which presentssimulation on the crankshaft with three different materials; Cast Iron, High carbon steel and Alloy steel (42CrMn) to obtain variation of stress magnitude at critical locations. The study compared numerical results with Theoretical results of von-misses and shear stress to validate the model(Mounika & Madhuri, 2015).

Citti, P. et al (2017) discussescurrent challenges in material choice for high-performance engine crankshaft. The study observed that segment of high-performance cars will progressively deal with the trade-off among cost saving, high performances and quality due to customers' higher expectations and the regulations requests for higher-power, safer, more intelligent and environmentally friendly cars. Dealing with these complicated systems requires additional designing phases and optimization of all components in terms of performances, reliability and costs. Among such mechanical parts assembled in an Internal Combustion Engine (ICE), the crankshaft is one that still requires extra attention regarding materials choice, thermal treatments, production processes and costs. The aim of this work is to analyse the actual and future scenarios about the material choice for the crankshaft of high-performance engines. In particular, what is considered here is the actual development and improved quality reached by base materials and manufacturing technologies for this critical component of the engine. In this context, different materials are analysed, together with surface hardening techniques, thermal treatments and their technical and cost saving potentials

2.8 Types of Three-Wheelers

Three-wheeled vehicles can be broadly divided into two categories – the passenger carriers and the goods carriers. Passenger carriers are of two types, one is the compact 4 persons carrier (3 passengers plus the driver) called the auto-rickshaw and the 7 persons carrier (6 passengers plus driver) – often called the Tempo. These two basic platforms also have corresponding goods versions (Iyer, 2012).

A majority of three-wheeled vehicles used in Ghana are designed to carry three passengers in addition to the driver and are called auto-rickshaws.Variants of the basic three-wheelers that are provided with a goods tray, or built like a delivery van, are quite popular for intra-city movement of small merchandize like vegetables, bread, kitchen gas cylinders etc. Most of these vehicles have a payload capacity of half to one tonne. These vehicles basically use a steel frame chassis with a goods tray mounted on it. The front of the vehicle where the driver sits is usually the same as in the corresponding passenger version. All the three-wheelers usually have maximum speed in the region of 50 to 55 km/h.

Another type of three-wheeled vehicle that typically carries six passengers has been growing in popularity in recent years. These vehicles are powered by small, single cylinder diesel engines and operate on fixed routes more or less like the omnibus, often providing a competition to the latter. This vehicle is made of a tubular frame with a sheet metal body mounted on it. This vehicle is also provided with a hood made of fabric and has no doors either in the driver or in the passenger compartments. It has two bench seats facing each other for the passengers and one bench seat in the front for the driver and one more passenger. However, government regulations do not permit a passenger to use that seat and the vehicle continues to be

referred to as the ‘six-seat-rickshaw’ or ‘tempo’. The vehicle is provided with a steering wheel like those in four-wheeled vehicles.

CHAPTER THREE

MATERIALS AND METHODS

3.1 Introduction

This chapter presents the tools, equipment and the methods (procedures) used for the study;it includes the theoretical design procedure for the crankshaft, design of shaft under flywheel as well as the physical and mechanical properties of the materials used (AISI 1018, AISI 1045 and ASTM A36).

3.2 Materials used for Modelling of TVS tricycle Crankshaft

A proper functioning crankshaft mustfulfil the following conditions:

i. Enough strength to withstand the forces to which it is subjected i.e., the bending and twisting moments.
ii. Enough rigidity to keep the distortion at minimum.
iii. Stiffness to minimize the stresses due to torsional vibration,
iv. Strength to resist the stresses due to torsional vibrations
v. Minimum weight.

The materials mostly used for TVS king tricycle crankshaft considered for this study are Mild Steel and forged steel, however, in this study structural steel was used as an implementing material.

3.2.1Structural steel

There are a number of different configurations of structural steel that can be found, but for the most part, all the stuff inside are the same. Just like other types of steel, the main components are iron and carbon. When more carbon is added to the alloy, it increases strength and lower the ductility of the finished product. Other chemicals or substances can be added in the production process that can result in the following:

i. Improve strength
ii. Deliver more or less ductility
iii. Improve economics of use

One of the most common additions to structural steel, after iron and carbon, is manganese. Manganese improves the machinability of steel, and also helps bind steel better to resist cracking and splitting during the rolling process. For the purpose of this study, structural steel (ASTM A36) was used as the implementing material.

3.2.2Mechanical properties of structural steel

Table 3.1Mechanical Properties of Structural Steel(ASTM A36)

S/NO.	MECHANICAL PROPERTIES	METRIC
1.	Density	7800 g/cm^3
2.	Coefficient of thermal expansion	1.2 x 10^{-5} C
3.	Young's Modulus	200 GPa
4.	Poisson's Ratio	0.3
5.	Shear Modulus	76.923 GPa
6.	Tensile Yield strength	2.5 x 10^8 Pa
7.	Compressive Yield strength	2.5 x 10^8 Pa

8. Tensile Ultimate strength 4.6×10^8 Pa

(Akinlabi&Agarana, 2018)

3.3 Method

3.3.1 Theoretical Design Procedure for Crankshaft

The following procedure was adopted for design and modelling of the crankshaft.

i. First of all, the magnitude of the various loads on the crankshaft was found.

ii. The distances between the supports and their position with respect to the loads was determined.

iii. For the sake of simplicity and also for safety, the crankshaft was considered to be supported at the centres of the bearings and all the forces and reactions to be acting at these points. The distances between the supports depend on the length of the bearings, which in turn depend on the diameter of the shaft because of the allowable bearing pressure.

iv. The thickness of the cheeks or webs is assumed to be from 0.4 ds to 0.6 ds, where ds is the diameter of the shaft. It may also be taken as 0.220 to 0.32D, where D is the bore of cylinder in mm.

v. Now calculate the distance between the supports.

vi. Assuming the allowable bending and shear stresses, determine the main dimensions of the crankshaft.

Also;

The crankshaft was designed to check for at least two crank positions: Firstly, when the crankshaft is subjected to maximum bending moments and secondly when the crankshaft is subjected to maximum twisting moment or torque.

The additional moment due to weight of flywheel, belt tension and other forces must be considered.

It is assumed that the effect of bending moment does not exceed two bearing between which a force is considered.

3.3.2 Design of centre crankshaft

The centre crankshaft was designed by considering the two crank positions, i.e. when the crank is at dead centre (or when the crankshaft is subjected to maximum bending moment) and when the crank is at angel at which the twisting moment is maximum. These two cases are discussed in detail as below:

3.3.3 When the crank is at dead centre.

At this position of the crank, the maximum gas pressure on the piston will transmit maximum force on the crankpin in the plan of the crank causing only bending of the shaft. The crankpin as well as ends of the crankshaft will be only subjected to bending moments.

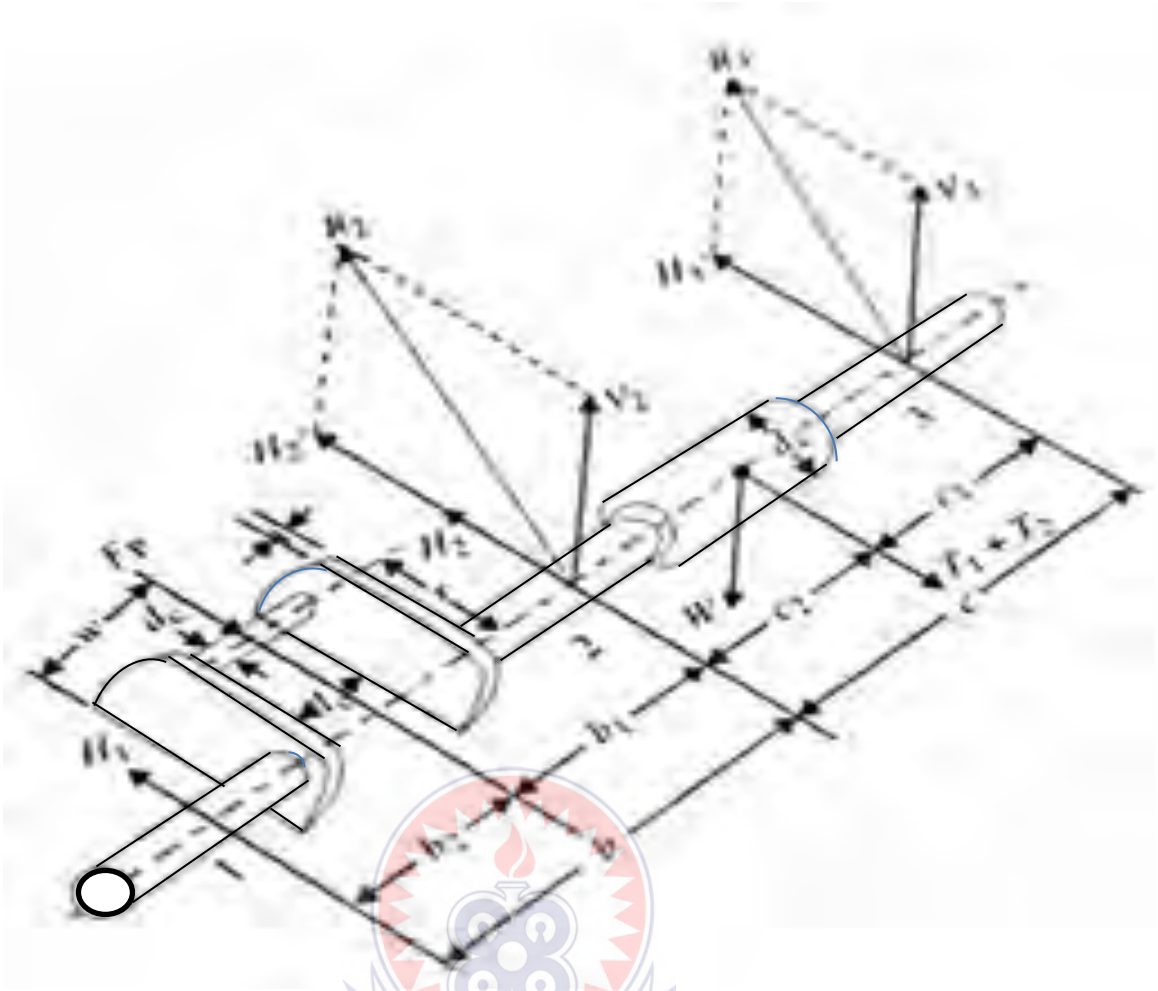

Fig.3.1 Centre Crankshaft at Dead Centre

Consider a single throw three bearing crankshaft as shown in Fig. 3.1

Let D= piston diameter or cylinder in mm,

P= maximum intensify of pressure on the piston in N/mm^2,

W= weight of the flywheel acting downwards in N, and

The resultant belt tension is as indicated in Eq. (3.1)

T1 + T2 =R (3.1)

The thrust in the connecting rod was equal to the gas load on the piston (Fp). It's known as gas load on the piston, as in Eq. (3.2)

$$F_P = \frac{\pi}{4} \times D^2 \times P \quad (3.2)$$

Due to this piston gas load (Fp) acting horizontally, there was two horizontal reactions H_1 and H_2 at bearings 1 and 2 respectively, as shown in Eqs. (3.3) and (3.4)

$$H_1 = \frac{Fp \times b1}{b}; \quad (3.3)$$

$$H_2 = \frac{Fp \times b2}{b} (3.4)$$

Due to the weight of the flywheel (W) acting downwards, there were two vertical reactions $\frac{1}{2}$ and V_3 at bearings 2 and 3 respectively, as in Eq. (3.5) and (3.6)

$$V_2 = \frac{W \times C_1}{C}; \quad (3.5)$$

$$V_3 = \frac{W \times C_2}{C} \quad (3.6)$$

Now, due to the resultant belt tension (T_1+T_2), acting horizontally, there were two horizontal reactions H_2 and H_3 at bearings 2 and 3 respectively, as indicated in Eq. (3.7) and (3.8)

$$H_2' = \frac{(T_1 + T_2)C_1}{C} (3.7)$$

$$H_3' = \frac{(T_1 + T_2)C_2}{C} \quad (3.8)$$

The resultant force at bearing 2 was given as shown in Eq. (3.9)

$$R_2 = \sqrt{(H_2 + H_2')^2 + (V_2)^2} (3.9)$$

Note: $T_1$was the belt tension in the tight side and $T_2$was the belt tension in the slack side.

The resultant force at bearing 3 was given as in Eq. (3.10)

$$R_3 = \sqrt{(H_3)^2 + (V_3)^2} (3.10)$$

Now the various parts of the centre crankshaft were designed for bending only, as discussed below:

i. Design of crankpin

Let d_c= diameter of the crankpin in mm,

l_c = length of the crankpin in mm,

σ_b= allowable bending stress for the crankpin in N/mm^2.

We know that bending moment at the centre of the crankpin,

From Eq. (3.11) and (3.12), diameter of the crankpin was determined. The length of the crankpin was given as shown in Eq. (3.13)

$$M_c = H_1 \times b_2 \quad (3.11)$$

Also know that;

$$M_c = \frac{\pi}{32}(d_c)^3 \times \sigma_b \quad (3.12)$$

$$l_c = \frac{Fp}{dc \times Pb} \quad (3.13)$$

Where Pb = permissible bearing pressure in N/mm2.

ii. Design of left-hand crank web

The crank web was designed for eccentric loading. There were two stresses acting on the crank web, one was direct compressive stress and the other was bending stress due to piston gas load (Fp)

The thickness (t) of the crank web was given empirically as

t = 0.4ds to 0.6 ds

= 0.22D to 0.32D

=0.65dc to 6.35mm

Where ds = shaft diameter in mm,

D = bore diameter in mm, and

ds = crank pin diameter in mm,

The width of crank web (w) was taken as

$$w = 1.125\ dc + 12.7mm,$$

We know that maximum bending moment on the crank web is as in Eq. (3.14)

$$M = H_1 \left(b_2 - \frac{l_2}{2} - \frac{t}{2}\right) \quad (3.14)$$

And section modulus as shown in Eq. (3.15),

$$Z = \frac{1}{6} x\ W\ x\ t^2 \quad (3.15)$$

∴ Bending stress as indicated in Eq. (3.16),

$$\sigma_b = \frac{M}{Z} = \frac{6H_1\left(b2 - \frac{l_2}{2} - \frac{t}{2}\right)}{W\ x\ t} \quad (3.16)$$

and direct compressive stress on the crank web as in Eq. (3.17)

$$\sigma_c = \frac{H_1}{W\ x\ t} (3.17)$$

∴ Total stress on the crank web is as in Eq. (3.15) = Bending stress + Direct stress

$$= \sigma_b + \sigma_c (3.18)$$

$$= \frac{6H_1\left(b2 - \frac{l_2}{2} - \frac{t}{2}\right)}{W\ x\ t} + \frac{H_1}{W\ x\ t}$$

This total stress was less than the permissible bending stress.

iii. Design of right-hand crank web

The dimensions of the right-hand crank web (i.e., thickness and width)were made equal to left hand crank web from the balancing point of view.

iv. Design of shaft under the flywheel

Let; d_s = Diameter of shaft in mm.

We know that bending moment due to the weight of flywheel as in Eq. (3.19)

$$M_w = V_3 \text{ x } C_1 (3.19)$$

And bending moment due to belt tension is as shown in Eq. (3.20)

$$M_T = H_3' \text{ x } C_1 \quad (3.20)$$

These two bending moments act at right angles to each other. Therefore, the resultant bending moment at the flywheel location is as indicated in Eq. (3.21)

$$M_S = \sqrt{(M_w)^2 + (M_T)^2} = \sqrt{(V_3 \text{ x } C_1)^2 + (H_3 \text{ x } C_1)^2} \quad (3.21)$$

We also know that the bending moment at the shaft is as in Eq. (3.22)

$$M_S = \frac{\pi}{32} (d_s)\ \sigma_b (3.22)$$

Where σ_b = allowable bending stress in N/mm2

From equations (3.11) and (3.12) we may determine the shaft diameter (ds).

3.3.4 Crank at an angle of maximum twisting moment

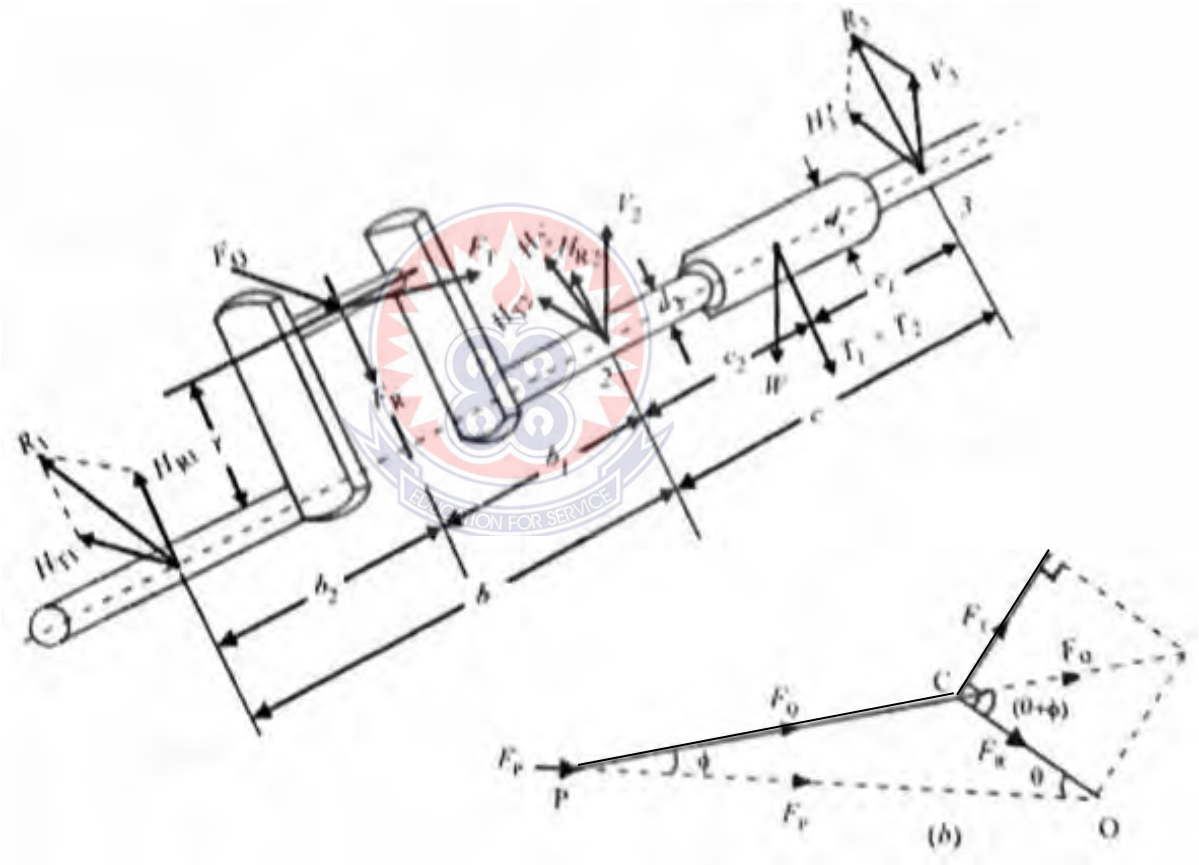

Figure 3.2 Crank at an angle of Maximum Twisting Moment and Forces

The twisting moment on the crankshaft was maximum when the tangential force on the crank (F_T) was maximum. The maximum value of tangential force lies when the crank is at angle of 25^0 to 30^0 from the dead centre for a constant value

combustion engine (i.e., petrol engines) and 30^0 to 40^0 for constant pressure combustion engines (i.e., Diesel engines).

Consider a position of the crank at an angel of maximum twisting moment as shown in fig. 3.2 (a).

If $P^{/}$ is the intensity of pressure on the position at this instant, then the piston gas load at this position of crank is as shown in Eq. (3.23)

$$F_P = \frac{\pi}{4} \times D^2 \times P^{/} \quad (3.23)$$

And thrust on the connecting rod is as indicated in Eq. (3.24)

$$F\sigma = \frac{FP}{Cos\ \emptyset} (3.24)$$

Where $\emptyset$ = Angel of inclination of the connecting rod with the line of stroke PO

The thrust in the connecting rod (F_Q) may be divided into two components, one perpendicular to the crank and the other along the crank. The components of F_Q perpendicular to the crank was the tangential force (F_T) and the component of F_Q along the crank was the radial force (F_R) which produces thrust on the crank shaft bearings. From fig. 3.2(b), we find as in Eq. (3.25) and (3.26)

$$F_T = F_Q \text{ Sin } (\Theta + \emptyset) \quad (3.25)$$

$$F_P = F_Q \text{ Cos } (\Theta + \emptyset) \quad (3.26)$$

It may be noted that the tangential force cause twisting of the crankpin and shaft while the radial force cause bending of the shaft.

Due to the tangential force (F_T), there were two reactions at bearings 1 and 2, such as shown in Eqs. (3.27) and (3.28)

$$H_{T1} = \frac{F_T - b1}{b} (3.27)$$

$$H_{T2} = \frac{F_T - b2}{b} (3.28)$$

Due to the radial force (F_R), there were two reactions at the bearings 1 and 2, as indicated in Eqs. (3.29) and (3.30)

$$H_{R1} = \frac{F_{R1} + b_1}{b} \quad (3.29)$$

$$H_{R2} = \frac{F_R + b_2}{b} \quad (3.30)$$

The reactions at the bearings 2 and 3 due to the flywheel weight (w) and resultant belt pull ($T_1 + T_2$) was same as discussed earlier.

Now the various parts of the crankshaft are designed as discussed below

3.3.5 Design of Crankpin

In designing of the crankpin, the following Eqs. (3.31), (3.32) and (3.33) was used.

Let; d_c = diameter of the crankpin in mm.

We know that bending moment at the centre of the crankpin,

$$M_c = H_{R1} \times b_2 \quad (3.31)$$

And twisting moment on the crankpin,

$$T_c = H_{R1} \times r \quad (3.32)$$

∴ Equivalent twisting moment on the crankpin,

$$T_e = \frac{\pi}{16} (d_c)^3 \tau \quad (3.33)$$

Where τ = Allowable shear stress in the crankpin.

From equation (i) and (ii), the diameter of the crankpin is determined.

3.3.6 Design of shaft under the flywheel

In the designing of the shaft under the flywheel, the following Eqs. (3.34), (3.35), (3.36) and (3.37) was used.

Let; d_s = Diameter of the shaft in mm.

We know that bending moment on the shaft,

$$M_s = R_3 \text{ x } C_1 \quad (3.34)$$

And twisting moment on the shaft,

$$T_S = F_T \text{ x } r \quad (3.35)$$

∴ Equivalent twisting moment on the shaft,

$$T_e = \sqrt{(M_S)^2 + (T_S)^2} = \sqrt{(R_3 \text{ x } C_1)^2 + (F_T \text{ x } r)^2} \quad (3.36)$$

We also know that equivalent twisting moment on the shaft,

$$T_e = \frac{\pi}{16}(d_c)^3\tau \quad (3.37)$$

Where τ= allowable shear stress in the shaft.

From equation (i) and (ii), the diameter of the shaft was determined.

3.3.7 Design of shaft at the juncture of right-hand crank arm

To enable the designing og the shaft at the juncture of right – hand crank arm, the following Eqs. (3.38), (3.39), (3.40) and (3.41).

Let d_{S1} = Diameter of the shaft at the juncture of right-hand crank arm.

We know that bending moment at the juncture of the right-hand crank arm,

$$M_{S1} = R_1 \left(b + \frac{lc}{2} + \frac{t}{2}\right) - F_R \left(\frac{lc}{2} + \frac{t}{2}\right) \quad (3.38)$$

and the twisting moment at the juncture of the right-hand crank arm,

$$T_{S1} = F_T \text{ x } r \quad (3.39)$$

∴ Equivalent twisting moment at the juncture of the right-hand crank arm

$$T_e = \sqrt{(M_{S1})^2 + (T_{S1}b)^2} \quad (3.40)$$

We also know that equivalent twisting moment,

$$T_e = \frac{\pi}{16}(d_{S1})^3\tau \quad (3.41)$$

Where; τ = allowing shear stress in the shaft.

3.3.8 Designed of right-hand crank web

In designing of the right-hand crank web the following Eqs. (3.42), (3.43), (3.44) and (3.45) was used.

The right-hand crank web was subjected to the following stresses:

(1) Bending stresses in two planes normal to each other, due to the radial and tangential components of F_Q,

(2) Direct compressive stress due to F_R, and

(3) Torsional stress.

The bending moment due to the radial component of $F_Q$was given by,

$$M_R = H_{R2}\left(b_1 - \frac{lc}{2} - \frac{t}{2}\right) \quad (3.42)$$

We also know that, $M_R = \sigma_{bR} \times Z = \sigma_{bR} \times \frac{1}{6} \times W \times t^2$ (3.43)

Where; σ_{bR} = bending stress in tangential direction, and

$$Z = \text{section modulus} = \frac{1}{6} \times W \times t^2$$

From equation (i) and (ii) the value of bending stress σ_{bR} is determined.

The bending moment due to the tangential component of F_Q was maximum at the juncture of crank and shaft.

It's given by; $$M_T = F_T\left(r - \frac{d_{S1}}{2}\right) \quad (3.44)$$

Where; d_{S1} = shaft diameter at juncture of right hand crank arm, i.e. at bearing 2

We also know that, $$M_T = \sigma_{Bt} \times Z = \sigma_{bT} \times \frac{1}{6} \times W \times t^2 \quad (3.45)$$

Where; σ_{bT} = bending stress in tangential direction. From Eqs. (3.44) and (3.45), the value of bending stress σ_{bT} was determined.

The direct compressive stress was given as in Eq. (3.46)

$$\sigma_d = \frac{F_R}{2\ x\ W\ x\ t} (3.46)$$

The maximum compressive stress (σ) will occur at the upper left corner of the cross-section of the crank as shown in Eq. (3.47)

$$\therefore\ \sigma_C = \sigma_{bR} + \sigma_{bT} + \sigma_d (3.47)$$

Now, the twisting moment on the arm is as in Eq. (3.48),

$$T = H_{T1}\ (b_2 + \frac{l_c}{2}) - F_T\ x\frac{l_c}{2} = H_{T2}(b_2 - \frac{l_c}{2}) (3.48)$$

We know that shear stress on the arm as indicated in Eq. (3.49)

$$\tau = \frac{T}{Z_p} = \frac{4.5\ x\ T}{W\ x\ t^2} (3.49)$$

Where Z_p = polar section modulus as in Eq. (3.50)

$$Z_p = \frac{W\ x\ t^2}{4.5} (3.50)$$

∴ Maximum or total combined stress is as in Eq. (3.51)

$$(\sigma_c)max = \frac{\sigma_c}{2} + \frac{1}{2}\sqrt{(\sigma_c)^2 + 4\tau^2} (3.51)$$

The value of (σ_c) max should be within safe limits. If it exceeds the safe value, then the dimension 'W' may be increased because it does not affect other dimensions.

3.3.9 Design of left-hand crank web

Since the left-hand crank web was not stressed to the extent as the right-hand crank web, the dimensions for the hand crank web was be made same as theright-hand crank web.

3.3.10 Design of crankshaft bearings

The bearing 2 was the most heavily loaded and should be checked for the safe bearing pressure.

We know that the total reaction at the bearing 2 is as shown in Eq. (3.52)

$$R_2 = \frac{F_p}{2} + \frac{W}{2} + \frac{T_{1+}T_2}{2} (3.52)$$

∴ Total bearing pressure as indicated in Eq. (3.53)

$$= \frac{R_2}{l_{2\,x\,d_{S1}}} (3.53)$$

Where l_2 = length of bearing 2

3.4 TVS king three-wheeler specifications

Engine type: Four (4) stroke Air cooled single cylinder Spark Ignition (SI)

Table 3.5Specifications of TVS king tricycle engine

Displacement	199.26 cc
Maximum power	6.42 kW at 5250 rpm
Maximum torque	14.965 Nm at 3250 rpm
Bore	62 mm
Stroke	62 mm
Compression ratio	9.6:1

TVS (2021)

3.4.1 Pressure calculation

Density of petrol ($C_8\,H_{18}$), P= 750 kg/m^3 = 750 x 10^{-9} kg/mm

Operating temperature, T= 293.15 K

Mass = Density x Volume = 750 x 10^{-9} x 199.26 x 10^3 = 149.445 x 10^{-3} kg

Molecular weight of petrol, M= 114.228 x 10^{-3} kg/mole

Gas constant for petrol, R= $\frac{8314.3}{114.228\ x\ 10^{-3}}$ = 72.79 x 10^3 J/kg. mole K

Where air constant = 8314.3 J/K

From Gas law equation:

PV = MRT

$$P = \frac{MRT}{V} = \frac{149.445 \text{ x } 10^{-3} \text{ x } 72.79 \text{ x } 10^{3} \text{ x } 293.15}{199.26 \text{ x } 10^{3}} = \frac{3188915.469}{199.26 \text{ x } 10^{3}}$$

∴ P = 16.00 MPa

3.4.2 The crankshaft designed for the maximum force

The crankshaft designed for the maximum force developed in engine cylinders

∴From Eq. 3.2, the force acting on the piston (F_P) = $\frac{\pi D^2}{4}$ x P

= $\frac{\pi(62)^2}{4}$xP

→ F_P = $\frac{\pi(62)^2}{4}$ x 16 = 48305.12864 N ≈ 48.305 kN

3.4.3 The distance (b) between the bearings 1 and 2

The distance (b) between the bearings 1 and 2 was equal to twice the piston diameter

b = 2D = 2 x 62 = 124 mm

$b_1 = b_2 = \frac{b}{2} = \frac{124}{2}$ = 62 mm

Because of the piston gas load, will be two horizontal reactions H_1 and H_2 at bearings 1 and 2 respectively, such that;

As in Eq. 3.3, $H_1 = \frac{F_P \text{ x } b_1}{b}$

= $\frac{48305.129 \text{ x } 62}{124}$ = 24152.5645 N = 24.1525645 kN

From Eq. 3.4, $H_2 = \frac{F_P \text{ x } b_2}{b}$

= $\frac{48305.129 \text{ x } 62}{124}$ = 24152.5645 N = 24.1525645 kN

3.4.4 Design of crankpin

Let;

d_c = Diameter of the crankpin in mm

l_c = Length of the crankpin in mm; and

σ_b = Allowable bending stress for the crankpin. It may be assumed as 75 MPa or N/mm^2

The bending moment at the centre of the crankpin from Eq. 3.11was given as:

$M_c = H_1 \text{ x } b_2$

= 24152.5645 x 62 = 1497458.999 Nmm

It is also known from Eq. 3.12 that;

$$M_c = \frac{(\pi d_c^3)}{32}\sigma_b$$

$$= \frac{\pi d_c^3}{32} \text{x } 75 = 7.364 d_c^3 \text{ Nmm}$$

Equating the two expressions for the bending moment gives:

$$1497458.999 = 7.364 d_c^3$$

$$d_c^3 = \frac{1497458.999}{7.36} = 203348.5876 \text{ mm}$$

$$d_c = \sqrt[3]{203348.5876} = 59 \text{ mm}$$

$$\therefore d_c = 59 \text{ mm}$$

3.4.5 The length of the crankpin

The length of the crankpin (l_c) was given from Eq. 3.13 as:

$$l_c = \frac{F_p}{d_c \text{ x } p_b}$$

$$= \frac{48305.12864}{59 \text{ x } 10} = \frac{48305.12864}{590} = 81.87 \text{ mm} \approx 82 \text{ mm}$$

3.4.6 Design of left-hand crank web

i. The thickness of the crank web was given as:

$$t = 0.65d_c + 6.35 \text{ mm}$$

$$t = 0.65 \times 59 + 6.35 = 44.7 \text{ mm} \approx 45 \text{ mm}$$

ii. The width of the crank web (w) was given as:

$$w = 1.125d_c + 12.7 \text{ mm} = 1.125 \times 59 \times 12.7 \text{ mm} = 79.075 \text{ mm} \approx 79 \text{ mm}$$

3.4.7 The maximum bending

The maximum bending moment on the crank web from Eq. 3.14was given as:

$$M = H_1\left(b_2 + \frac{l_c}{2} + \frac{t}{2}\right)$$

$$M = 24152.5645\left(62 - \frac{82}{2} - \frac{45}{2}\right) = 24152.5645\ (62 - 41 - 22.5)$$

$$M = 24152.5645\ (-1.5)$$

$$M = -36228.85 \text{ Nmm (Compressive)}$$

3.4.8 Section modulus

Section modulus wasgiven from Eq. 3.15 as:

$$Z = \frac{1}{6} \times w \times t^2$$

$$Z = \frac{1}{6} \times 79 \times 45^2 = 26662.5 \text{ Nmm}^3$$

3.4.9 Bending stress

From Eq. 3.16, bending stress (σ_b) was given as:

$$\sigma_b = \frac{M}{Z}$$

$$= \frac{36228.85}{26662.5} = 1.359 \text{ N/mm}^2$$

3.4.10 The direct compressive stress on the crank web:

The direct compressive stress on the crank web from Eq. 3.17 was given as:

$$\sigma_c = \frac{H_1}{w \times t}$$

$$= \frac{24152.5645}{79 \times 45} = \frac{24152.5645}{3555} = 6.75 \text{ N/mm}^2$$

3.4.11 The total stress on the crank web

Total stress on the crank web from Eq. 3.18was given as:

$$\sigma_b + \sigma_c$$

$$= 1.359 + 6.75 = 8.109 \text{ MPa}$$

Since the total stress on the crank web is far less than the allowable bending stress of 75 MPa, the design of the left-hand crank web is therefore very safe.

3.4.12Design of right-hand crank web

From the balancing point of view, the dimensions of the right-hand crank web (thickness and width) are made equal to the dimensions of the left-hand crank web.

3.5 Stressesinduced

We know that,

$$\text{Sin } Ø = \text{Sin } \theta/(\text{L.R}) = \text{Sin } \frac{35^0}{4}$$

Which implies $Ø = 8.24^0$

We know from Eq. 3.26 that thrust in connecting rod, $F_Q = \frac{F_P}{Cos Ø}$

$$F_Q = \frac{48305.129}{Cos\ (8.24)}$$

Therefore, $F_Q = 48809.013$ N

Tangential force on the crankshaft,

As shown in Eq. 3.25, $F_T = F_Q \text{ Sin } (Ø + \theta)$

$F_T = 48809.013 \text{ Sin } (8.24 + 35)$

Therefore, $F_T = 33436.9$ N

Twisting moment, $T = F_T (0.75l_c + 0.5t)$

$T = 33436.9 (0.75 \text{ x } 82 + 0.5 \text{ x } 45$

Therefore, T = 2808699.6 N-mm

As indicated in Eq. 3.27, $H_{T1} = \frac{F_T \text{ x } b_1}{b}$

$H_{T1} = \frac{33436.9\, x 62}{124}$

Therefore, $H_{T1} = 16718.8$ N

As in Eq. 3.32, $T_C = H_{T1} \text{ x } r$

$T_C = 16718.8 \text{ x } 31$

Therefore, $T_C = 518282.8$ N-mm

From Eq. 3.31, $M_C = H_{T1} \text{x } b_2$

$M_C = 24.1525645 \text{ x } 62$

Therefore, $M_C = 1497.459$ N-mm

3.5.1 Equivalent twisting moment

From Eq. 3.36, $Te = \sqrt{(M_S)^2 + (T_S)^2}$

$T_e = \sqrt{(1497.45899)^2 + (518.2828)^2}$

Therefore, $T_e = 1584.61$ Kn-mm

If from Eq. 3.37, $Te = (\frac{\pi}{16}) \text{ x } (d_c)^3 \text{ x } \tau$

Shear stress is as indicated in Eq. (3.54)

Then, $\tau = \frac{T_{e\ x\ 16}}{\pi\ x\ d_c^3}$ (3.54)

$\tau = \frac{1584.61\ x\ 16}{3.142\ x\ 59^3}$

Therefore, theoretical shear stress τ = 0.0392898 kN-mm^2 = 39.2898 N/mm^2

3.5.2 Von-Misses stress induced in the crankpin

According to theory of distortion energy, the Von-Misses stress in the crank-pin was given as in Eq. (3.55).

$Mev = \sqrt{((K_b\ x\ M_c)^2 + \frac{3}{4}\ x\ (K_t\ x\ T_c)^2)}$ (3.55)

$M_{ev} = \sqrt{(K_b\ x\ M_c)^2 + \frac{3}{4}\ (K_t\ x\ T_c)^2}$

Where, K_b = 2 (combined shock and fatigue factor for bending)

K_t = 1.5 (shock and fatigue factor for torsion)

$M_{ev} = \sqrt{(2\ x\ 1497458.99)^2 + \frac{3}{4}\ (1.5\ x\ 518282.8)^2}$

$M_{ev} = \sqrt{8969533706927.28 + 453291290059.23}$

M_{ev} = 3069662.03 N-mm

Also, $M_{ev} = \frac{\pi}{32}\ x\ (d_c)^3\ x\ \sigma_{von}$

Therefore, $\sigma_{von} = \frac{M_{ev\ x\ 32}}{\pi\ x\ d_c^3}$

$\sigma_{von} = \frac{3069662.03\ x\ 32}{3.142\ x\ 59^3} = 152.22$

Theoretical Von-misses stress σ_{von} = 152.22 N/mm^2

3.5.3 Maximum principal stress theory

In order to determine maximum principal stress, the following Eq. (3.56) and (3.57) was used.

Maximum principal stress

$$\sigma_{max} = \frac{\sigma_x}{2} + \sqrt{(\frac{\sigma_x}{2})^2 + \tau^2} \quad (3.56)$$

$$\sigma_x = \frac{32\ x\ M}{\pi d^3} - \frac{4F_T}{\pi d^2} \quad (3.57)$$

$$\sigma_x = \frac{32\ x\ 36228.85}{3.142\ x\ 59^3} - \frac{4\ x\ 33437.6}{3.142\ x\ 59^2}$$

σ_x = 1.7966 -12.2288

σ_x = -10.4322 N/mm^2

Therefore, $\sigma_{max} = \frac{-10.4322}{2} + \sqrt{(\frac{-10.4322}{2})^2 + 39.2898^2}$

σ_{max} = -5.2161+ 39.6345

σ_{max} = 34.4184 N/mm^2

3.6 Weight of the crankshaft of forged steel

The volume of the crankshaft used is:

$$1187960 mm^3 = 0.001187960\ m^3$$

The density of forged steel is:

$$7.87\ g/cm^3 = 7.87\ x\ 10^6\ g/m^3$$

Mass (m) of forged steel crankshaft = Volume (V) of component x density (ρ) of material

$$m = V \times \rho$$

$$m = 0.001187960 \times 7.87 \times 10^6 \ m^3 \times \frac{g}{m^3}$$

$$m = 9349.2452g \approx 9.3493 \ kg$$

weight of crankshaft (w) = mass of crankshaft (m) x acceleration due to gravity (g)

$$w = mg$$

$$w = 9.3493 \times 9.81 \ kg \times \frac{m}{s^2}$$

$$w = 91.71 \ kgm/s^2 = 91.71 \ N$$

Therefore, the weight of forged steel crankshaft was 91.71 N

3.6.1 Weight of the crankshaft of mild steel

The volume of the crankshaft used is:

$$1187960mm^3 = 0.001187960 \ m^3$$

The density of mild steel is:

$$7.87 \ g/cm^3 = 7.87 \times 10^6 \ g/m^3$$

Mass (m) of mild steel crankshaft = Volume (V) of component x density (ρ) of material

$$m = V \times \rho$$

$$m = 0.001187960 \times 7.87 \times 10^6 \ m^3 \times \frac{g}{m^3}$$

$$m = 9349.2452g$$

$$= 9.3493 \ kg$$

weight of crankshaft (w) = mass of crankshaft (m) x acceleration due to gravity (g)

$$w = mg$$

$$w = 9.3493 \text{ x } 9.81 \text{ kg x } \frac{m}{s^2}$$

$$w = 91.71 \text{ kgm/s}^2 = 91.71 \text{ N}$$

Therefore, the weight of mild steel crankshaft was 91.71 N

3.6.2 Weight of the crankshaft of structural steel

The volume of the crankshaft used is:

$$1187960\text{mm}^3 = 0.001187960 \text{ m}^3$$

The density of structural steel is:

$$7.800 \text{ g/cm}^3 = 7.80 \text{ x } 10^6 \text{ g/m}^3$$

Mass (m) of structural steel crankshaft = Volume (V) of component x density (ρ) of material

$$m = V \text{ x } \rho$$

$$m = 0.001187960 \text{ x } 7.80 \text{ x } 10^6 \text{ m}^3 \text{ x } \frac{g}{m^3}$$

$$m = 9266.088\text{g}$$

$$m = 9.266088 \text{ kg}$$

weight of crankshaft (w) = mass of crankshaft (m) x acceleration due to gravity (g)

$$w = mg$$

$$w = 9.266088 \text{ x } 9.81 \text{ kg x } \frac{m}{s^2}$$

$$w = 90.90032 \text{ kgm/s}^2$$

$$w = 90.90032 \text{ N}$$

Therefore, the weight of structural steel crankshaft was 90.9003 N

3.7 Method used for the study

In this study, Autodesk Inventor 2017 suit was used for the design and modelling of the crankshaft using the following parameters as indicatedin table 3. 6. Again, the model 3-D model was imported onto the ANSYS bench for structural analysis.

Table 3.2 Parameters used for modelling TVS king tricycle crankshaft

S/No.	Symbol	Meaning	Value
1.	P	Pressure	16.00 MPa
2.	F_P	Force acting on piston	48305.12864 N
3.	b	Distance between bearings 1 & 2	124 mm
4.	H_1 & H_2	Reactions at bearings 1 & 2	24.1525645 kN
5.	M_C	Bending moment at centre of crankpin	1497458.999 Nmm
6.	d_c	Diameter of the crankpin	59 mm
7.	l_c	Length of the crankpin	81.87 mm
8.	t	Thickness of the crank web	44.7 mm
9.	w	Width of the crank web	79.075 mm
10.	M	Maximum bending moment	-36228.85 N/mm^2 (compressive)
11.	Z	Section modulus	26662.5 Nmm^3
12.	σ_b	Bending stress	1.359 N/mm^2
13.	σ_c	Direct compressive stress on crank web	6.75 N/mm^2
14.	σ_{max}	Total stress on crank web	8.109 MPa

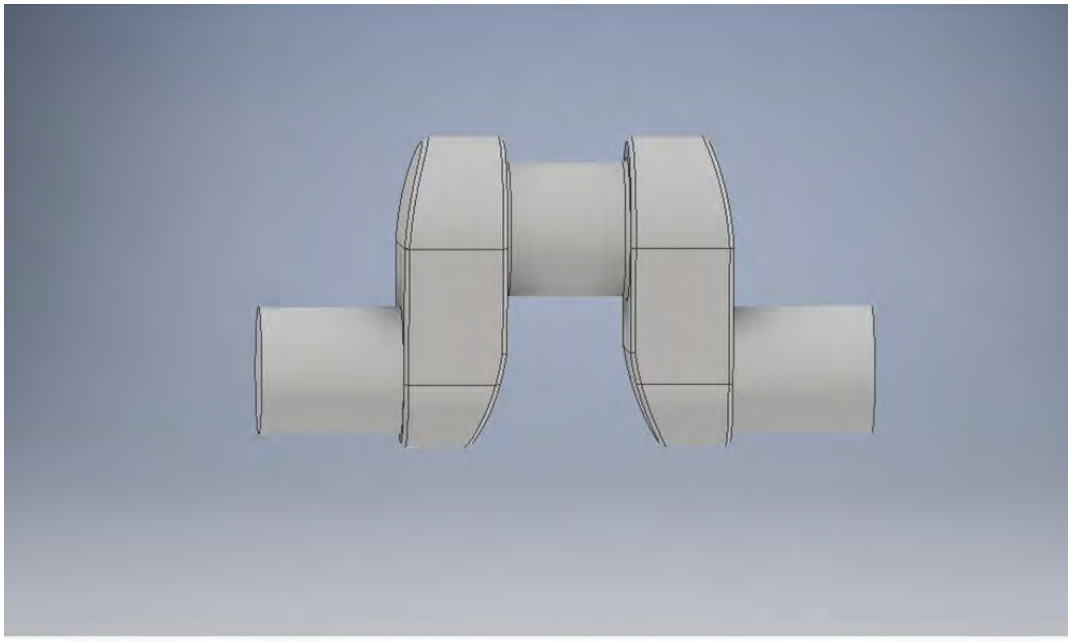

Figure 3.3Model of TVS king tricycle Crankshaft

3.7.1 Boundary conditions

In any analysis, boundary conditions play an important role. It's the boundary conditions that decide the part of the geometry which is fixed.

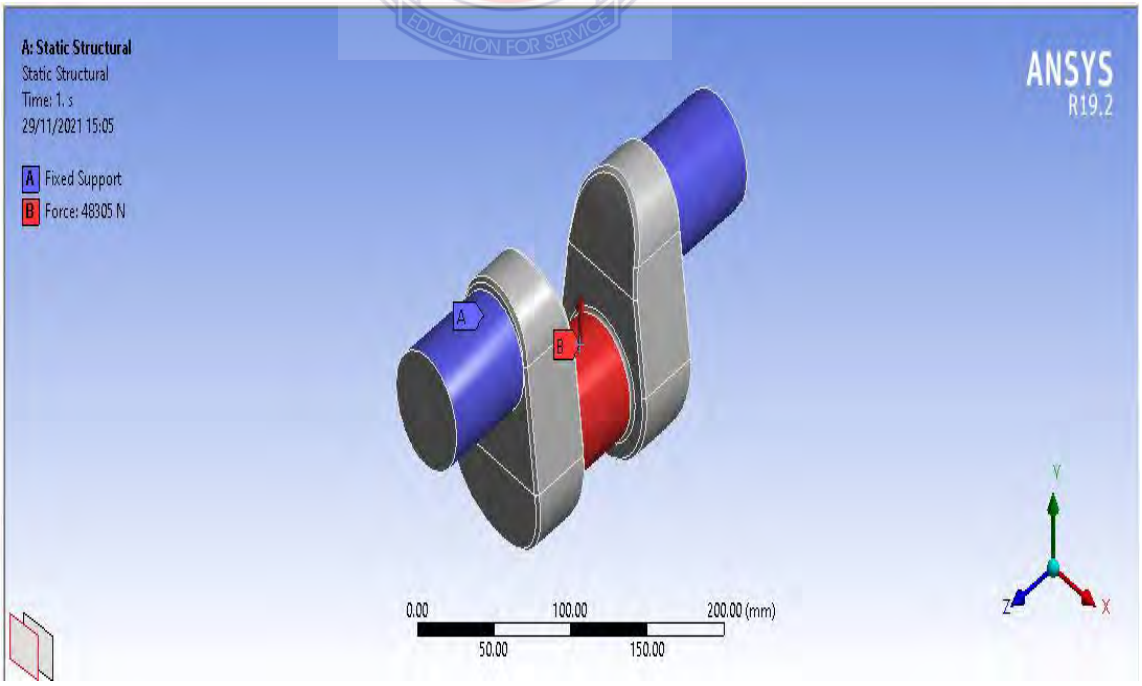

Figure 3.4 Boundary Condition of TVS king tricycle crankshaft

3.7.2 Meshing

In finite element analysis, the structure was divided into finite number of elements. These elements are then analysed independently for stresses and deformation. The first step of finite element analysis was meshing.

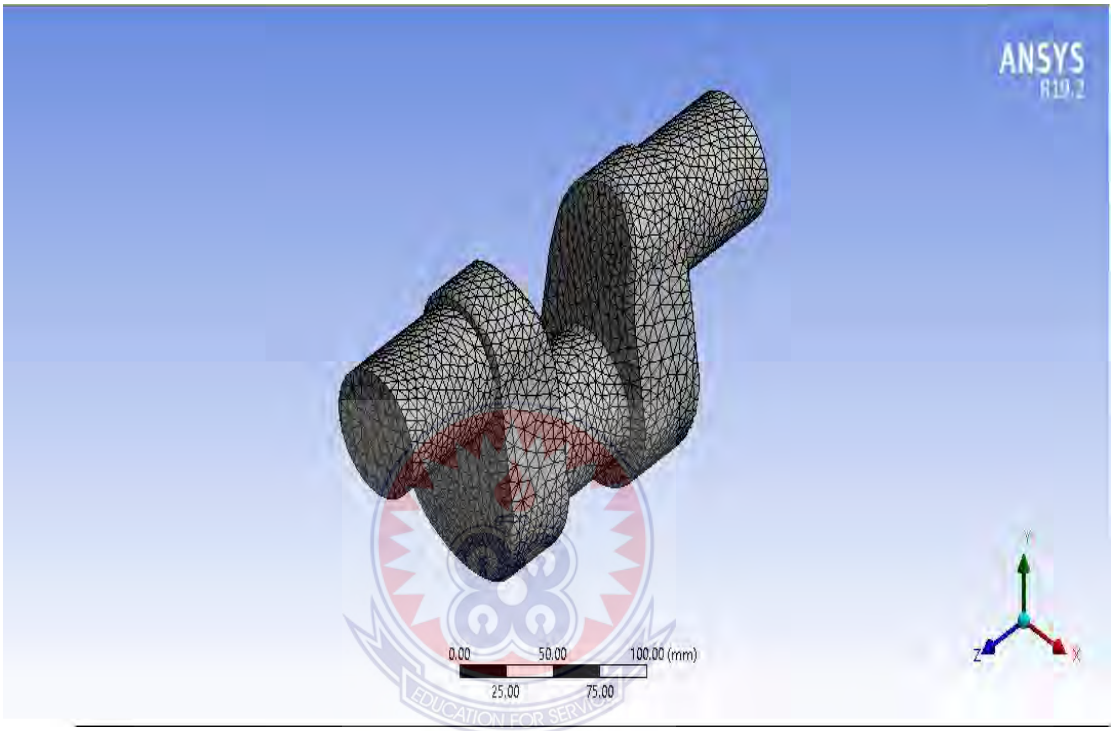

Figure 3.5 Component Meshed with ANSYS

In the process of meshing, the structure of the crankshaft was divided into a finite number of tetrahedrons which will be analysed individually for deformation at different frequencies of a given frequency range. the structure of the crankshaft was divided into 21324 elements and 34951 nodes. The mesh influences the accuracy, convergence and speed of the simulation. If meshing is precise, then the results are also expected to be practicable.

3.7.3 Grid Independent Test

The size of the mesh for the crankshaft was cautiously chosen, having in mind the influence of mesh size to the validity of the results. Free test for five (5) iterations

were conducted with mesh sizes 1 mm, 2 mm, 3 mm 4 mm and 5 mm and the best iteration number which is 3mm was selected as the mesh size.

Table 3.3 Grid Independent Test Results

MESH SIZE	*NUMBER OF NODES*	*VON-MISES*
5 mm	21450	429.72 MPa
4mm	22321	420.67 MPa
3 mm	22510	378.75 MPa
2 mm	31835	378.75 MPa
1 mm	34624	378.75 MPa

CHAPTER FOUR

RESULTS AND DISCUSSION

4.1 Introduction

This chapter presents analysis of results and discussion for the study includingdeformation, equivalent elastic strainand stress of the materials.

4.2 Results of Static Structural Analysis

The following result was in terms of load applied on the crankpin of a TVS king tricycle crankshaft. The results were presented based on three (3) materials, the materials used for construction of TVS king tricycle crankshaft (Forged steel and Mild steel) which are the controlled materials, and Structural steel the implementing material.

4.2.1Total Deformation

When a load of 48305.13 N from Eq. 3.2 as calculated in page 33 was imposed on the forged steel crankshaft for TVS king tricycle (Pragya), it was observed that, the maximum deformation of 0.0079249 mm occurred at the lower centre portion of the crankpin, whiles the minimum deformation of 0.00088054 mm was recorded at the main journal of crankshaft.Total Deformation Observed in Crankshaft Made of Forged Steel is shown in Fig. 4.1.

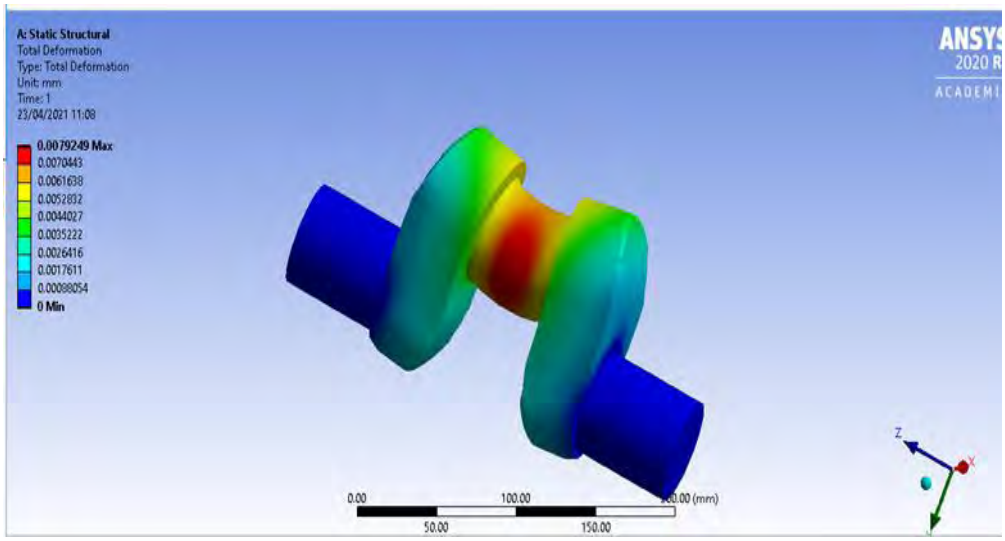

Figure 4.1 Total Deformation of Forged Steel Crankshaft for TVS

As shown in Fig. 4.2, when the same load was imposed on mild steel crankshaft for TVS king tricycle (Pragya), it was discovered that, the maximum deformation of 0.0085204 mm took place at the lower centre portion of the crankpin, whiles the minimum deformation of 0.00094671 mm was noticed at the main journal of the crankshaft.

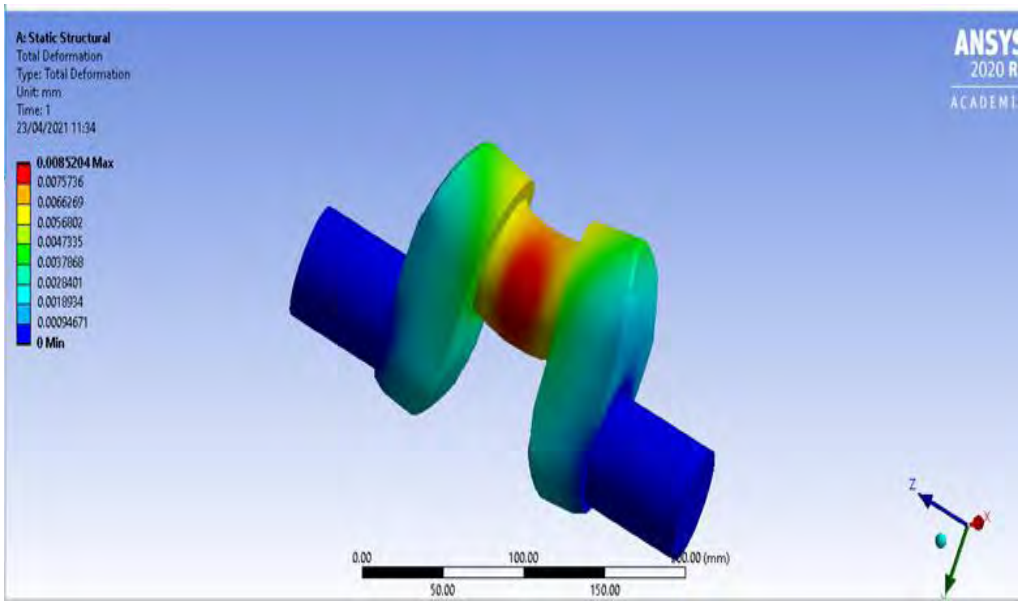

Figure 4.2 Total Deformation of Mild Steel Crankshaft for TVS

A load of 48305.13 N was obtruded on the structural steel crankshaft for TVS king tricycle (Pragya), it was noticed that, the minimum deformation of 0.000973 mm occurred at the crankshaft main journal, whereas the maximum deformation 0.008757 mm was observed at the lower centre portion of the crankpin which received the load. Total Deformation of Structural Steel Crankshaft for TVS is shown in Fig. 4.3.

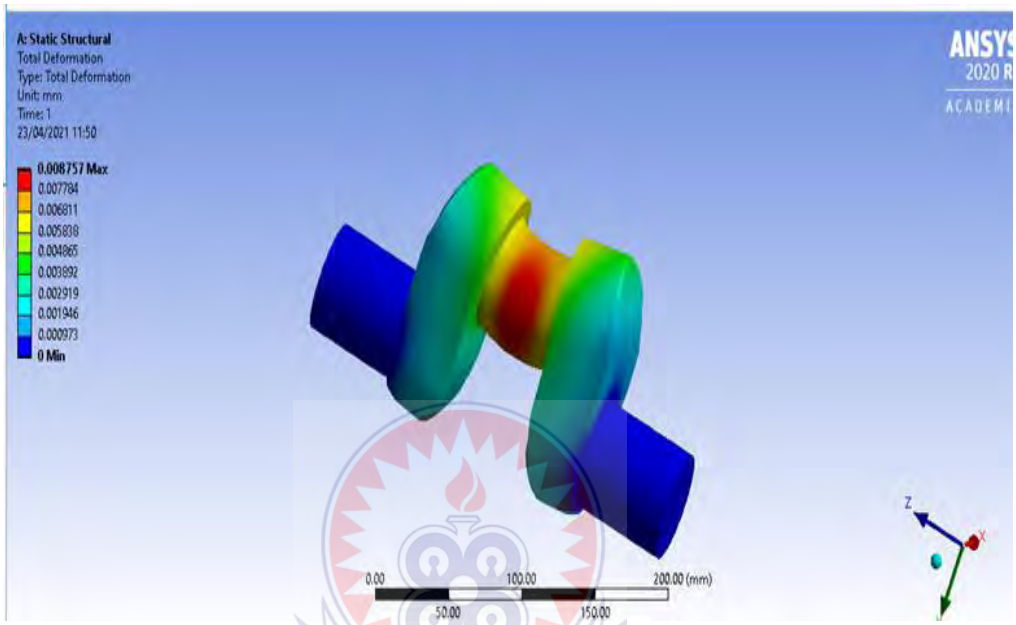

Figure 4.3 Total Deformation of Structural Steel Crankshaft for TVS

4.2.2 Directional Deformation

As indicated in Fig. 4.4, with a load of 48305.13 N applied on the crankpin of TVS king tricycle crankshaft made of forged steel, it was observed that a maximum directional deformation of 0.000063254 mm occurred at lower portion of the crankpin, whiles a minimum directional deformation of -0.00074287 mm was noted at the centre of the crankpin.

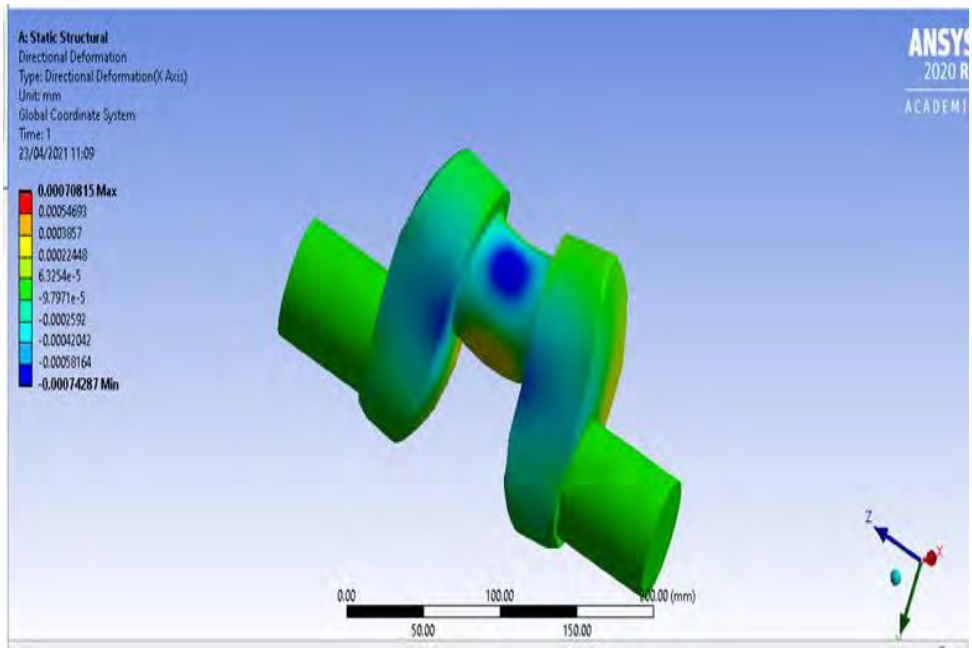

Figure 4.4 Directional Deformation of Forged Steel Crankshaft for TVS

When a load of 48305.13 N was imposed on mild steel crankshaft for TVS tricycle, it was discovered that, a maximum directional deformation of 0.00006631 mm took place at the lower portion of the crankpin and some portions of the crank web, whereas a minimum directional deformation of -0.00077953 mm was recorded at the middle portion of the crankpin. The directional deformation diagram for Mild Steel Crankshaft is indicated in Fig. 4.5.

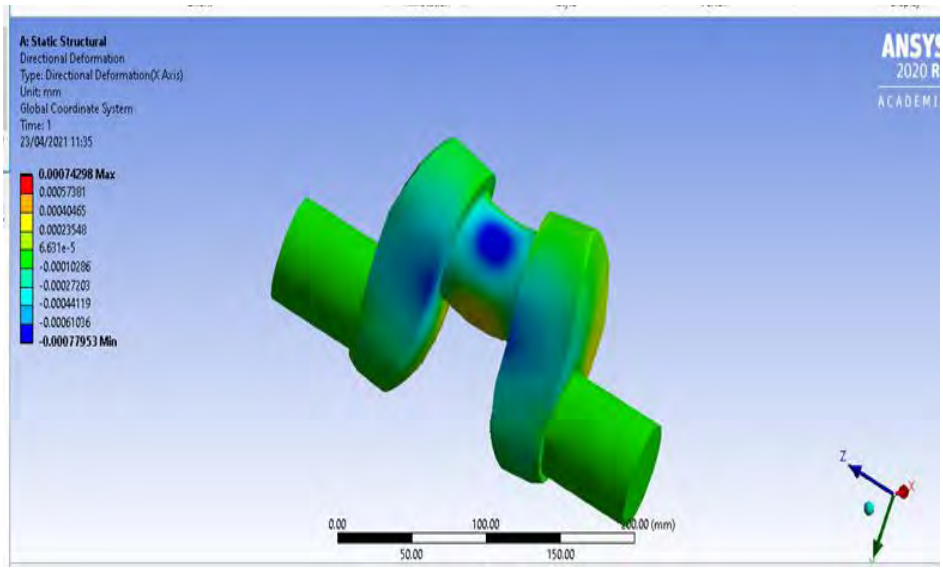

Figure 4.5 Directional Deformation of Mild Steel Crankshaft for TVS

Fig. 4.6 shows the directional deformation of crankshaft made of Structural Steel. As a structural steel crankshaft for TVS king tricycle was subjected to load of 48305.13 N on the crankpin, it was realised that, a maximum directional deformation of 0.000069895 mm took place at the lower portion of the crankpin, whilst a minimum directional deformation of -0.00082087 mm occurred at the centre of the crankpin.

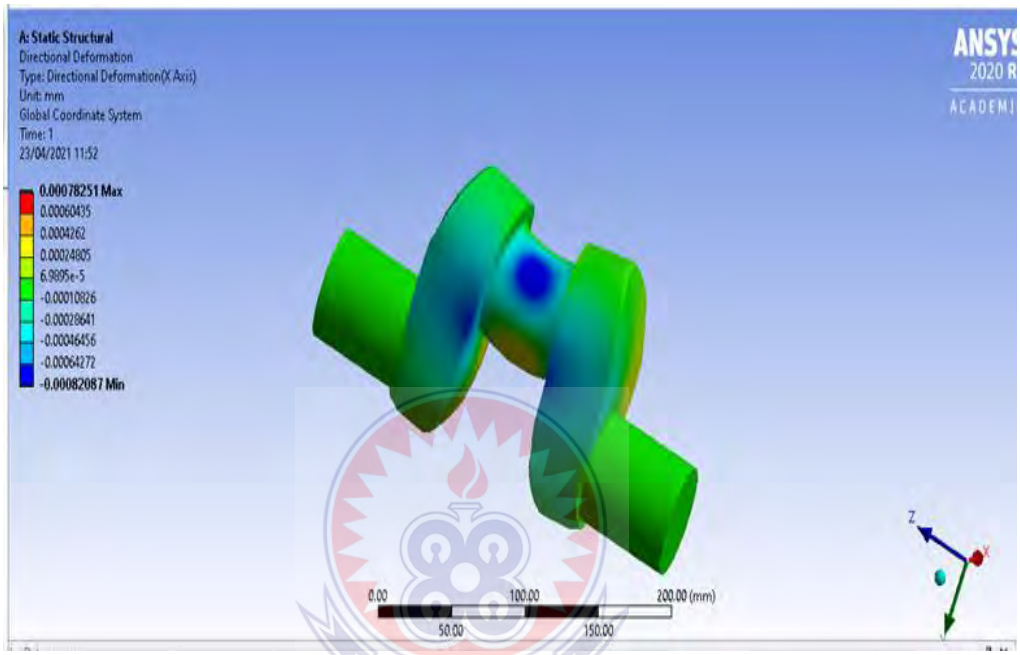

Figure 4.6 Directional Deformation of Structural Steel Crankshaft for TVS

It is known that total deformation is a summation of all deformations under study. It was observed from Figures of maximum directional and total deformation of forged steel, one of the materials used for producing crankshaft of TVS king tricycles which recorded 0.00070815 mm and 0.0079249 mm.This material appeared to be the material with lowest deformation among the group of materials adopted for the study. Mild Steel was next in the hierarchy with a maximum directional deformation of 0.00074298 mm and a total deformation of 0.0085204 mm been the second highest. Structural steel which was the implementing material for the study recorded a maximum directional deformation of 0.0007825 mm and a total deformation of

0.008757 mm as the material with highest deformation among the group of materials used for the study. Ultimately, since the yield starts for most steels at approximately 0.2% elongation, all the three crankshafts on the study were found to have deformed within the acceptable limits, and as such all the materials are fit for purpose. It was also observed that, for both controlled and implementing materials, the deformation was concentrated at the centre of the crankpin.

4.2.3 Equivalent Elastic Strain

With a load of 48305.13 N exerted on the crankpin of a TVS king tricycle crankshaft made of forged steel, it was noted that, a maximum equivalent elastic strain of 0.000083416 took place at the centre of the crankpin and between the crank web and the main journal, whereas a minimum equivalent elastic strain of 0.00000017296 was recorded at the ends of the main journals and at the top portion of the crank web. The equivalent elastic strain for forged steel crankshaft for TVS is shown in Fig. 4.7.

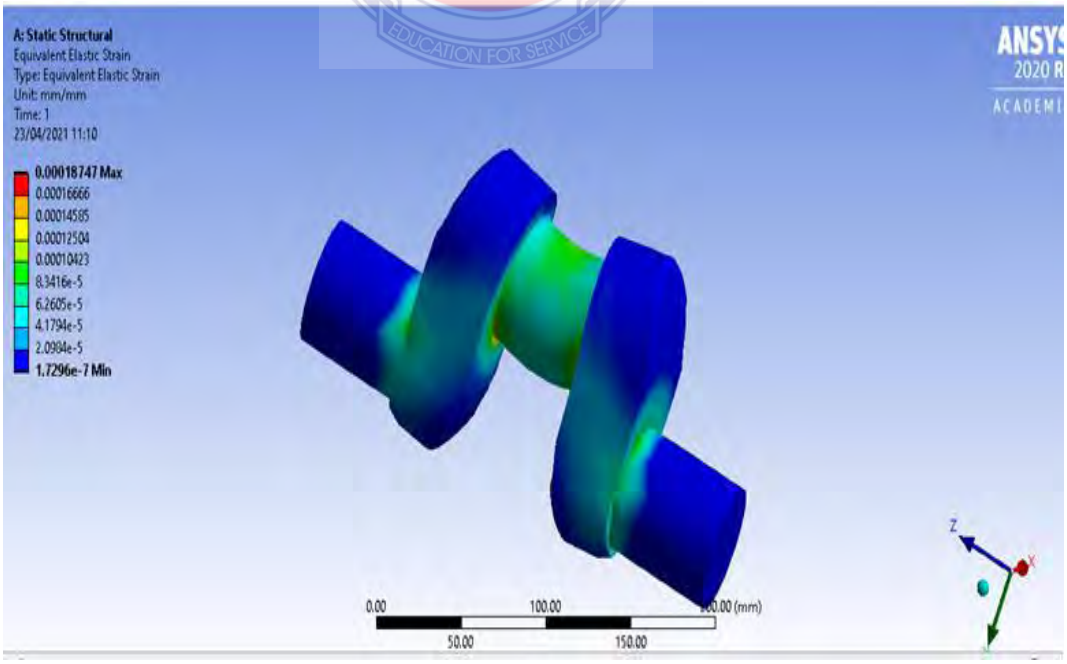

Figure 4.7 Equivalent Elastic Strain of Forged Steel Crankshaft for TVS

As shown in Fig. 4.8, when a load of 48308.13 N was imposed on mild steel crankshaft for a TVS king tricycle, it was realised that a maximum equivalent elastic strain of 0.000090069 occurred at the middle portion of the crankpin and also at the joint between the crank web and the main journal. A minimum equivalent elastic strain of 0.00000020587 was discovered at the ends of the main journals and the upper part of the crank web.

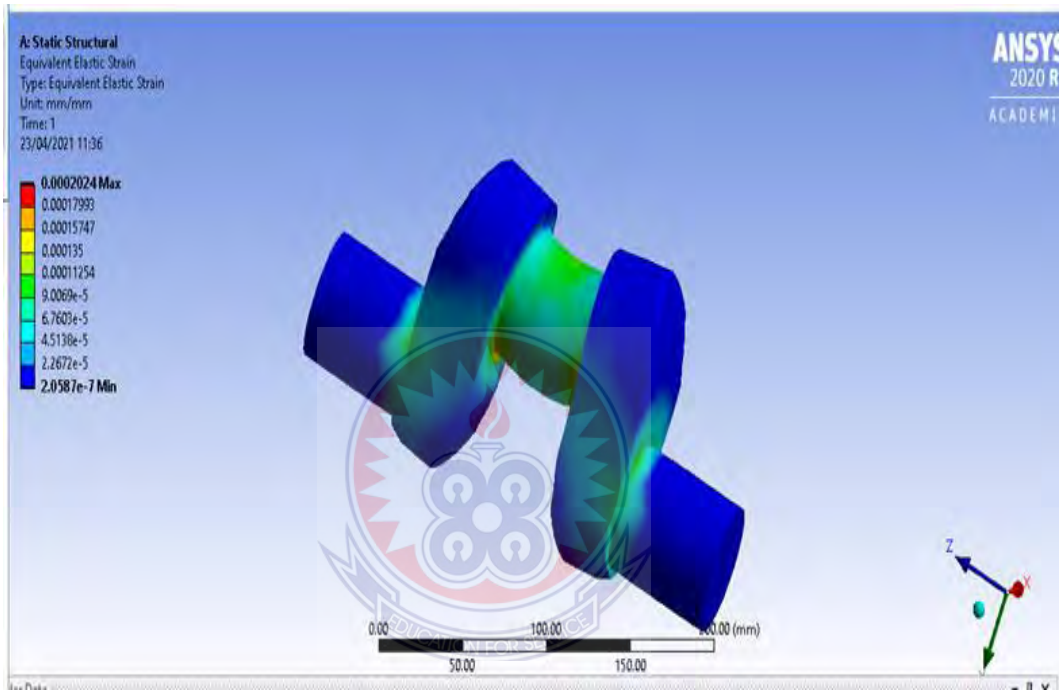

Figure 4.8 Equivalent Elastic Strain of Mild Steel Crankshaft for TVS

A load of 48305.13 N was placed on a structural steel crankshaft for TVS king tricycle. From Fig. 4.9, it was observed that a maximum equivalent elastic strain of 0.0000921714 occurred at the mid-point of the crankpin and also at the meeting point of the main journals and crank webs. Based on the same load, a minimum equivalent elastic strain of 0.00000019112 was discovered at the upper ends of the crank webs and the ends of the main journals of the crankshaft.

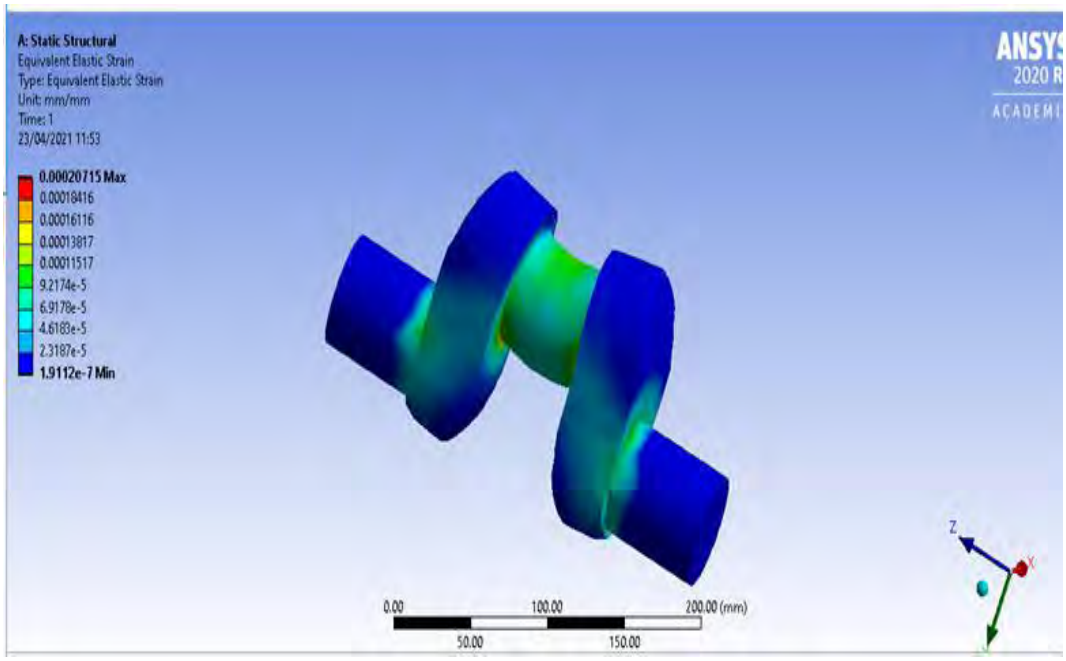

Figure 4.9 Equivalent Elastic Strain of Structural Steel Crankshaft for TVS

From the Figures for all three materials for the study, it is observed that forged steel one of the controlled materials recorded the lowest maximum strain of 0.00018747 MPa representing, followed by mild steel which recorded a maximum strain of 0.0002024 MPa representing, and finally, structural steel the implementing material of the study recorded a maximum strain of 0.00020715 MPa representing 35%. It's observed that equivalent elastic strain of both controlled and implementing materials was below the compressive strength of the materials used on the study, hence the materials can be considered as fit for purpose.

4.2.4 Von-Misses Stress

From Fig. 4.10 when a load of 48305.13 N was imposed on a TVS king tricycle crankshaft made of forged steel, a maximum equivalent Von-Mises stress of 20.867 MPa occurred at the centre of the crankpin and at the lower part of the joint between the crankpin and the crank webs, whilst a minimum equivalent Von-Mises stress of 0.030536 MPa was observed at ends of the main journals and the upper ends of the crank webs.

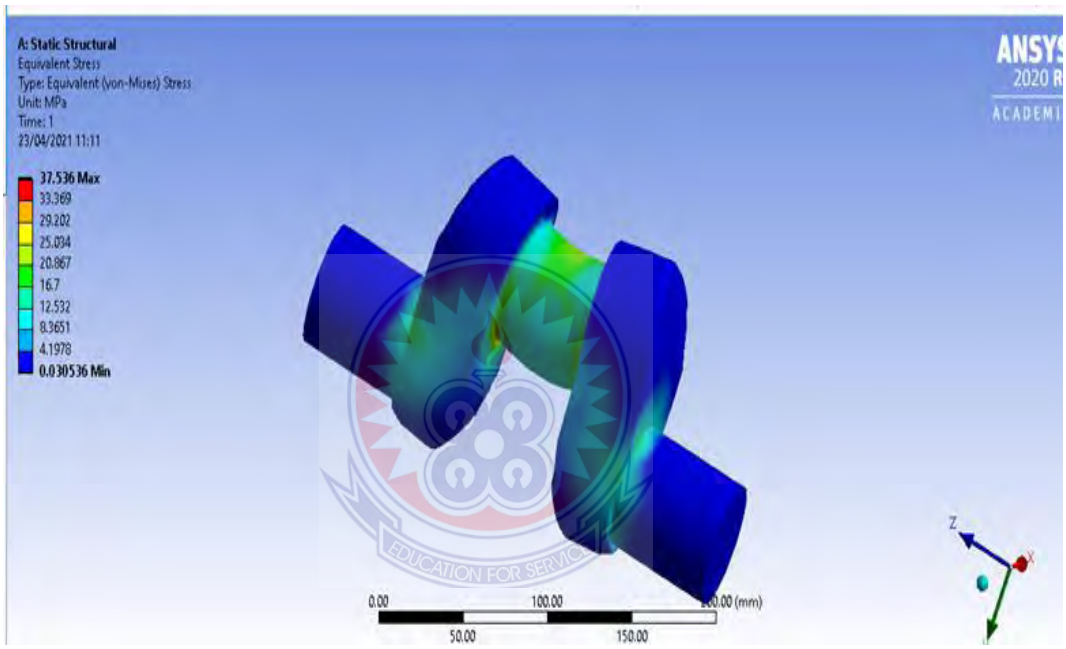

Figure 4.10 Equivalent Von-Mises Stress of Forged Steel Crankshaft for TVS

As indicated in Fig. 4.11, a maximum equivalent Von-Mises Stress of 20.897 MPa was realised at the middle portion of a TVS king tricycle crankshaft made of mild steel, when a load of 48305.13 N was exerted on the crankshaft. Also, a minimum equivalent Von-Mises stress of 0.035622 MPa took place at the main journal ends and the upper portion of the crank webs.

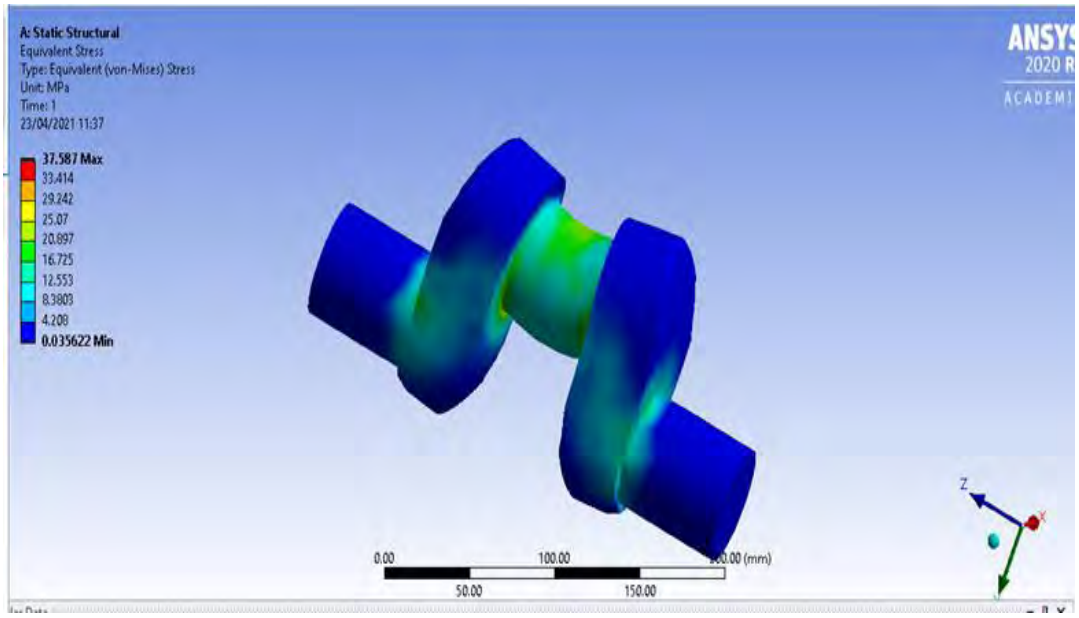

Figure 4.11 Equivalent Von-Mises Stress of Mild Steel Crankshaft for TVS

As shown in Fig. 4.12, with a load of 48305.13 N placed on TVS king tricycle crankshaft made of structural steel, it was discovered that a maximum equivalent Von-Mises Stress of 20.867 MPa occurred at the mid-point of the crankpin and the lower sections of the joints between the crank webs and the crankpin. A minimum equivalent Von-Mises Stress of 0.030536 MPa was also noticed at the ends of the main journals and the upper sections of the crank webs.

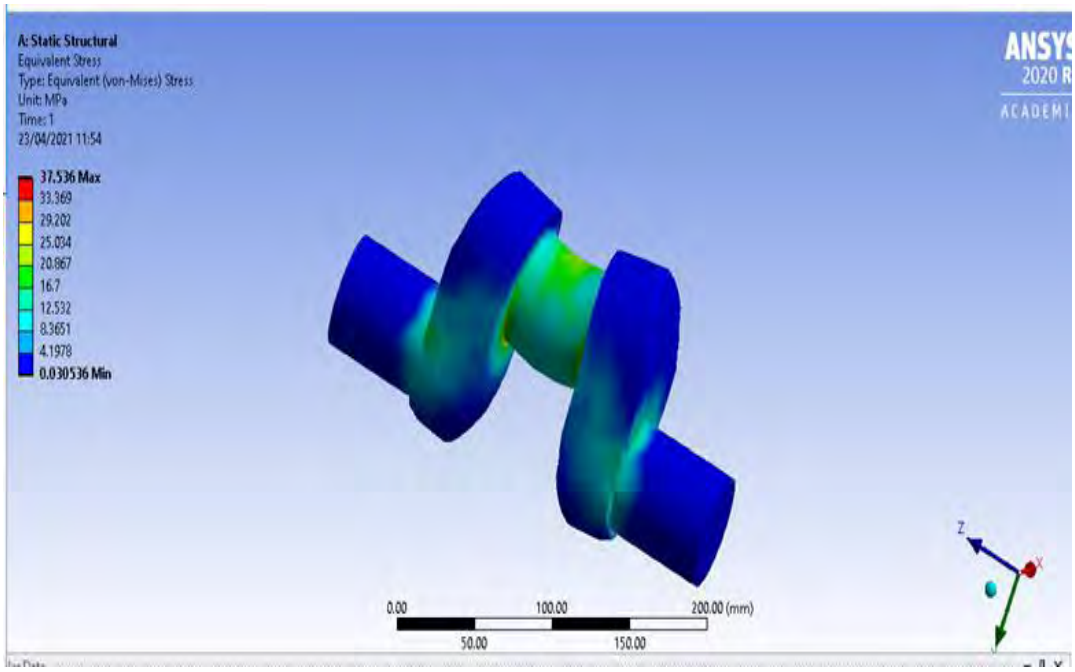

Figure 4.12 Equivalent Von-Mises Stress of Structural Steel Crankshaft for TVS

From Figures of equivalent von-mises stress for materials used for the study, it was observed that, Mild steel one of the controlled materials for the study recorded the highest stress of 37.567 MPa, while forged steel the other controlled material and structural steel the implementing material both recorded 37.536 MPa. The yield stress of the various materials used for the study ranges from 250 MPa to 625 MPa. Juxtaposing the Von-Mises recorded values to the yield stress of the materials indicates that the materials can withstand any load imposed on them by the TVS king tricycle engine. This further confirmed that all three materials were fit for purpose.

4.2.5 Maximum Principal Stress

From Fig. 4.13, when a load of 48305.13 N was exerted on a TVS ding tricycle crankshaft made of forged steel, it was noticed that a maximum of the maximum principal stress of 12.498 MPa was observed at the lower section of the crankpin. A

minimum of the maximum principal stress of -3.6458 MPa was recorded at the ends of the main journals of the crankshaft.

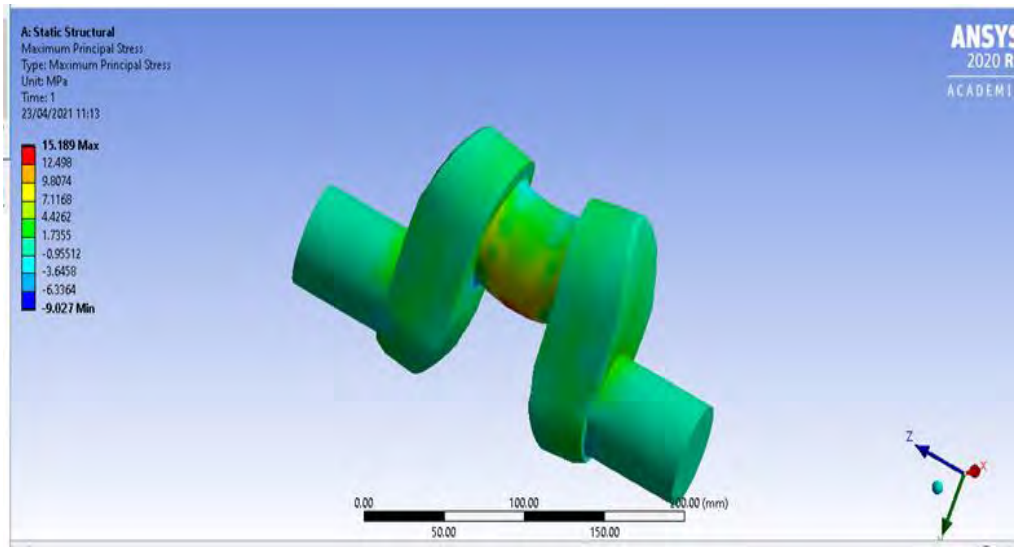

Figure 4.13 Maximum Principal Stress of forged steel crankshaft for TVS

During a static structural analysis of a TVS king tricycle crankshaft made of mild steel, it was noticed that, a maximum of the maximum principal stress of 12.599 MPa occurred at the lower portion of the crankpin when a load of 48305.13 N was imposed on the crankshaft. Under the same load, a minimum of the maximum principal stress of -3.343 MPa was observed at the main journals. This is shown in Fig. 4.14.

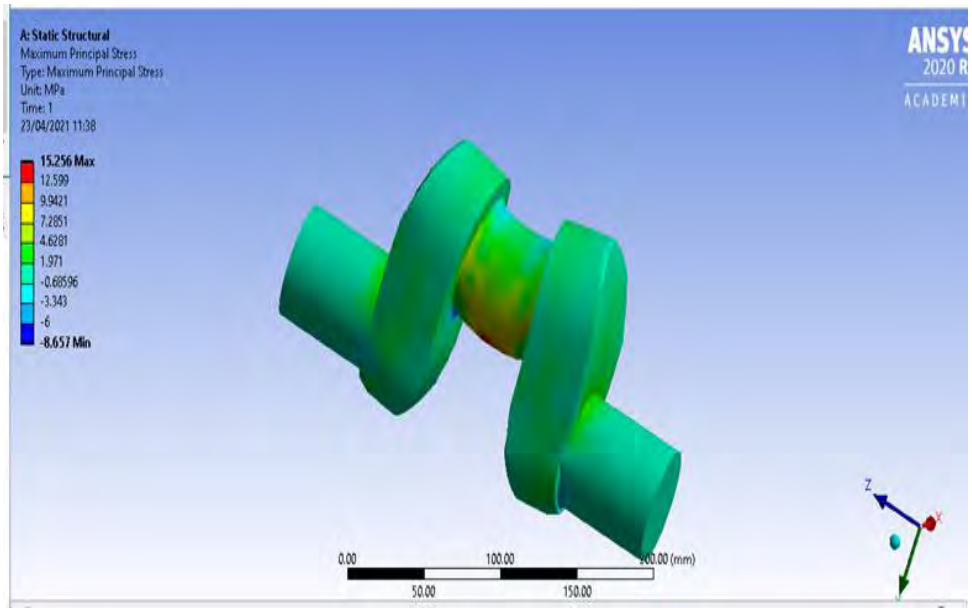

Figure 4.14 Maximum Principal Stress of Mild Steel Crankshaft for TV

With a load of 48305.13 N placed on a TVS king tricycle crankshaft made of structural steel for static structural analysis, it was observed that a maximum of the maximum principal stress of 12.498 MPa was noticed at the lower part of the crankpin. With the same load in place, a minimum of the maximum principal stress of -3.6458 MPa was realised at the main journals of the crankshaft. This is indicated in Fig. 4.15.

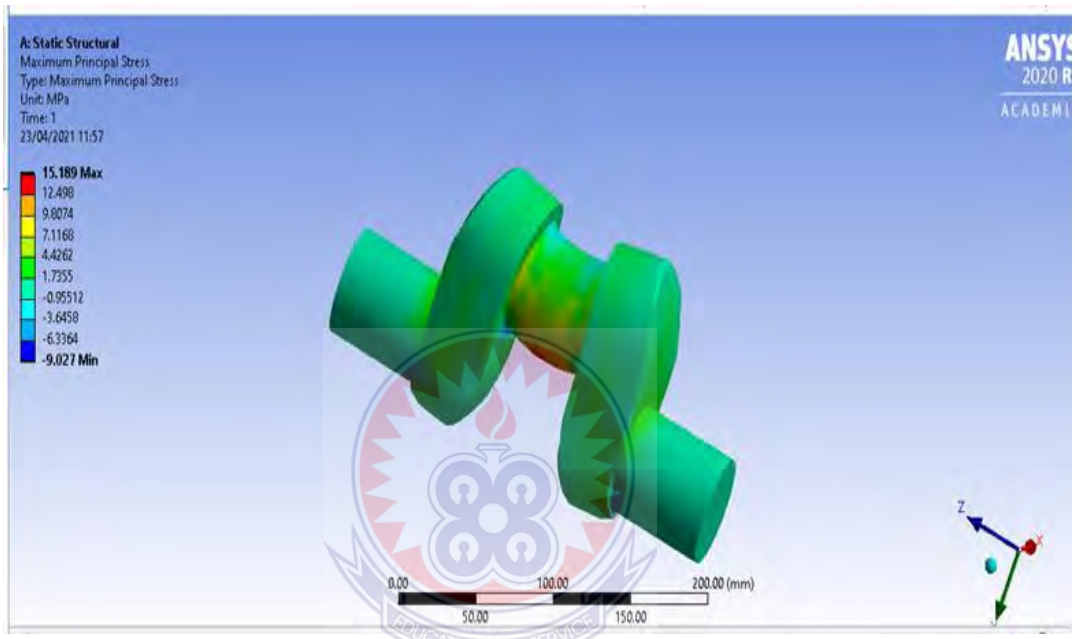

Figure 4.15 Maximum Principal Stress of Structural Steel Crankshaft for TVS

4.2.6 inimum Principal Stress

From Fig. 4.16, a maximum of the minimum principal stress of 1.2373 MPa was observed at the ends of the main journal and the upper ends of the crank webs when a load of 48305.13 N was imposed on the crankshaft. With the same load in place, a minimum of the minimum principal stress of -25.108 MPa was noticed at the tip centre of the crankpin and the lower portion of the joint between the crankpin and the crank webs.

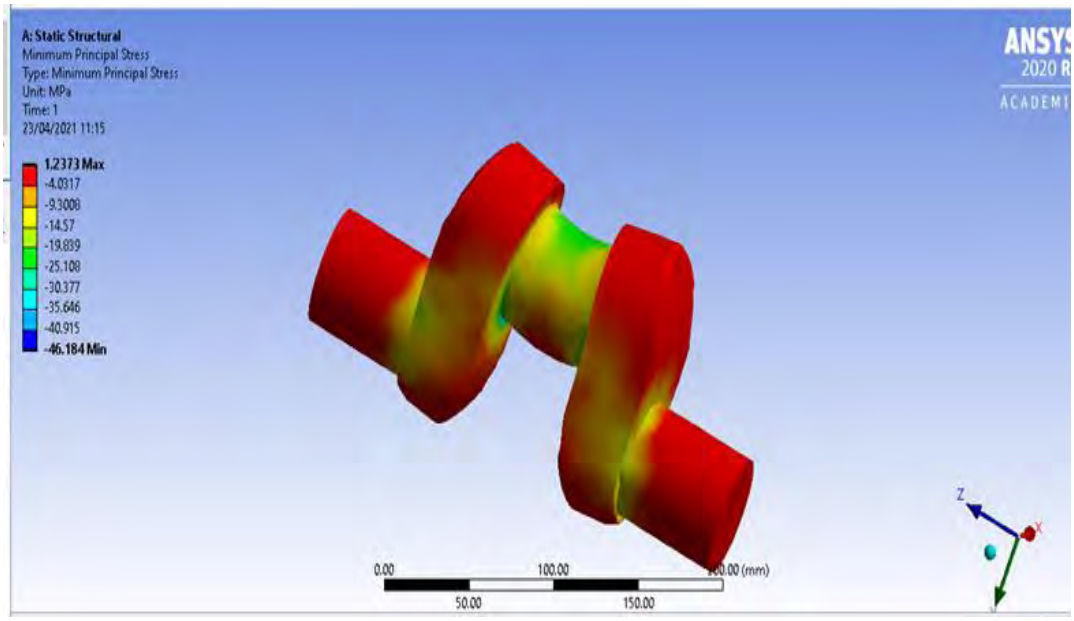

Figure 4.16 Minimum Principal Stress of Forged Steel Crankshaft for TVS

As shown in Fig. 4.17, when a load of 48305.13 N was exerted on a TVS king tricycle crankshaft made of mild steel, it was discovered that a maximum of the minimum principal stress of 1.0995 MPa occurred at the ends of the main journals and at the upper ends of the crank webs. With the same load imposed, a minimum of the minimum principal stress of -25.006 MPa was observed at the middle portion of the crankpin and the lower section of the joint between the crankpin and crank webs of the crankshaft.

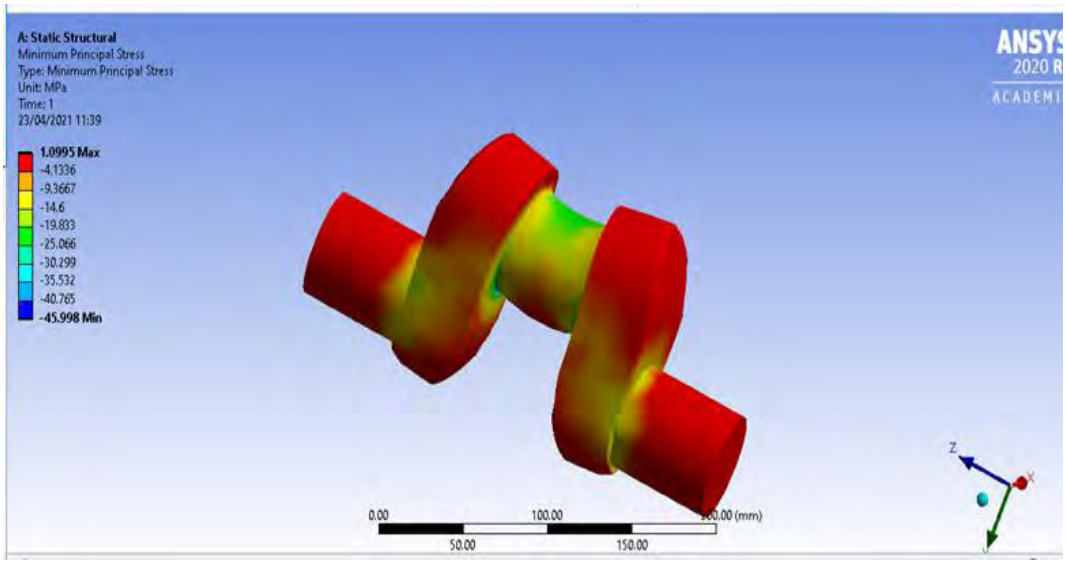

Figure 4.17 Minimum Principal Stress of Mild Steel Crankshaft for TVS

From Fig. 4.18, during a static structural analysis of a TVS king tricycle crankshaft made of structural steel, it was observed that a maximum of the minimum principal stress of 1.2373 MPa took place at the ends of the crank webs and at the ends of the main journals of the crankshaft when a load of 48305.13 N was placed on the crankshaft. Under the same load, it was realised that a minimum of the minimum principal stress of -25.108 MPa was recorded at the joints between the crankpin and the main journals of the crankshaft.

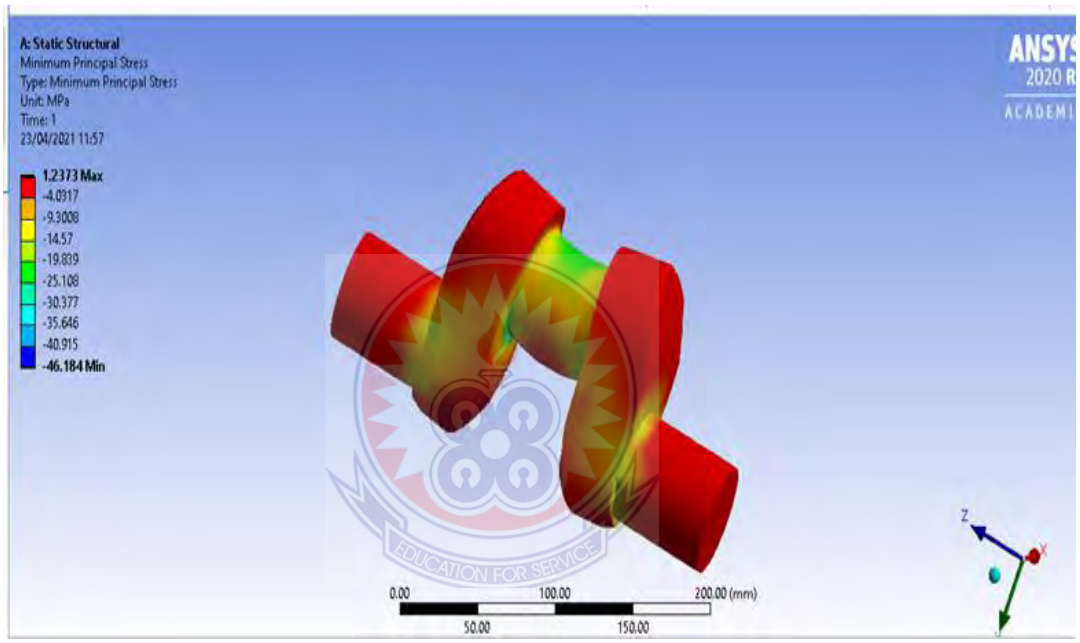

Figure 4.18 Minimum Principal Stress of Structural Steel Crankshaft for TVS

Observing from Figures of maximum principal stress and minimum principal stress for all three materials for the study, it is realised that mild steel, one of the controlled materials on the study recorded the highest maximum principal stress of 15.256 MPa, whereas forged steel, the other controlled material and structural steel the implementing material both recorded 15.189 MPa. Maximum principal stress theory asserts that, yielding occurs when the largest principal stress equals the yield strength. Since the principal stresses are far below the yield strength of both the controlled

material and the implementing materials, it was concluded that all the materials can be used to produce crankshafts for TVS king tricycle (Pragya).

4.2.6 Maximum Shear Stress

From Fig. 4.19, it was observed during a static structural analysis of a TVS king tricycle crankshaft made of forged steel that, a maximum shear stress of 12.971 MPa was noticed at the centre of the crankpin and at the lower portion of the joint between the crankpin and the crank webs when a load of 48305.13 N was imposed on the crankshaft. Maintaining the same load on the crankshaft, a minimum shear stress of 0.019187 MPa was recorded at the main journals of the crankshaft.

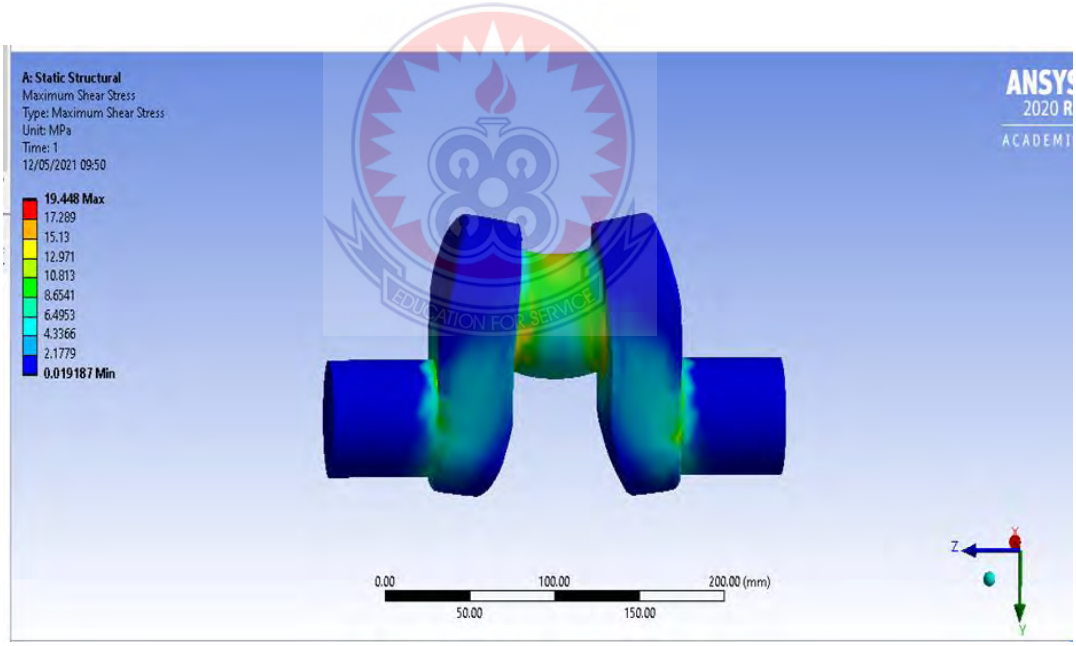

Figure 4.19 Maximum Shear Stress of Forged Steel Crankshaft for TVS

When a load of 48305.13 N was placed on a TVS king tricycle crankshaft made of mild steel, it was observed that a maximum shear stress of 12.971 MPa occurred at the centre of the crankpin and the lower part of the joint between the crankpin and the

crank webs. With same on the crankshaft, a minimum shear stress of 0.019787 MPa was noticed at the main journals of the crankshaft. This is shown in Fig. 4.20.

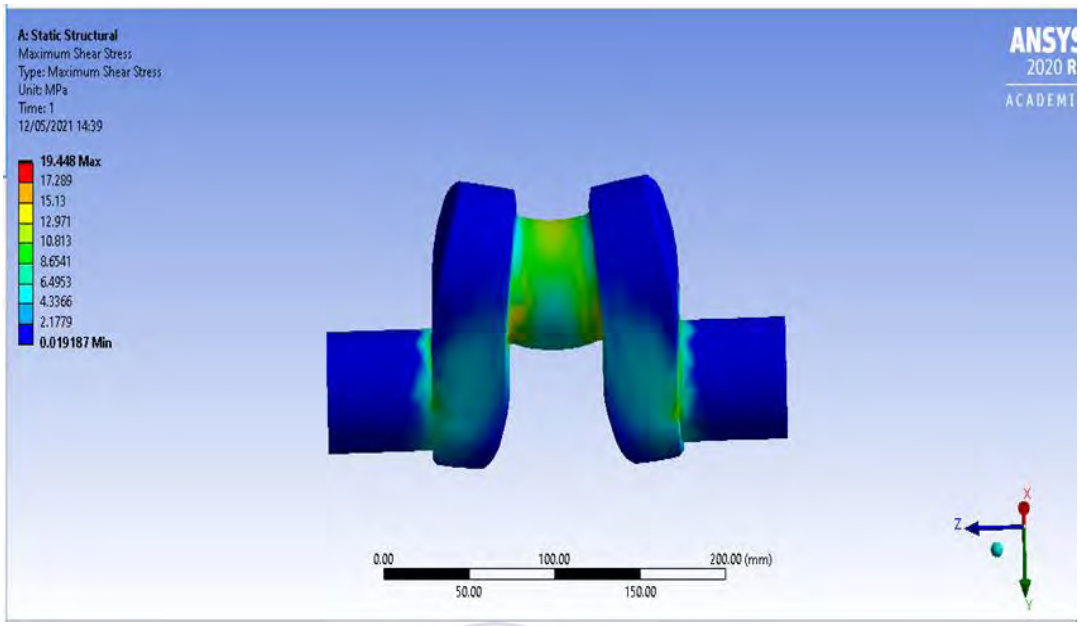

Figure 4.20 Maximum Shear Stress of Mild Steel Crankshaft for TVS

A maximum shear stress of 12.971 MPa was realised at the middle portion of TVS king tricycle crankshaft made of structural steel, and the lower portion of the joint between the crankpin and crank webs when a load of 48305.13 N was imposed on the crankshaft. With the same load maintained, a minimum shear stress of 0.019187 MPa was discovered at the ends of the main journals. Fig. 4.21 shows maximum shear stress of crankshaft made of structural steel.

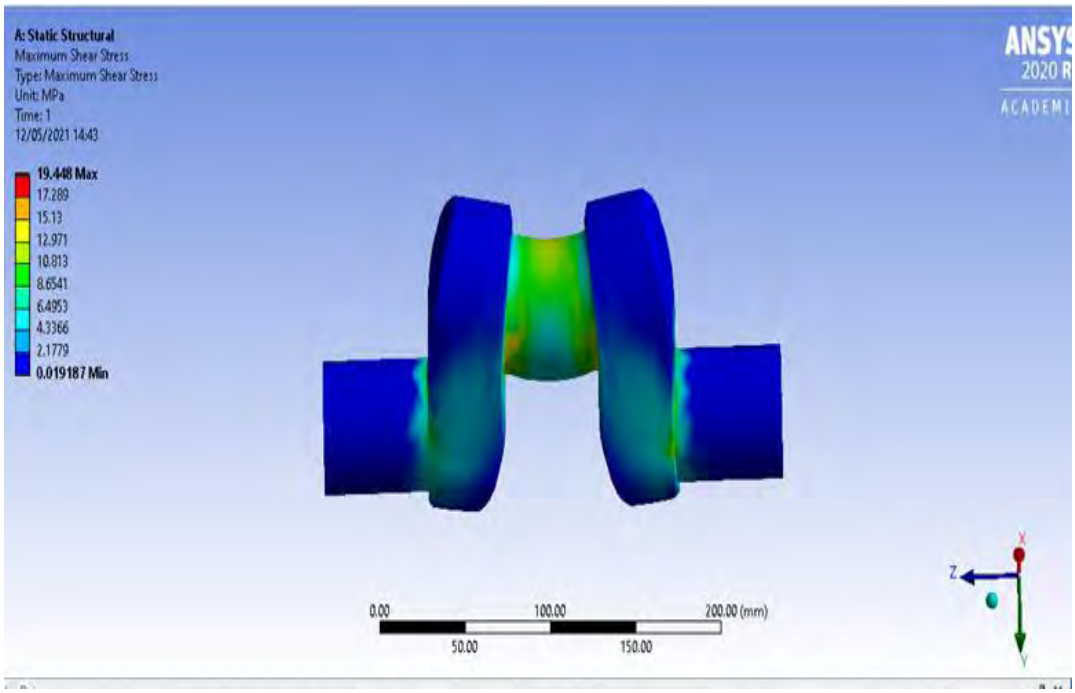

Figure 4.21 Maximum Shear Stress of Structural Steel Crankshaft for TVS

From Fig. 4.21, it can be seen that both controlled materials (Forged steel and Mild steel) and the implementing material (Structural steel) had the same maximum shear stress of 19.448 MPa. The FEA value as compared the yield stress of the controlled and implementing material further confirmed that all the materials could be used to produce crankshafts for TVS king tricycle (Pragya).

4.2.8 Factor of Safety

During a static structural analysis, a load of 48305.13 N was imposed on TVS king tricycle crankshaft made of forged steel. The crankshaft recorded 15 as its maximum factor of safety. This indicated in Fig. 4.22.

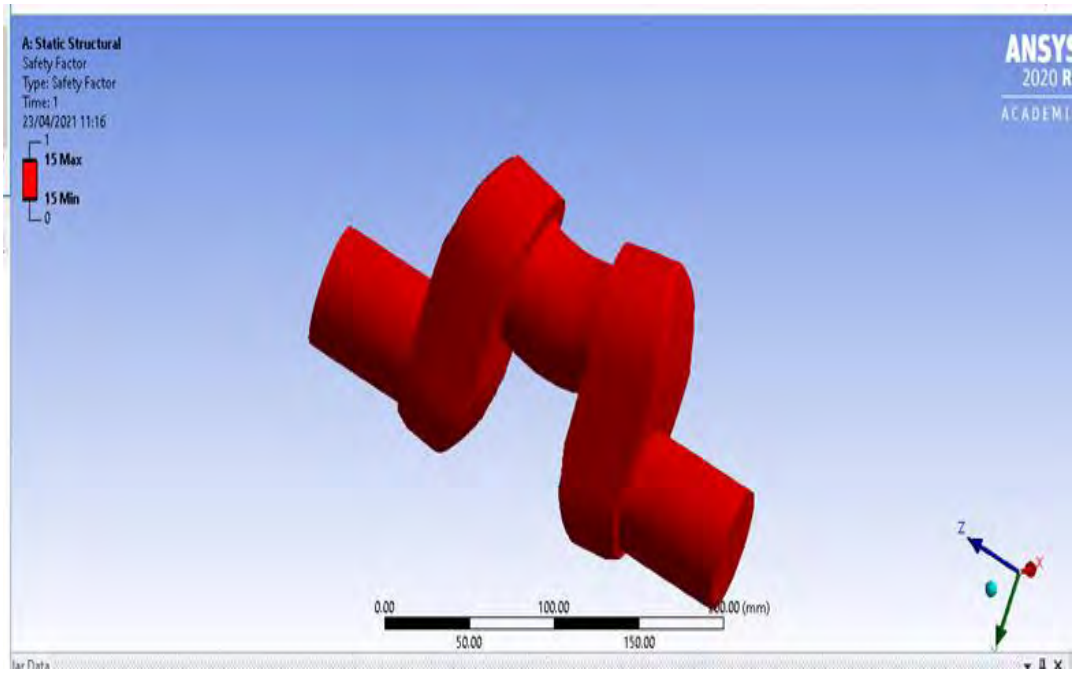

Figure 4.22 Factor of Safety of Forged Steel Crankshaft used for TVS

From Fig. 4.23, when a load of 48305.13 N was exerted on TVS king tricycle crankshaft made of mild steel, 15 was discovered as the maximum factor of safety.

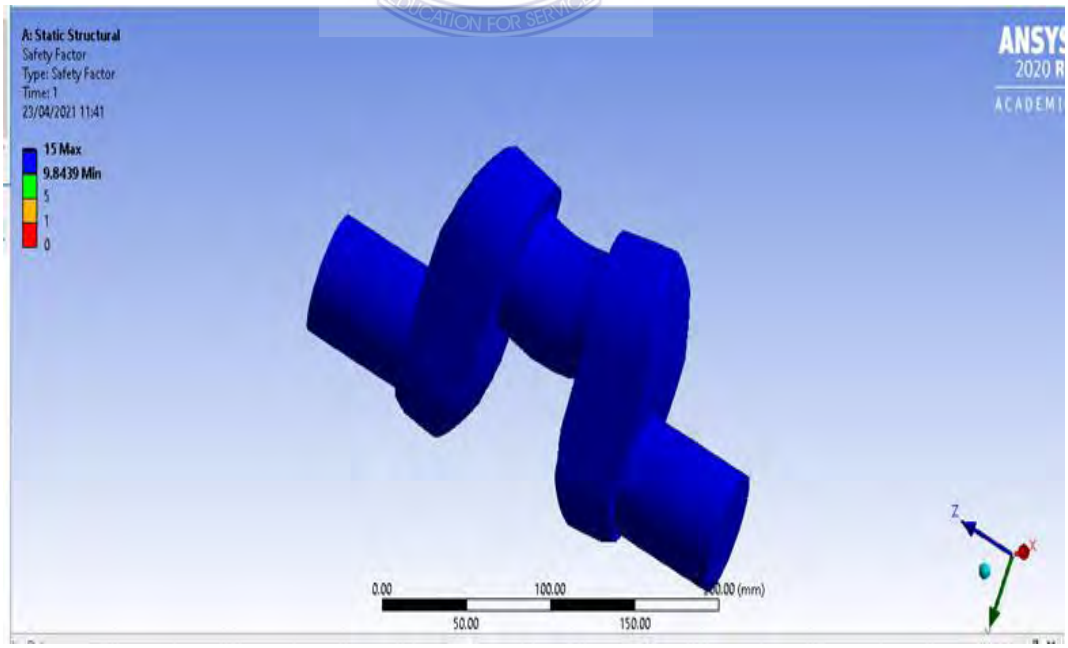

Figure 4.23 Factor of Safety of Mild Steel Crankshaft used for TVS

From Fig. 4.24, a factor of safety of 15 was realised when a load of 48305.13 N was placed on TVS king tricycle crankshaft made of structural steel.

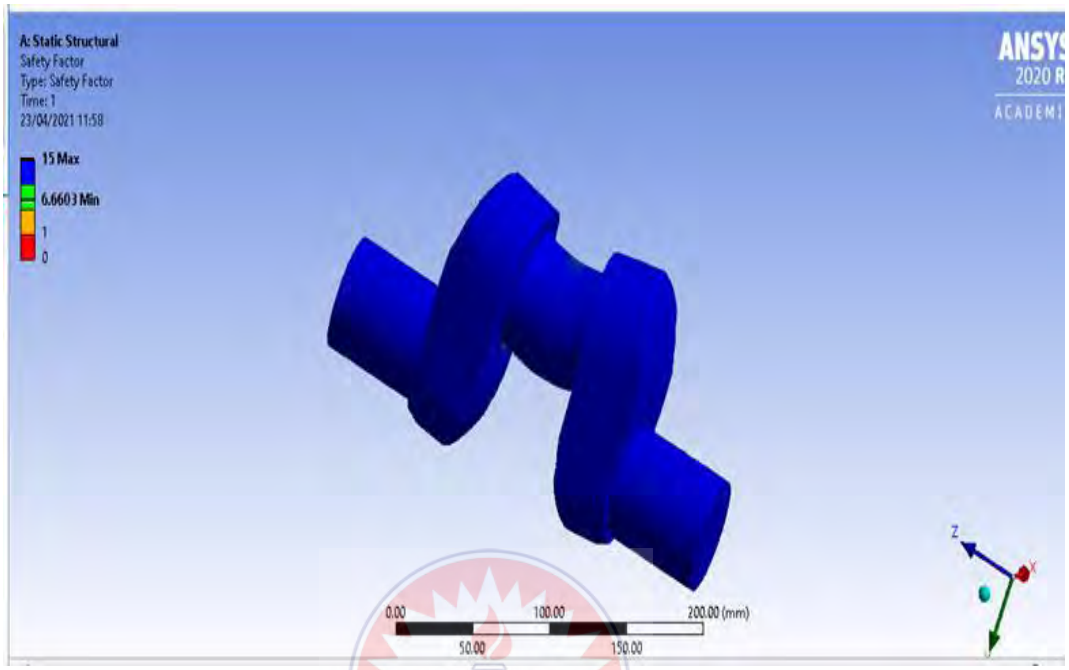

Figure 4.24 Factor of Safety of Structural Steel Crankshaft used for TVS

From the figures showing factor of safety of all materials used for the study, it was observed that all three materials recorded 15 as maximum factor of safety. Since the maximum factor of safety for ANSYS is 15, it was concluded that all three materials are safe to be used to produce crankshafts for TVS king tricycle.

4.3 Modal Analysis

Model analysis could be explained in brief as the study of the dynamic properties of structures under vibrational excitation. Modal analysis is the field of measuring and analysing the dynamic response of structures and or fluids during excitation. Following was the results obtained from the modal analysis based on the three materials under study:

4.3.1 Modal Analysis Results for Forged Steel

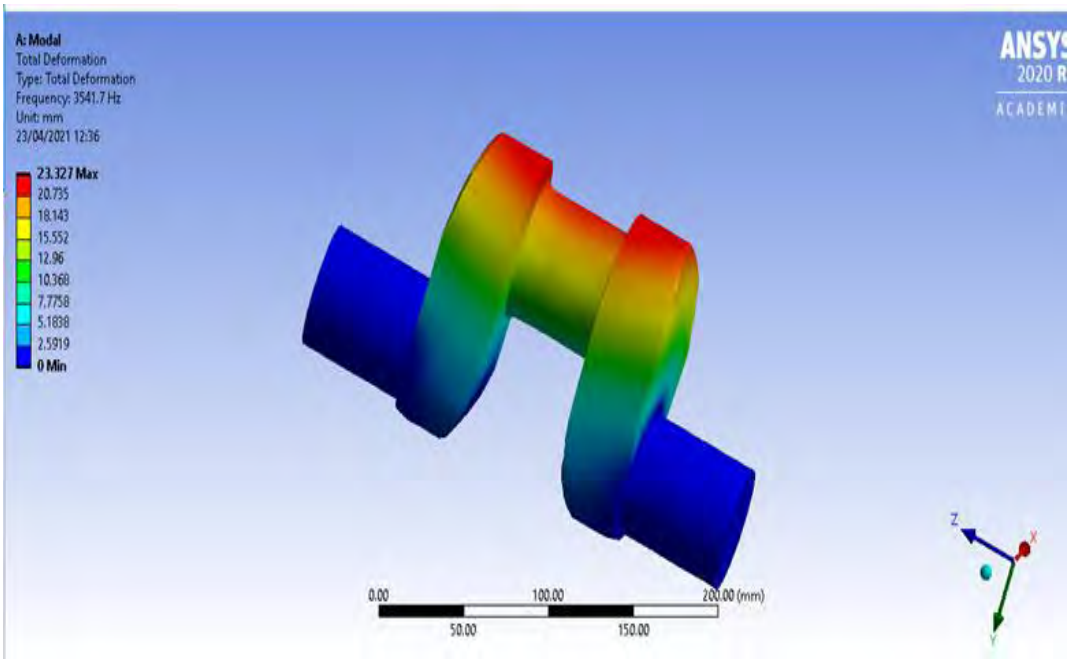

Figure 4.25 Mode 1 and Frequency of 3541.7 Hz

Report on modal analysis conducted on TVS king tricycle crankshaft made of forged steel revealed that, on mode 1in Fig. 4.25, which is the first mode for this study, a maximum deformation of 23.327 mm occurred at the upper parts of the crank webs and crankpin, whiles a minimum deformation of 2.5919 mm was noticed on the main journals at a frequency of 3541.7 Hz.

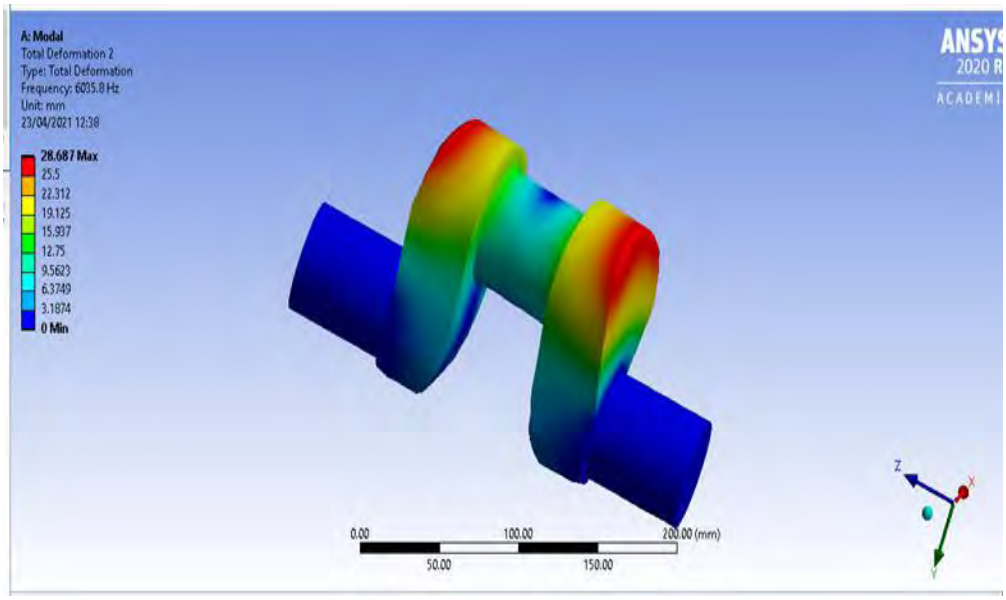

Figure 4.26 Mode 2 and Frequency of 6035.8 Hz

When a modal analysis was conducted on TVS king tricycle crankshaft made of forged steel, it was observed on mode 2 (Fig. 4.26) that, a maximum deformation of 28.687 mm occurred at the top most parts of the crank webs, with a minimum deformation of 2.5919 mm recorded at the main journals and the centre of the crankpin at a frequency of 6035.8 Hz.

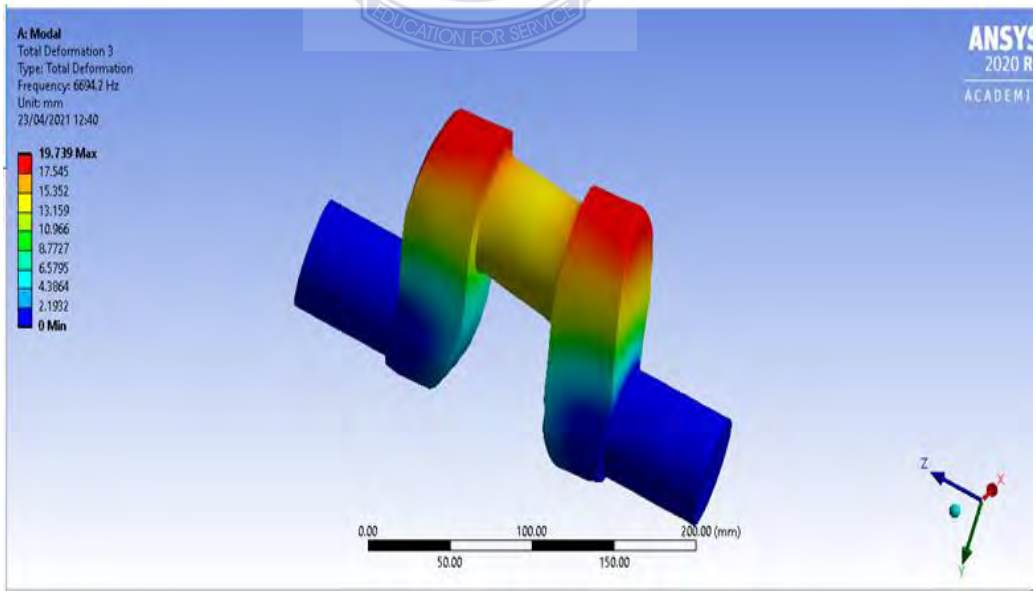

Figure 4.27Mode 3 and Frequency of 6694.2 Hz

It was realised during a modal analysis on TVS king tricycle crankshaft made of forged steel that, at frequency of 6694.2 Hz, a maximum deformation of 19.739 mm was noticed at the upper ends of the crank webs on mode 3, with a minimum deformation of 2.8879 mm recorded at the main journals and the lower portions of the crank webs. Fig. 4.27 shows the Modal Analyses (Mode) for Forged Steel.

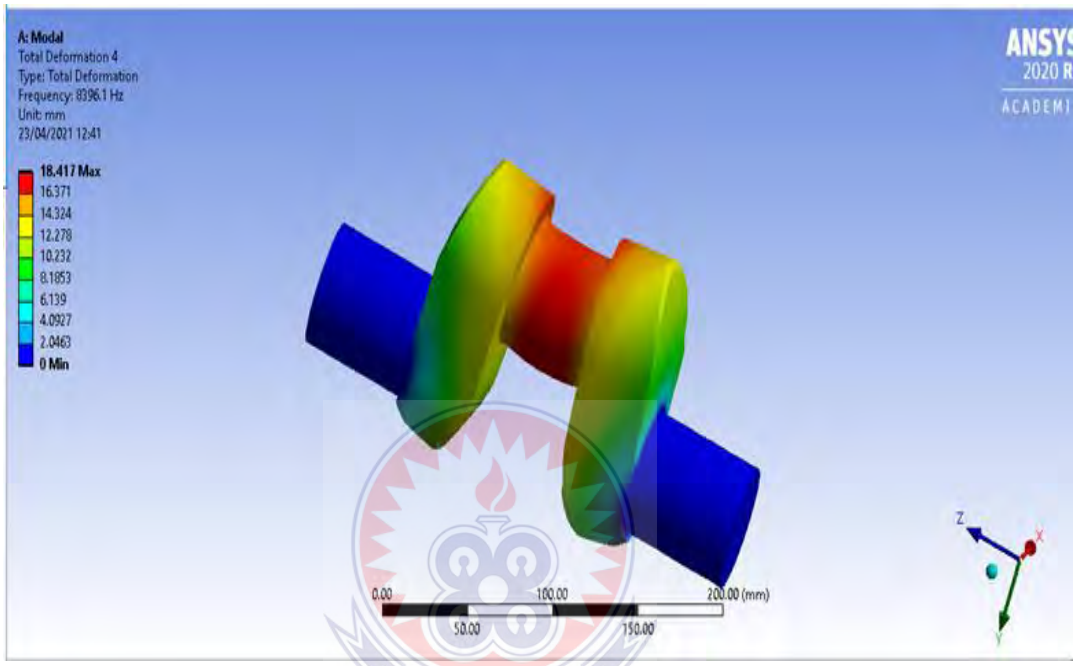

Figure 4.28Mode 4 and Frequency of 8396.1 Hz

A maximum deformation of 18.417 mm was noticed at the crankpin and upper edges of the crank webs of mode 4, during a modal analysis conducted on TVS king tricycle crankshaft made of forged steel. Minimum deformation of 2.0463 mm was recorded at the main journals at a frequency of 8396.1 Hz. This is indicated in Fig. 4.28.

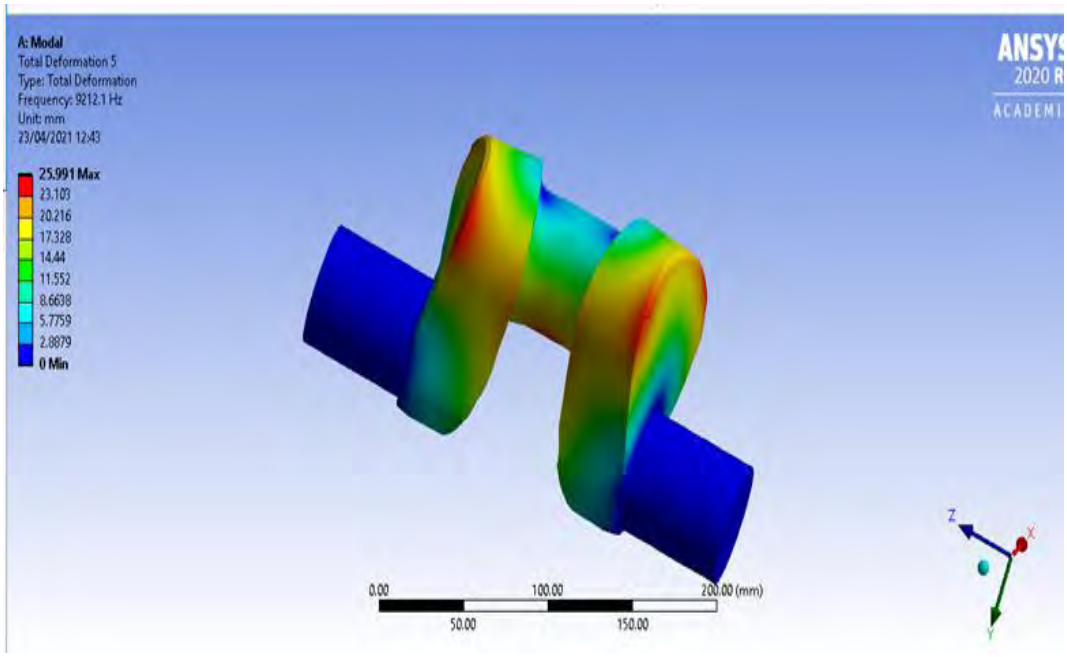

Figure 4.29Mode 5 and Frequency of 9212.1 Hz

During a modal analysis on a TVS king tricycle crankshaft, a maximum deformation of 25.991 mm was discovered at the upper edges of the crank webs on mode 5. From Fig. 4.29, a minimum deformation of 2.8879 mm occurred at the crankshaft main journals at a frequency of 9212.1 Hz.

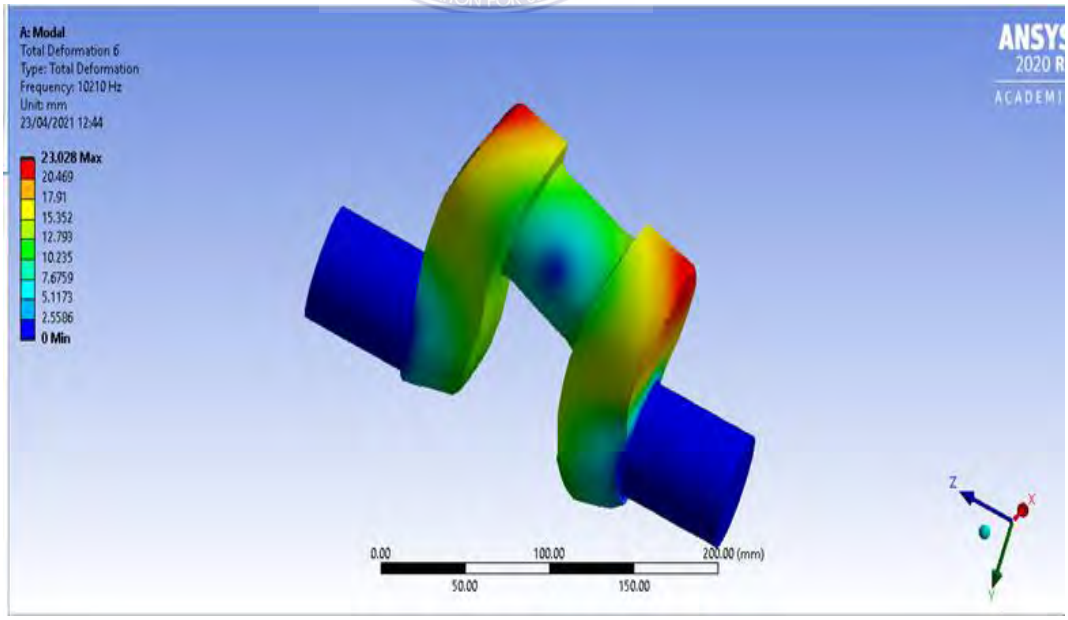

Figure 4.30 Mode 6 and Frequency of 10210 Hz

From Fig. 4.30, at a frequency of 10210 Hz during a modal analysis on TVS king tricycle crankshaft made of forged steel, it was realised on mode 6 that, a maximum deformation of 23.028 mm took place at the upper edges of the crank webs, whiles a minimum deformation of 2.5586 mm was noticed on the main journals and at the side of thecrankpin.

4.3.2 Modal Analysis Results for Mild Steel

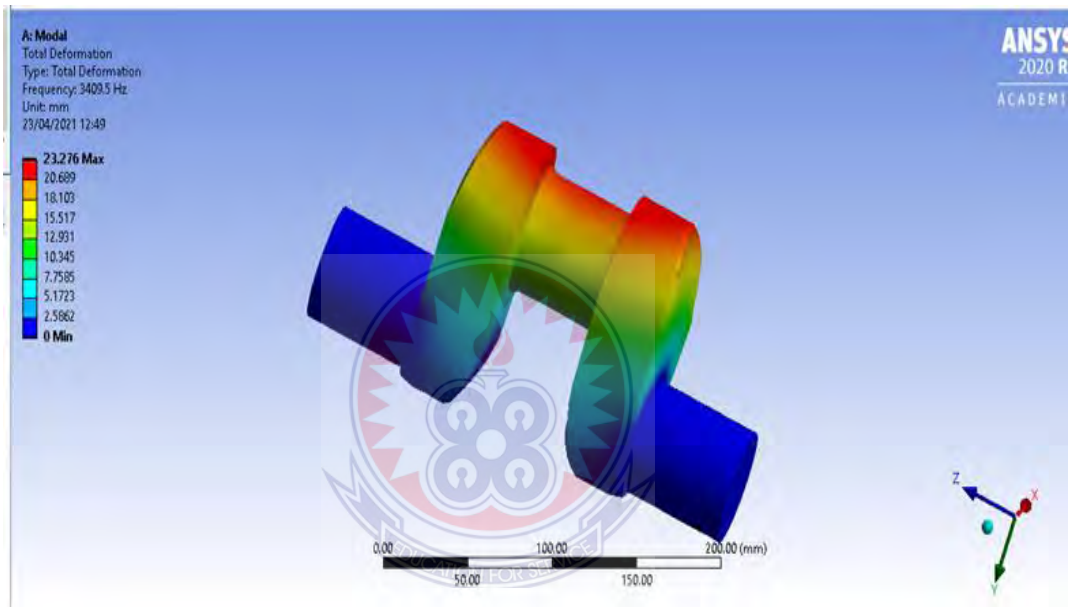

Figure 4.31 Mode 1 and Frequency of 3409.5 Hz

When a modal analysis was conducted on TVS king tricycle crankshaft made of mild steel, it was observed on mode 1 in Fig. 4.31 that, a maximum deformation of 23.276 mm occurred at the top most parts of the crank webs and the upper part of the crankpin, whilst a minimum deformation of 2.5862 mm was recorded at the main journals and the lower parts of the crank webs at a frequency of 3469.5 Hz.

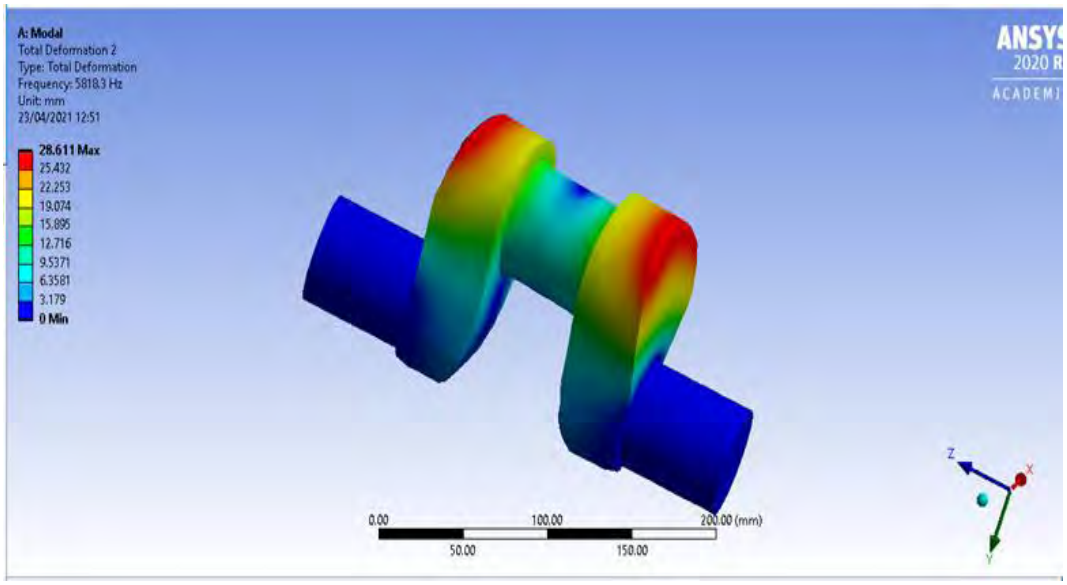

Figure 4.32 Mode 2 and Frequency of 5818.3 Hz

From Fig. 4.32, a maximum deformation of 28.611 mm was noticed at the upper outer edges of the crank webs on mode 2, during a modal analysis conducted on TVS king tricycle crankshaft made of mild steel. A minimum deformation of 3.179 mm was recorded at the main journals, lower portions of the crank webs, and centre of the crankpin at a frequency of 5818.3 Hz.

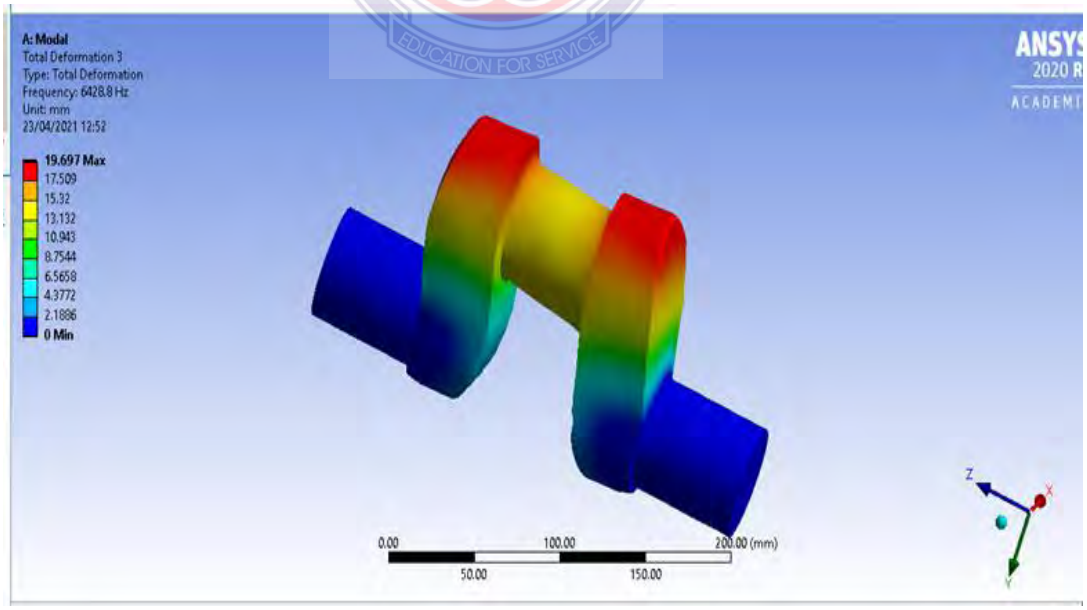

Figure 4.33 Mode 3 and Frequency of 6428.8 Hz

During a modal analysis on a TVS king tricycle crankshaft made of mild steel, a maximum deformation of 19.697 mm was discovered at the upper ends of the crank

webs on mode 3. A minimum deformation of 2.1886 mm occurred at the lower ends of the crank webs and main journals at a frequency of 6428.8 Hz. This is shown in Fig. 4.33.

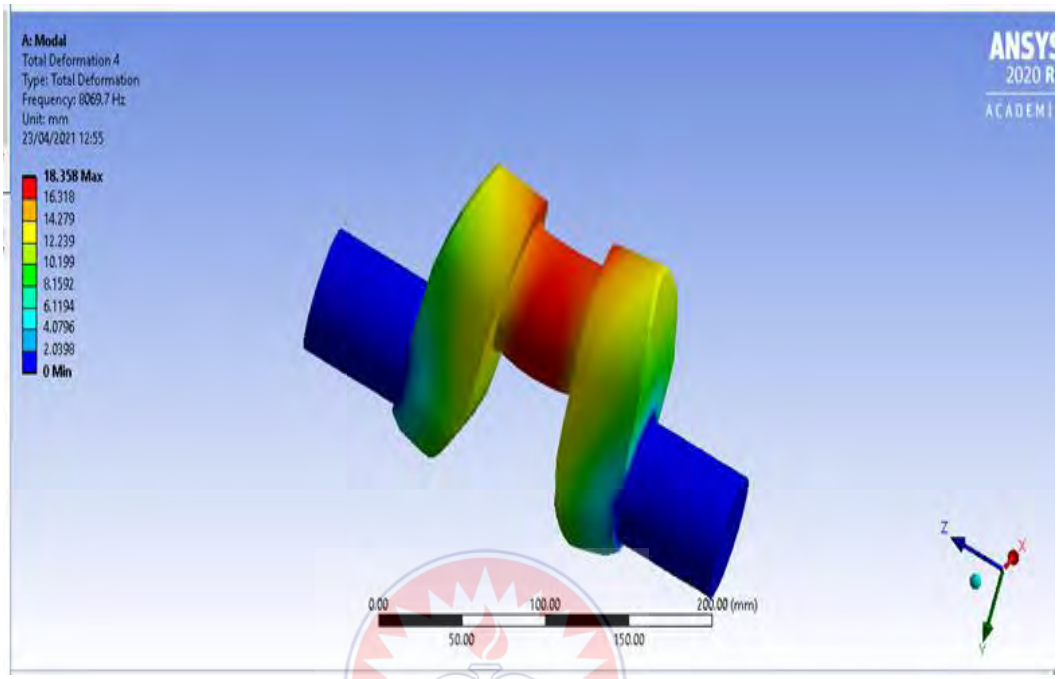

Figure 4.34Mode 4 and Frequency of 8069.7 Hz

At a frequency of 8069.7 Hz during a modal analysis on TVS king tricycle crankshaft made of mild steel, it was realised on mode 4 in Fig. 4.34 that, a maximum deformation of 18.358 mm took place on the crankpin and the inner upper edges of the crank webs, whiles a minimum deformation of 2.0398 mm was noticed on the main journals.

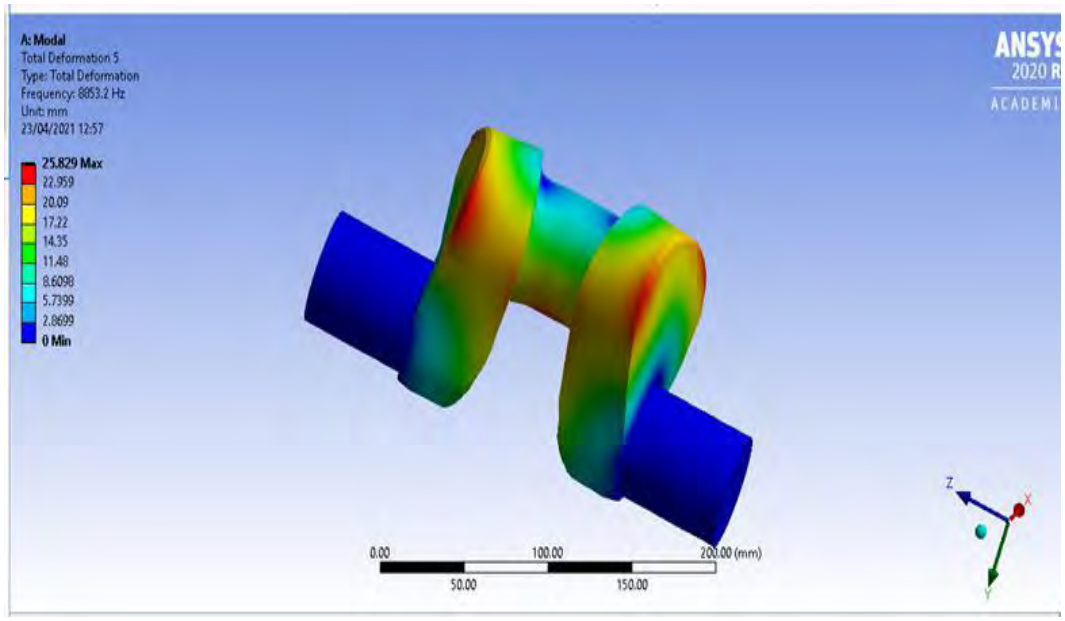

Figure 4.35 Mode 5 and Frequency of 8853.2 Hz

From Fig. 4.35, it was realised during a modal analysis on TVS king tricycle crankshaft made of mild steel that, on mode 5, at frequency of 8853.2 Hz, a maximum deformation of 25.829 mm was noticed at the upper edges of the crank webs with a minimum deformation of 2.8699 mm recorded at the main journals and the upper portion of the joint between the crank webs and the crankpin.

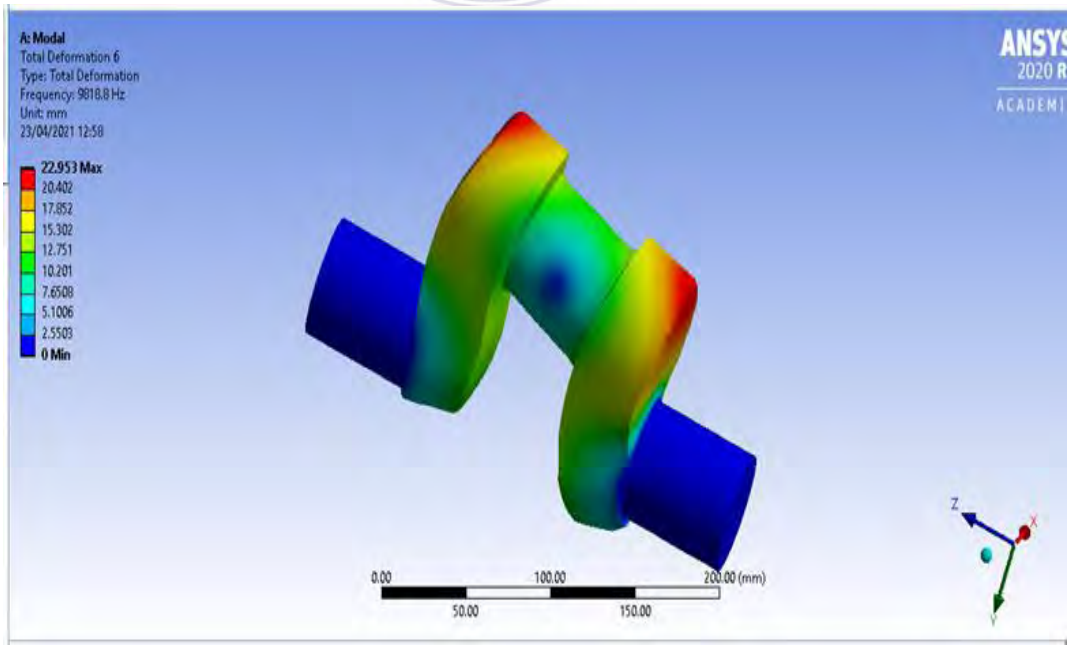

Figure 4.36 Mode 6 and Frequency of 9818.8 Hz

Modal analysis conducted on TVS king tricycle crankshaft made of mild steel revealed that, on mode 6 in Fig. 4.36, which is the final mode for this study, a maximum deformation of 22.953 mm occurred at outer upper edges of the crank webs, whiles a minimum deformation of 2.5503 was noticed at the side of the crankpin and the main journals at a frequency of 9818.8 Hz.

4.3.3 Modal Analysis Results for Structural Steel

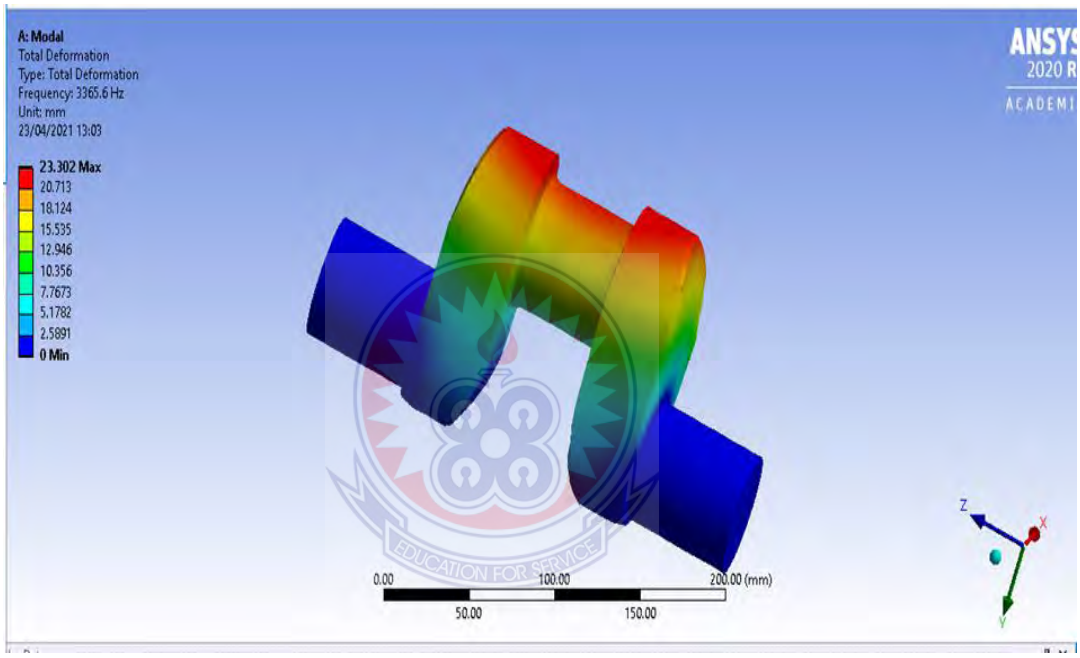

Figure 4.37 Mode 1 and Frequency of 3365.6 Hz

During a modal analysis on a TVS king tricycle crankshaft made of structural steel, a maximum deformation of 23.302 mm was discovered at the upper ends of the crank webs and crankpin on mode 1 in Fig. 4.37. A minimum deformation of 2.5891 mm occurred at the ends of the crankshaft main journals and lower ends of the crank webs at a frequency of 6694.2 Hz.

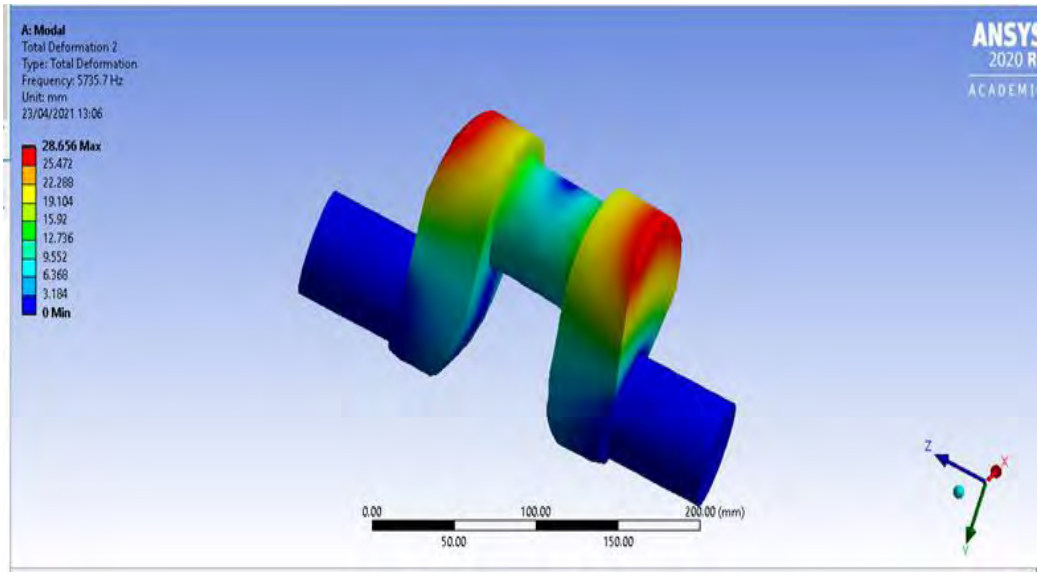

Figure 4.38Mode 2 and Frequency of 5735.7

It was realised in Fig. 4.38 that, during a modal analysis on TVS king tricycle crankshaft made of structural steel that, at frequency of 5735.7 Hzon mode 2, a maximum deformation of 28.656 mm was noticed at the upper edges of the crank webs with a minimum deformation of 3.184 mm recorded at the main journals, lower ends of the crank webs, and the centre of crankpin.

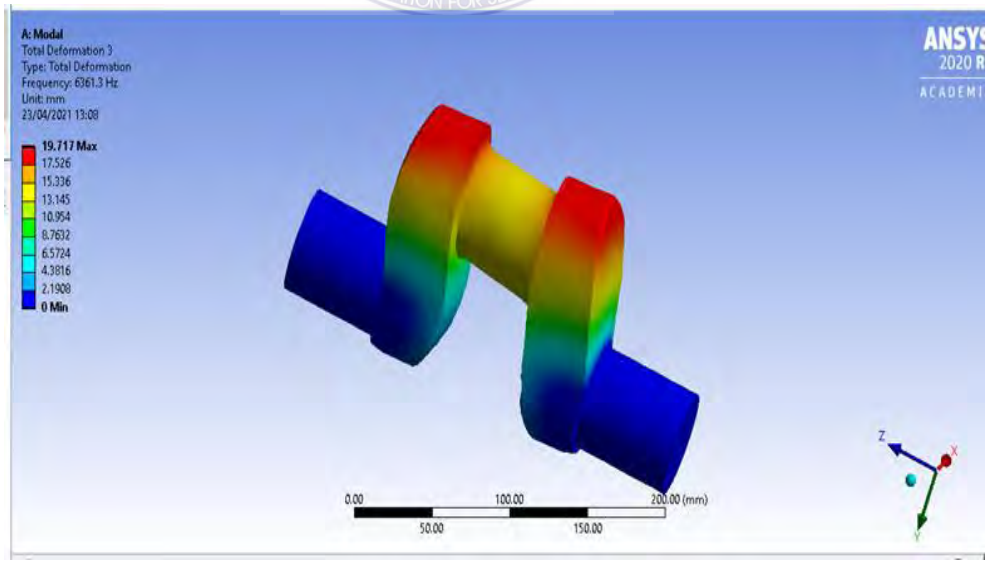

Figure 4.39Mode 3 and Frequency of 6361.3 Hz

At a frequency of 6361.3 Hz during a modal analysis on TVS king tricycle crankshaft made of structural steel, it was realised on mode 3in Fig. 4.39that, a maximum deformation of 19.717 mm took place at the upper ends of the crank webs, whiles a minimum deformation of 2.108 mm was noticed at the main journals and the lower parts of the crank webs.

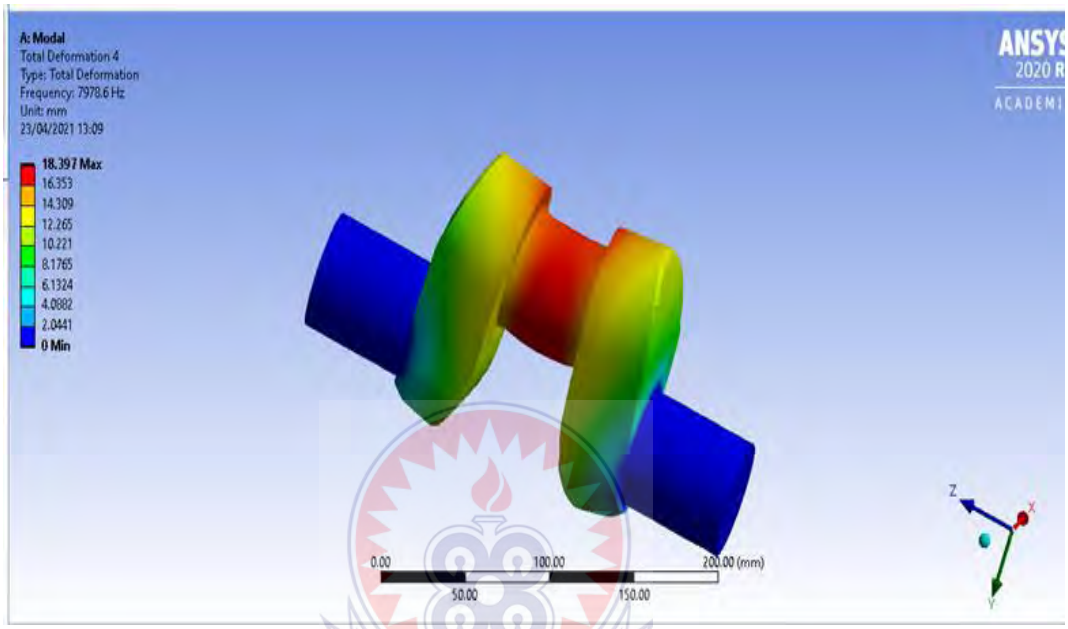

Figure 4.40 Mode 4 and Frequency of 7978.6 Hz

In Fig. 4.40, a maximum deformation of 18.397 mm was noticed at the crankpin and upper inner edges of the crank webs on mode 4 during a modal analysis conducted on TVS king tricycle crankshaft made of structural steel. Minimum deformation of 2.0441 mm was recorded at the main journals at a frequency of 7978.6 Hz.

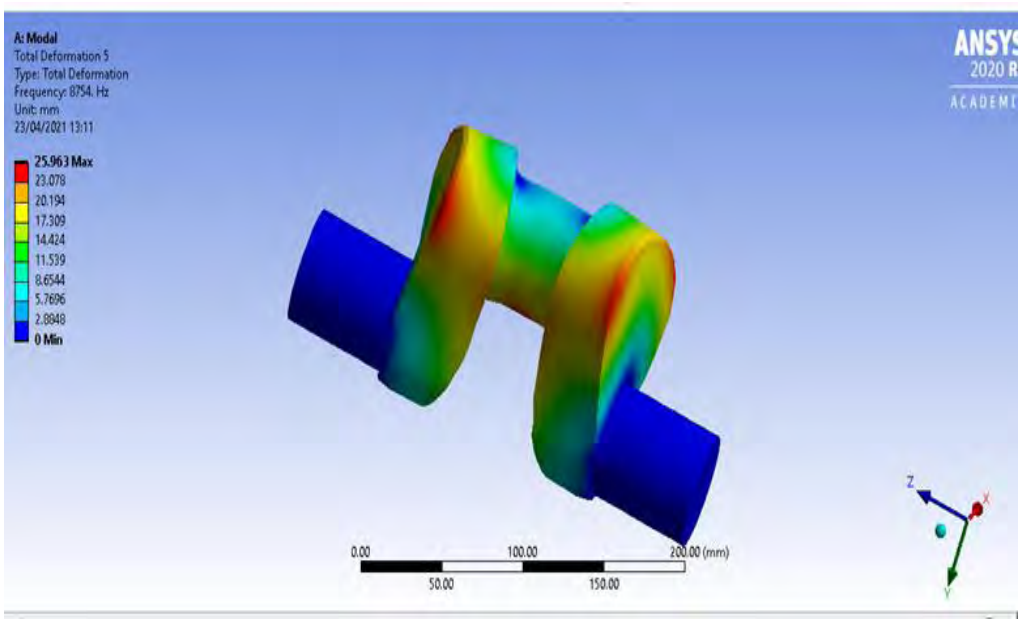

Figure 4.41 Mode 5 and Frequency of 8754.0 Hz

Modal analysis conducted on TVS king tricycle crankshaft made of structural steel revealed that, on mode 5 a maximum deformation of 25.963 mm occurred at outer upper edges of the crank webs, whiles a minimum deformation of 2.8848 mm was noticed at the main journals and upper portion of the joint between the crankpin and webs of the crankshaft. This is shown in Fig. 4.41.

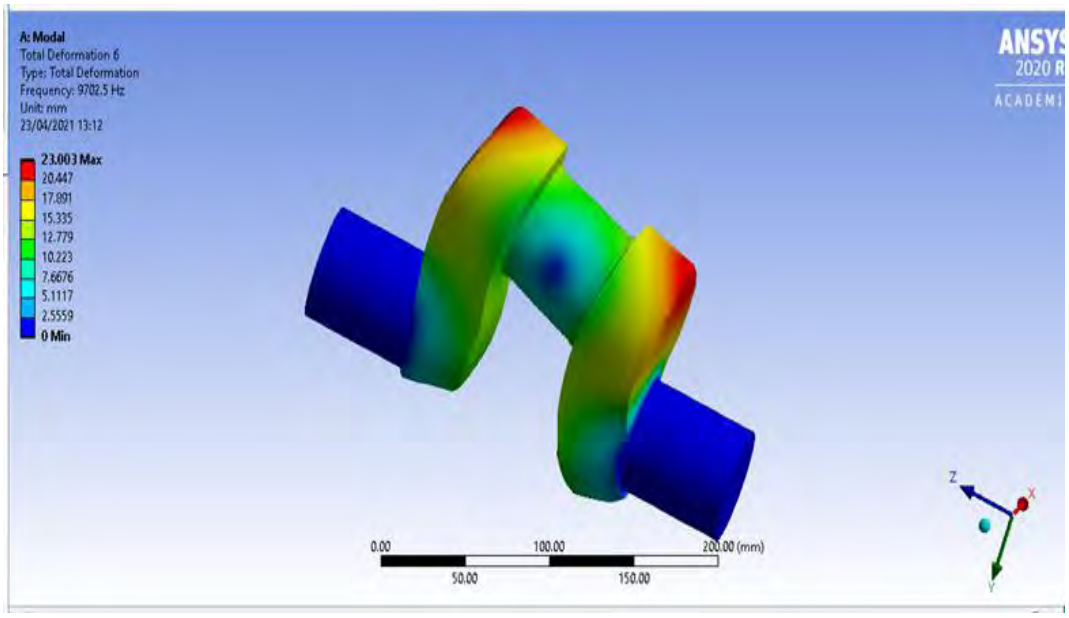

Figure 4.42Mode 6 and Frequency of 9702.5

When a modal analysis was conducted on TVS king tricycle crankshaft made of structural steel, it was observed on mode 6 in Fig. 4.42 that, a maximum deformation of 23.003 mm occurred at the outer top ends of the crank webs, whilst a minimum deformation of 2.5559 mm was recorded at the main journals and the side of the crankpin at a frequency of 9702.5 Hz.

It was observed from the simulation results that, materials used for the study recorded highest deformationsfor forged steel, mild steel, and structural steel onmode 2 (Figs. 4.38, 4.32, 4.26, and 4.20), whiles the lowest deformations for all the three materials adopted for the study was recorded on mode 4 (Figs. 4.40, 4.34, 4.28, and 4.22).It was also realized from the simulation that, the lowest frequencies for both controlled materials and the implementing material was noticed on mode 1 (Figs. 4.37, 4.31, 4.25, and 4.19), while the highest frequencies were observed on mode 6 (Figs. 4.42, 4.36, 4.30, and 4.24).It was therefore discovered that, with the TVS king tricycle crankshaft, as the modes proceed so also the frequency increases, hence the highest frequency been on the last mode, while the deformation is independent of the frequency.

4.4 Validation of Results

The analytical results were compared with the numerical results for validation purpose as shown in Table 4.1

Table 4.1Comparison of Theoretical and Numerical Results

S/No.	Types of Stresses	Theoretical Results (MPa)	Numerical Results (MPa)		
			Forged Steel	Mild Steel	Structured Steel
1.	Maximum principal stress	34.418	15.189	15.256	15.189
2.	Von - Mises	152.22	37.536	37.587	37.536
3.	Shear stress	39.2898	19.448	19.448	19.448

The comparison between the theoretical and simulation results for both controlled materials and the implementing material clearly indicated that all three materials had less stress levels and are fit for purpose.

CHAPTER FIVE

SUMMARY OF FINDINGS, CONCLUSION AND RECOMMENDATIONS

5.1 Introduction

This chapter presentsa summary of the main findings, conclusions, and recommendations.

5.2 Summary of findings

The following are findings made out of the study:

i. It was revealed from the study that, structural steel which is an implementing material for the construction of TVS king tricycle crankshaft in this study had the lowest yield strength of 250 MPa as compared to the materials that were used for the production of this crankshaft. Mild Steel which is one of the controlled materials had a yield strength of 370 MPa whiles Forged Steel, the other controlled material had a yield strength of 625 MPa. This presupposes that, structural steel is most likely to undergo severe deformation as compared to the controlled materials when subjected to the same load.

ii. Also, it was discovered from the study that, when the load of 48305.13N was applied on the crankpin of the crankshaft of all three materials for the study, this was how their various total deformation played out; maximum and minimum total deformation of mild steel TVS king tricycle crankshaft was 0.0085204mm and 0.0009467mm congruently, the maximum and minimum total deformation of forged steel for same crankshaft was 0.007925mm and 0.00088054mm respectively, whiles structural which is the implementing material recorded a maximum and minimum total deformation of 0.008757mm and 0.000973mm correspondingly. It is obvious from the

comparison that Forged steel deformed less, with the greatest total deformation going to structural steel. Since the yield starts for most steels at approximately 0.2% elongation, all the three crankshafts on the study were found to have deformed within the acceptable limits.

iii. Furthermore, when the maximum principal stresses of the three crankshafts was compared, mild steel crankshaft recorded the highest principal stress of maximum 15.256 MPa and minimum of -8.657 MPa, whereas forged steel and structural steel crankshafts recorded a maximum of 15.189 MPa and a minimum value of -9.027 MPa respectively. The maximum principal stresses induced in the crankshafts as gathered by FEA was lower than the theoretical maximum principal stress of 34.418 MPa.

iv. Again, from a comparison of equivalent Von-Mises stress induced in crankshafts of the three different materials, the maximum and minimum values recorded for forged steel and structural steel was 37.536 MPa and 0.030536 MPa accordingly. Comparatively, the equivalent Von-Mises stress induced in the crankshafts of all three materials on this study as recorded by FEA was lower than the theoretical equivalent Von-Mises stress of 152.22 MPa.

v. Also, when the maximum shear stress for the three crankshafts was compared, it was revealed that crankshafts of the three different materials recorded the same maximum shear stress of 19.448 MPa and a minimum of 0.019187 MPa respectively. The maximum shear stress recorded from the FEA for all the three crankshafts on the study was lower than the theoretical maximum shear stress of 39.2898 MPa.

vi. When the modal analysis results were compared with the structural static results, it was revealed that the trend of deformation between the two (2) analysis conducted was reliable. Whiles on the structural static analysis the highest deformation was observed at the centre of the crankpin for all the three crankshafts, the highest deformation was recorded on mode 2 for all the three crankshafts when the no load vibration analysis was compared. Mild steel crankshaft recorded a maximum deformation of 28.611mm, forged steel crankshaft recorded a maximum deformation of 28.687mm, while structural steel crankshaft recorded a maximum deformation of 28.656mm.

vii. Again, when the natural frequencies of all the crankshafts made of three different materials was compared, it was observed that the highest frequency was recorded on mode 6. Mild steel crankshaft had the highest natural frequency of 9818.8 Hz, whiles forged steel crankshaft had the highest natural frequency of 10210 Hz, and structural steel crankshaft also had a highest natural frequency of 9702.5 Hz. Comparatively, forged steel crankshaft had the highest natural frequency among the three, followed by mild steel crankshaft and lastly the structural steel crankshaft.

viii. Also, it was observed that the weight of forged steel crankshaft was 91.71N, mild steel crankshaft also had the same weight of 91.71N, whiles that of structural steel crankshaft was 90.9003N.Comparatively, structural steel which was the implementing material showed 0.81N which was equal to 82.6g less the weight of mild steel and forged steel crankshafts.

ix. Lastly, from a comparison of the factor of safety of crankshafts made of mild steel, forged steel, and structural steel, it was revealed that all three crankshafts recorded the same maximum factor of safety which 15.

5.3 Conclusion

The following were the main conclusions of the study:

The primary objective of the study which was to ascertain the possibility of using structural steel to model a crankshaft for weight optimisation whiles maintaining strength of the crankshaft. The weights of the crankshafts were compared, the results showed that, the weights of crankshafts made of the controlled materials (mild steel and forged steel) was the same, while the weight of the implementing material (structural steel) was slightly less than that of the controlled materials. Consequently, the main objective of the study which was to introduce another material for making the TVS king tricycle crankshaft of a lesser weight was realised.

Findings from the simulation showed that stresses in all the three crankshafts made of the three different materials for this study were below the yield strength of the materials. Based on the aforementioned assertion, it was concluded that all crankshafts of the three different materials can withstand the compressive load that was applied.Hence. all the three crankshafts are fit for purpose.

The results were validated by comparing the numerical results with the theoretical results. It was observed that FEA results were also below the theoretical results, which further confirms that all the three crankshafts were fit for purpose.

Failure of TVS tricycle crankshaft in Tamale is not as a result of manufacturing defect but may arise from bad handling on the part of drivers.

5.4 Recommendations

i. Structural steel can be considered as one of the materials for TVS king tricycle crankshaft. Analysis results shows that it can withstand the induced stresses and is also lighter in weight as compared to the controlled materials.

ii. It is further recommended that the design of a structural steel crankshaft for TVS king tricycle crankshaft be actualised and tested on an engine.

5.5 Suggestion for Future Study

i. Further analysis could be done on the structural steel crankshaft by refining the size of the mesh and also changing the loading conditions of the crankshaft.

ii. It is also suggested that a dynamic analysis be perform on the structural steel crankshaft.

REFERENCES

Akinlabi E. T. &Agarana M. C. (2018). *Modelling of A36 Steel Plate Dynamic Response to Uniform Partially Distributed Moving Iron Load using Differential Transform Method*. IOP Conf. Series: Materials Science and Engineering 413 (2018) 012011 doi:10.1088/1757-899X/413/012011. Retrieved from https://iopscience.iop.org/article/10.1088/1757-899X/413/1/012011/pdf on March 14, 2021

Azom (2012). *AISI 1045 Medium Carbon Steel.* Retrieved from https://www.azom.com/article.aspx?ArticleID=6130 on March 14, 2021

Azom (2013) *AISI 1018 Carbon Steel (UNS G10180) - Azom.com*. retrieved from https://www.azom.com on March 14, 2021

Basavaraj S. T., Kurbet S. N. &Kuppast V. V. (2015). *Static Structural Analysis Of 2-Cylinder Crankshaft Using ANSYS, International Journal for Technological Research in Engineering Volume* 3, Issue 2, October-2015 ISSN (Online): 2347 – 4718. Retrieved fromhttp://ijtre.com/images/scripts/2015030217.pdf on February 20, 2021

Citti P., Giorgetti A. &Millefanti U. (2017). *Current challenges in material choice for high-performance engine crankshaft, AIAS 2017 International Conference on Stress Analysis, AIAS 2017, 6-9 September 2017, Pisa, Italy*. Retrieved from http://www.sciencedirect.com/ on March 13, 2021

Garrett, T.K. (2001). *The MotorVehicle, Butterworth-Heinemann Linacre House, Jordan Hill*, Oxford OX2 8DP 225 Wildwood Avenue, Woburn, MA 08101-2041 *A division of Reed Educational and Professional Publishing* Ltd. Thirteenth Edition

Hillier V. A. W. & Peter C. (2004). *Fundamentals of Motor Vehicle Technology Book 1, Nelson Thornes Ltd, Delta Place 27 Bath Road CHELTENHAM* GL53 7TH United Kingdom, ISBN 0748780823, 9780748780822. Fifth Edition

Iyer N.V., (2012). A Technical Assessment of Emissions and Fuel Consumption Reduction Potential from Two and Three Wheelers in India. Prepared for: The International Council on Clean Transportation. Washington, DC

Jagruti K. C. Barjibhe R. B. (2016). *Experimental and Numerical Analysis of Crankshaft Used in Hero Honda Splendor Motorcycle, International Journal of New Technology and Research (IJNTR) ISSN*:2454-4116, Volume-2, Issue-7, July 2016 Pages 83-94

Jian Meng, et al (2011). *"Finite Element Analysis of 4-Cylinder Diesel Crankshaft," I.J. Image, Graphics and Signal Processing*, 5, 22-29

Katari A et al. (2011), "*Fatigue Fracture Expertise of Train Engine Crankshafts*", Engineering Failure Analysis, Vol. 18, pp. 1085-1093.

Metkar R. M. et al (2011). *A fatigue analysis and life estimation of crankshaft - a review, International Journal of Mechanical and Materials Engineering* (IJMME), Vol.6 (2011), No.3, 425-430. Retrieved from http://www.sciencepublishinggroup.com/journal/paperinfo?journalid=525&paperId=10022782 on March 12, 2021

Montazersadgh, F. &Fatemi, A. (2009). *Optimization of a Forged Steel Crankshaft Subject to Dynamic Loading. SAE International Journal of Materials and Manufacturing, 1*(1), 211-217. Retrieved from http://www.jstor.org/stable/26282649 on March, 2021

Mounika B., Madhuri R. P. (2015). *Structural Static Analysis of Crankshaft, International Journal of Science and Research* (IJSR) ISSN (Online): 2319-7064 Index Copernicus Value (2015): 78.96 | Impact Factor (2015): 6.391

Muse D., Prabhu P., Tamana D., & Venkatesh K.S. (2017). *Optimization and Finite Element Analysis of Single Cylinder Engine Crankshaft for Improving Fatigue Life*, *American Journal of Mechanical and Materials Engineering*. Vol. 1, No. 3, 2017, pp. 58-68. doi: 10.11648/j.ajmme.20170103.11

Pandiyan A., Arun K. G., Amit P. & Shaik A. S. (2018). *Design and Optimization of Crankshaft for Single Cylinder 4 – Stroke Spark Ignition Engine Using Coupled Steady-State Thermal Structural Analysis, International Journal of Mechanical Engineering and Technology*, 9(7), 2018. Retrieved from https://www.researchgate.net/publication/326461109_DESIGN_AND_OPTIMIZATION_OF_CRANKSHAFT_FOR_SINGLE_CYLINDER_4_- on December 12, 2020

Pratiksha M. N. (2015). *Analysis of Crankshaft, International Journal of Scientific Engineering and Research (IJSER) ISSN (Online):* 2347-3878 Index Copernicus Value (2015): 62.86 | Impact Factor (2015): 3.791 Volume 5 Issue 4, April 2017. Retrieved from https://www.ijser.in/archives/v5i4/IJSER151332.pdf on December 10, 2020

Raja S. J. I., Sathishkumar G., Sivaganesan S. & Sridhar R. (2018). *DESIGN AND DYNAMIC ANALYSIS OF CRANKSHAFT IN LIGHT WEIGHT, International Journal in Recent Trends in Engineering,* ISSN (ONLINE):2455-1457, IMPACT FACTOR: 4.101

Raju R. &Namcharaiah K. (2018) *Design and Fatigue Analysis of Crankshaft, International Journal of Innovative Research in Science, Engineering and*

Technology (A High Impact Factor, Monthly, Peer Reviewed Journal) Visit: www.ijirset.com Vol. 7, Issue 2, February 2018. Retrieved fromhttp://www.ijirset.com/upload/2018/february/40_13_Design.pdf on April 10, 2021

Rinkle G. et al (2012). "*Finite Element Analysis and Optimization of Crankshaft Design "International Journal of Engineering and Management Research*, Vol.-2, Issue-6, December 2012 ISSN No.: 2250-0758 Pages: 26-31. Retrieved from https://www.indianjournals.com/ijor.aspx?target=ijor:ijemr&volume=2&issue=6&article=004 on December 10, 2020

Shahane V. C. &Pawar R.S. (2017). *Optimization of the crankshaft using finite element analysis approach*, Automot. Engine Technol. 2:1–23. Retrieved from https://doi.org/10.1007/s41104-016-0014-0 on December 5, 2020

Souza T. N. F. &Nogueirac R. A. P. S. (2014). *Mechanical and Microstructural Characterization of Nodular*, DOI: http://dx.doi.org/10.1590/1516-1439.249413. Retrieved fromhttps://www.scielo.br/j/mr/a/zrYNRvfJ7qzZKRf8ttnSrJp/?lang=en&format=pdf on December 10, 2020

Springer, V. (2006) *Crankshafts and connecting rods*. In: Vehicular Engine Design. Der Fahrzeugantrieb/Powertrain. Springer, Vienna, ISBN:978-211-21130-4. Retrieved from https://doi.org/10.1007/3-211-37762-X_16 on March 10, 2021

Sriramireddy K., Venkaiah G. &Hareesh M. V. (2018). *Mechanical Model Vibration Analysis of Crankshaft of I.C Engine*. IJESC (2018) Volume 8, Issue No. 6. Retrieved from

https://ijesc.org/upload/e02b73da023e38e6098312267574999c.Mechanical%20Modal%20Vibration%20Analysis%20of%20Crank on March 12, 2021

Talikoti B., Kurbet S. N., Kuppast V. V., &Yadwad A. M. (2015). *Modal analysis of a 2-cylinder crankshaft using ANSYS, Int. Journal of Engineering Research and Applications*. Retrieved from https://www.ijera.com/papers/Vol5_issue12/Part%20-%201/D512012630.pdfon December 10, 2020

TVS (2021) *Commercial Vehicles*. Retrieved from https://commercialvehicleinfo.com/200cc-tvs-king-three-wheeler-price-specification-features/ on March 14, 2021

Wang, J. H., Hua, J., & Li, C. (2011). *Fatigue Strength and Modal Analysis of S195 Engine Crankshaft. Applied Mechanics and Materials*, 120, 81–84. Retrieved from https://doi.org/10.4028/www.scientific.net/amm.120.81on March 10, 2021

WWH (2021) *Crankshaft Materials*, retrieved from: https://what-when-how.com/crankshaft/crankshaft-material/ on March 15, 2021

Yamagata, H. (2005). *The Science and Technology of Materials in Automotive Engines*. Woodhead Publishing Limited, Abington Hall, Abington Cambridge CB1 6AH, England www.woodheadpublishing.com retrieved March 11, 2021

APPENDIX

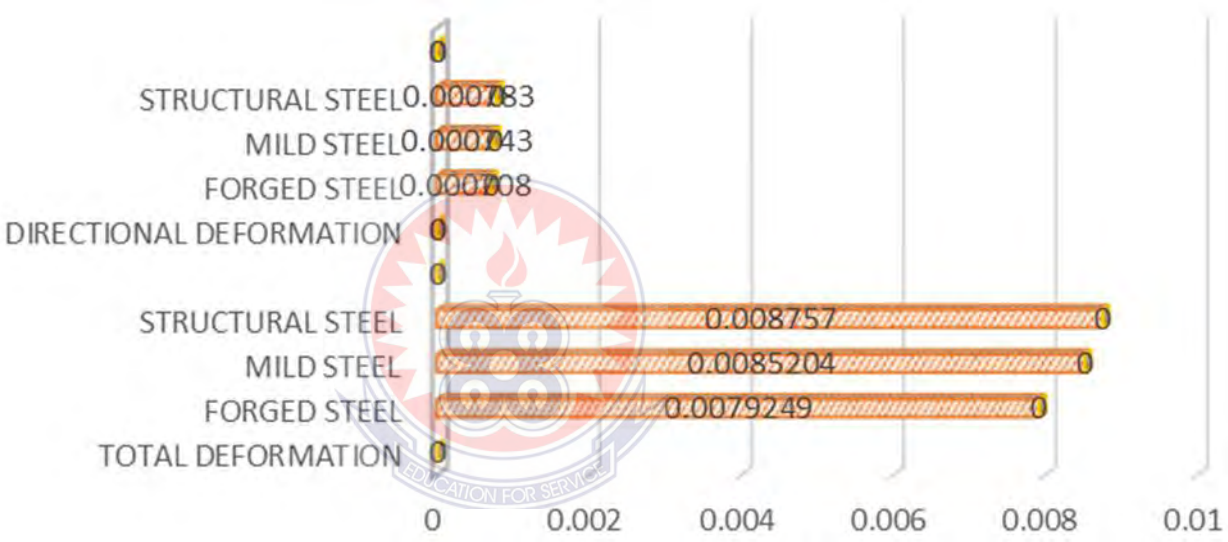

Graph showing Total deformation and Directional Deformations of Material used for the Study

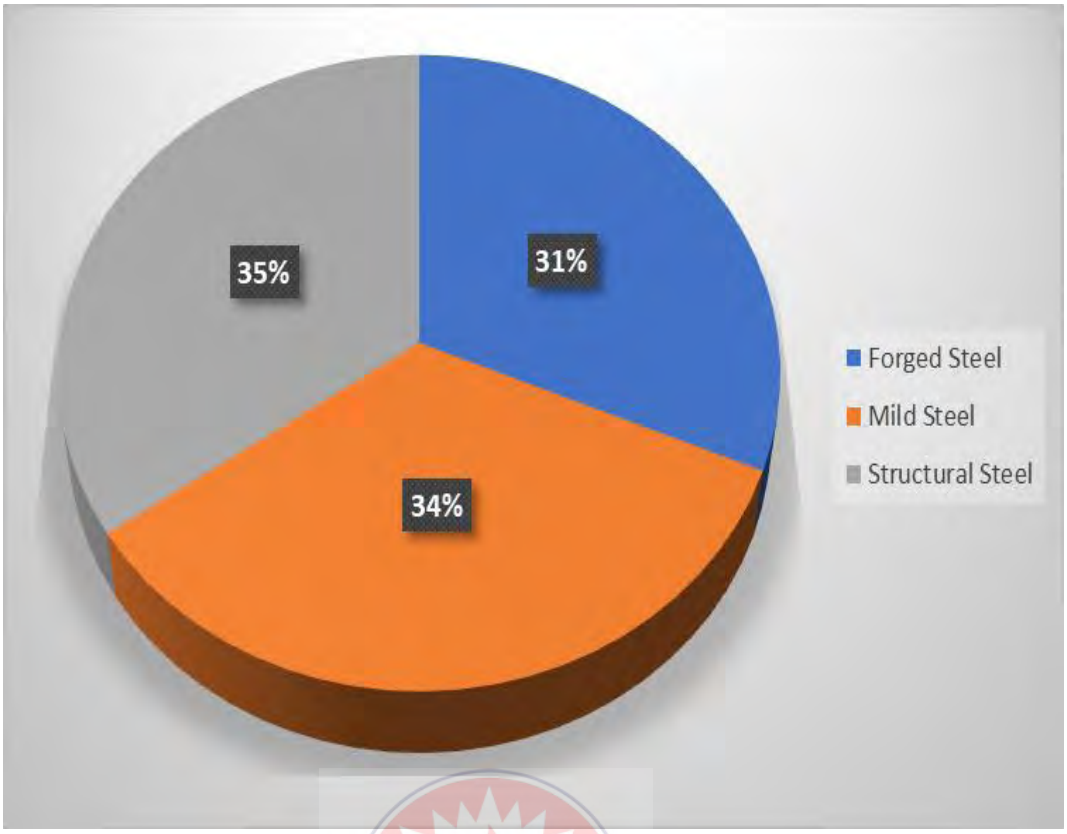

Pie chart showingEquivalent Elastic Strain of all materials used in the Study

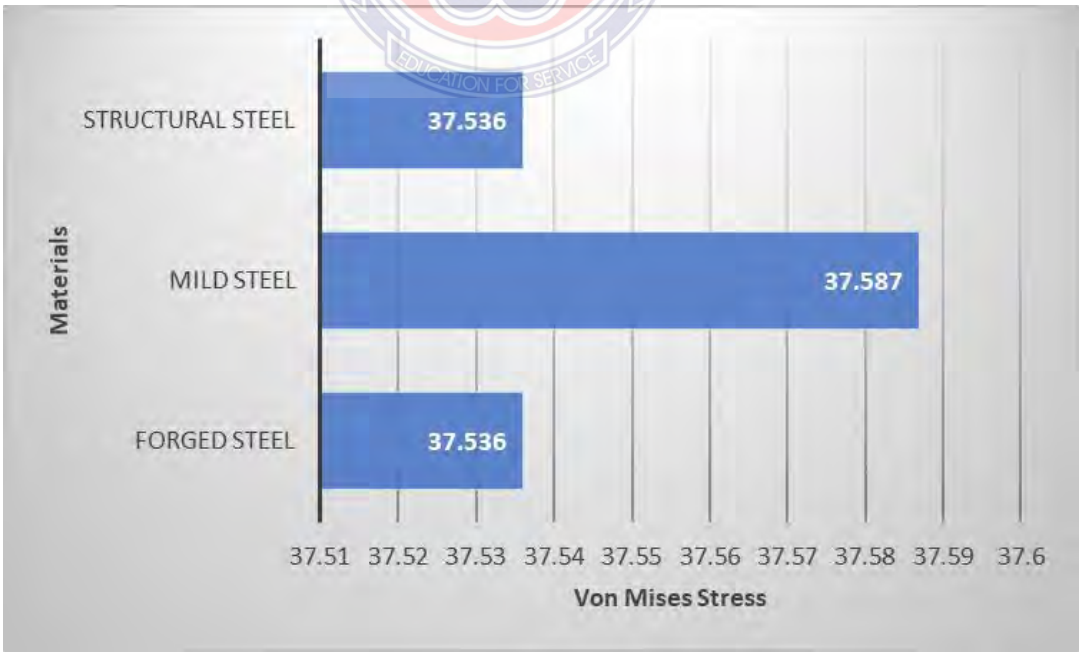

Graph showing Equivalent Von-Mises Stress for all Materials used in the Study

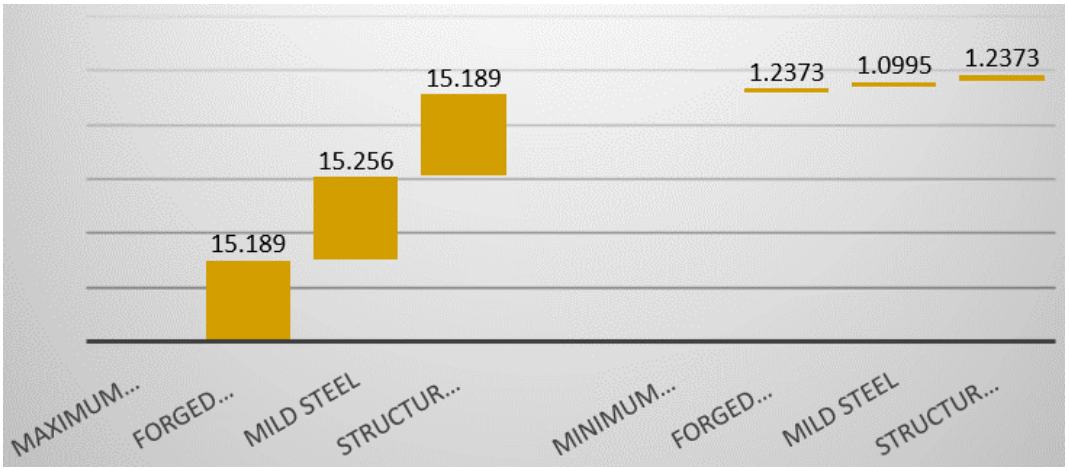

Graph showing Maximum and Minimum Principal Stresses for Materials used on the Study

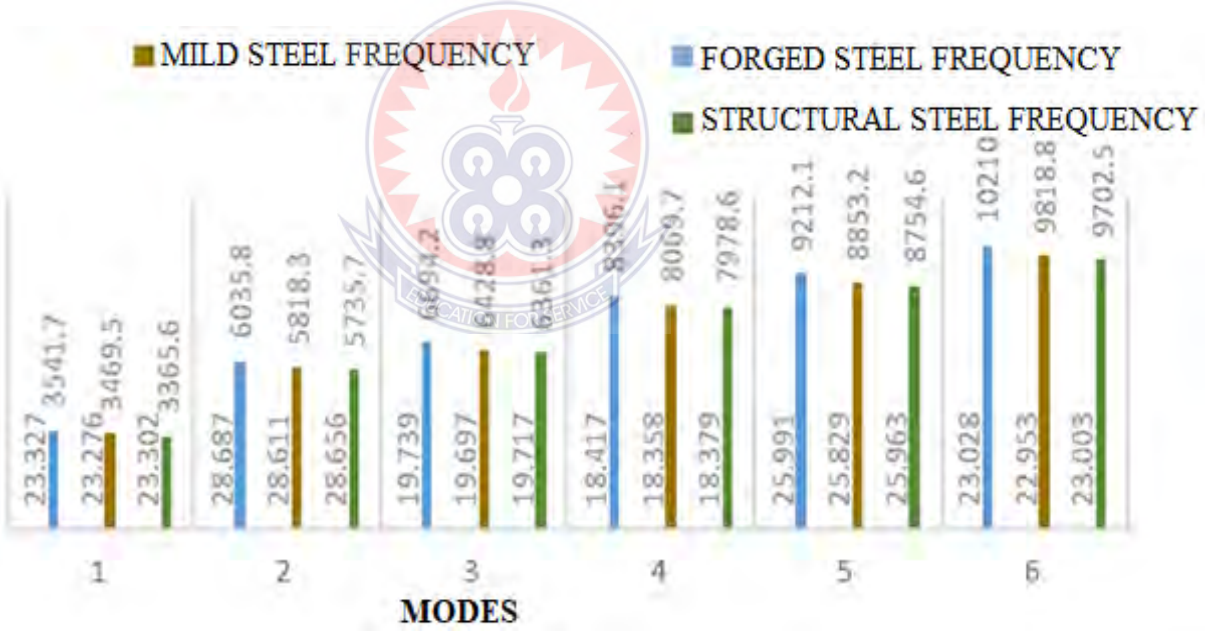

Combined Graph showing of Modal Analysis of Materials used for the Study

Table 4.2 Autodesk report summary showing volume of crankshaft

Paramter	Minimum	Maximum
Volume	1187960 mm^3	
Mass	9.32545 kg	

Von Mises Stress	0.0360247 MPa	453.299 MPa
1st Principal Stress	-32.2269 MPa	82.4945 MPa
3rd Principal Stress	-438.565 MPa	17.1872 MPa
Displacement	0 mm	0.0327006 mm
Safety Factor	0.551512 ul	15 ul
Stress XX	-143.334 MPa	31.8266 MPa
Stress XY	-202.096 MPa	49.3355 MPa
Stress XZ	-87.7865 MPa	134.615 MPa
Stress YY	-164.55 MPa	33.9251 MPa
Stress YZ	-97.3792 MPa	112.346 MPa
Stress ZZ	-150.921 MPa	38.4259 MPa
X Displacement	-0.0266491 mm	0.00133763 mm
Y Displacement	-0.0047053 mm	0.0232581 mm
Z Displacement	-0.00852241 mm	0.0085499 mm
Equivalent Strain	0.000000154465 ul	0.00191004 ul
1st Principal Strain	0.000000106005 ul	0.000981438 ul
3rd Principal Strain	-0.00210178 ul	-0.0000000972106 ul
Strain XX	-0.000274164 ul	0.000332353 ul
Strain XY	-0.00125107 ul	0.00030541 ul
Strain XZ	-0.00054344 ul	0.000833334 ul
Strain YY	-0.000661649 ul	0.00029146 ul
Strain YZ	-0.000602824 ul	0.000695478 ul
Strain ZZ	-0.000511022 ul	0.000169906 ul